PAVEMENT PERFORMANCE MONITORING USING DYNAMIC CONE PENETROMETER AND GEOGAUGE DURING CONSTRUCTION

by

AHMED NAWAL AHSAN

Presented to the Faculty of the Graduate School of

The University of Texas at Arlington in Partial Fulfillment

of the Requirements

for the Degree of

MASTER OF SCIENCE IN CIVIL ENGINEERING

THE UNIVERSITY OF TEXAS AT ARLINGTON

December 2014

ACKNOWLEDGEMENTS

First, I would like to express my deepest gratitude to my supervisor Dr. Sahadat Hossain, for his valuable time, guidance, encouragement, help and unconditional support throughout my Master's studies. Without his guidance and support throughout my Master's study, this thesis would not have been completed.

I would like to give my special thanks to Dr. Stefan A. Romanoschi and Dr. Xinbao Yu, for their time and participation as my committee members and for their valuable suggestions and advice.

My utmost appreciation to Texas Department of Transportation (TxDOT) for their constant help and collaboration at site.

I am really grateful to Dr. Sadik Khan for his constant guidance, valuable input, cooperation and assistance in all stages of work.

Special thanks extended to Dr. Golam Kibria, Dr. Sonia Samir, Mohammad Faysal, Asif Ahmed, Masrur Mahedi and all my colleagues for their active cooperation and assistance.

Finally, and most of all, I would like to thank my parents for all their love, encouragement, and great support.

November 12, 2014

ABSTRACT

PAVEMENT PERFORMANCE MONITORING USING DYNAMIC CONE PENETROMETER AND GEOGAUGE DURING CONSTRUCTION

Ahmed Nawal Ahsan

The University of Texas at Arlington, 2014

Supervising Professor: Sahadat Hossain

Proper design life of road network system requires adequate quality control measures during the construction process to ensure proper material quality and sufficient strength in between the materials. Laboratory tests are often time consuming and sometimes, are not practical while the construction work is going on, in-situ techniques can efficiently evaluate the material properties through simple and less time consuming procedures. Dynamic Cone Penetrometer and Geogauge can play a vital role as an in-situ testing equipment because both have the potential to measure the change in material properties through field tests being performed in the field. Both in-situ techniques was not extensively used in North Texas area. Frequent use of these two equipment during the construction process can expedite the whole construction process because both are hand-held devices and can be conducted within a short amount of time, often in minutes. For this study, Dynamic Cone Penetrometer and Geogauge was used to assess the material properties from the tests performed on five construction sites of Horseshoe Project around Dallas, TX. Several points across the width of the pavement have been considered to perform these in-situ tests along with Nuclear Density Gauge test in two of these sites. A

thorough analysis has been conducted for the material properties to be determined. Dynamic Cone Penetrometer and Geogauge both were consistent to measure the change in in-place material characteristics of the pavement materials. The design thickness of cement treated base layer where the tests were being performed was 6". DCP was efficient enough to detect the layer thickness up to a proximity of 0.5 inch and was also able to distinguish layer anomalies between the pavement layers. Cement stabilized base layer provided with a DCPI value which ranges from 0.5 mm/blow to 8 mm/blow whereas, DCPI values were observed to remain within a range of 2 mm/blow to 22 mm/ blow. For the top 6" cement treated base layer, unconfined compressive strength was found vary between 210 psi to 1023.5 psi. The highest resilient moduli value was found at the middle of the cement stabilized base layer where it varied from 40,500 psi – 623,285 psi. Young's moduli values for cement stabilized base layer measured with Geogauge also followed the same trend of resilient moduli obtained from the measurements taken with Dynamic Cone Penetrometer.

Table Of Contents

Acknowledgements iii

Abstract iv

List of Illustrations xii

List of Figures xv

Chapter 1- Introduction 1

1.1 Background 1

1.2 Problem Statement 3

1.3 Objectives 3

1.4 Organization 4

Chapter 2- Literature Review 6

2.1 Introduction 6

2.2 Dynamic Cone Penetrometer 6

2.2.1 Background 6

2.2.2 Principle 8

2.2.3 Terminology 13

2.2.4 Application Of Dynamic Cone Penetrometer 16

2.2.5 Factors Affecting DCP Measurements 18

2.2.5.1 Material Effects 18

2.2.5.2 Vertical Confinement Effects 20

2.2.5.3 Side Friction Effect 20

2.2.6. Existing Correlations Between DCP And California Bearing Ratio (CBR) 20
2.2.7 Existing Correlation Between DCP And Different Moduli 25
2.2.8 Existing Correlation Between DCP And Shear Strength Of Soil 30
2.2.9 Correlation Between DCPI And Unconfined Compressive Strength 33
2.2.10 Soil Classification Based On DCPI 34
2.3 Soil Stiffness Gauge (Geogauge) 37
2.3.1 Introduction 37
2.3.2 Principle Of Operation 38
2.3.3 Geogauge Stiffness And Moduli Calculation 40
2.3.4 Geogauge Application 42
2.3.5 Factors Affecting Geogauge Measurement 43
2.3.6 Correlation Between Geogauge And Resilient Modulus 43
2.3.7 Recent Use Of Geogauge 47
Chapter 3- Site Selection And Test Methodology 48
3.1 Introduction 48
3.2 Site Location And Layout Of The Tests 49
3.2.1 Location-1 (Avery St.) 49
3.2.2 Location-2 (I-35E Northbound Frontage Road) 50
3.2.3 Location-3 (S Riverfront Blvd.) 52
3.2.4 Location-4 (Jefferson Viaduct Blvd.) 53
3.2.5 Location-5 (Near Sylvan Ave.) 55

3.2.6 Summary Of The Tests Performed In Each Location 56
3.3 Test Methodology And Analysis Of Obtained Data 57
3.3.1 Dynamic Cone Penetration Test 57
3.3.2 Analysis Of Dynamic Cone Penetrometer (DCP) Data 57
3.3.2.1 DCP Index (DCPI) 58
3.3.2.2 Determination Of CBR 58
3.3.2.3 Determination Of Resilient Modulus (M_r) 58
3.3.2.4 Determination Of Unconfined Compressive Strength (qu) 59
3.3.3 Geogauge Test 59
3.3.4 Analysis Of Geogauge Data 60
3.3.4.1 Determination Of Young's Modulus, (E) 60
3.3.5 Nuclear Density Gauge Test 60
3.3.6 Analysis Of Nuclear Density Gauge Test Data 61
Chapter 4- Results And Analysis 62
4.1 Introduction 62
4.2 Data Collection 62
4.3. Field Tests On Avery St. (Location-1) 62
4.3.1 Approximation Of Level Of Compaction From DCPI Profile With Depth 62
4.3.2 Determination Of Layer Thickness From DCPI Profile 64
4.3.3 Resilient Moduli Profile Along Depth 66
4.3.4 Variation Of Resilient Moduli In Different Layers 67

4.3.5 Variation Of Unconfined Compressive Strenth In Base Layer Across Width Of The Pavement 68

4.3.6 Variation Of Young's Moduli From Geogauge 69

4.3.7 Comaprison Of Resilient Moduli From Dcp Measurement With Young's Moduli From Geogauge For Cement Stabilized Base Layer With Prime Coat……..….70

4.4 Field Tests Near I-35E Northbouth Frontage Road (Location-2) 71

4.4.1 Variation Of Young's Moduli With Moisture Content 71

4.4.2 Variation Of Young's Moduli With Change In Density 72

4.5 Field Tests Near South Riverfront Blvd. (Location-3) 74

4.5.1 Approximation Of Level Of Compaction From DCPI Profile With Depth 74

4.5.2 Determination Of Layer Thickness From DCPI Profile 75

4.5.3 Resilient Moduli Profile Along Depth 76

4.5.4 Variation Of Resilient Moduli In Different Layers 77

4.5.5 Variation Of Unconfined Compressive Strenth In Base Layer Across Width Of The Pavement 78

4.5.6 Variation Of Young's Moduli From Geogauge 79

4.5.7 Comaprison Of Resilient Moduli From DCP Measurement With Young's Moduli From Geogauge For Cement Stabilized Base Layer With Prime Coat……80

4.6 Field Tests Near Jefferson Viaduct Blvd. (Location-4) 81

4.6.1 Variation Of Young's Moduli With Moisture Content 81

4.6.2 Variation Of Young's Moduli With Change In Density 82

4.7 Field Tests Near Sylvan Ave. (Location-5) 84

4.7.1 Approximation Of Level Of Compaction From DCPI Profile With Depth 84

4.7.2 Determination Of Layer Thickness From DCPI Profile 85

4.7.3 Resilient Moduli Profile Along Depth 86

4.7.4 Variation Of Resilient Moduli In Different Layers 87

4.7.5 Variation Of Unconfined Compressive Strenth In Base Layer Across Width Of The Pavement 88

4.7.6 Variation Of Young's Moduli From Geogauge: 89

4.7.7 Comaprison Of Resilient Moduli From DCP Measurement With Young's Moduli From Geogauge For Cement Stabilized Base Layer With Prime Coat……..……90

4.8 Comparison With Literature 91

4.8.1 Comparison Of Resilient Modulus From DCPI 91

4.8.1.1 Cement Stabilized Base With Prime Coat 91

4.8.1.2 Lime Stabilized Subgrade 93

4.8.1.3 Compacted Subgrade 95

4.8.2 Comparison Of Unconfined Compressive Strength (UCS) From DCPI For Cement Stabilized Base Materials With Laboratory Data And Literature…….....96

4.8.3 Comparison Of Young's Modulus From Geogauge…….98

Chapter 5- Conclusions And Recommendations 101

5.1 Summary And Conclusions 101

5.2 Recommendations 102

References 103

Biographical Information 109

List Of Illustrations

Figure 2.1: Dynamic Cone Penetrometer 7

Figure 2.2: Dynamic Cone Penetrometer Schematic (Source: MnDOT DCP Design) 9

Figure 2.3: The Dynamic Cone Penetration (DCP) Test Procedure (Salgado and Yoon, 2003) 11

Figure 2.4: DCPI Profile of a Flexible Pavement (Gudishala, 2004) 12

Figure 2.5: Foundation Balance Graph (Kleyn) (1 inch = 25.4 mm) 14

Figure 2.6: Strength-Balance Curve (Kleyn) (1 inch = 25.4 mm) 15

Figure 2.7: Average Strength Profile of a Flexible Pavement 17

Figure 2.8: Trend among the trends obtained from Laboratory results (Harison, 1987) .. 19

Figure 2.9: Correlation chart between CBR vs DCPI 21

Figure 2.10: Comparison of Different CBR - Modulus Relationships (Wu and Sargand, 2007) 22

Figure 2.11: Comparison of Predicted UCS and Actual UCS 34

Figure 2.12: Geogauge 37

Figure 2.3: Schematic of Geogauge (Humboldt, 1998) 39

Figure 3.1: Location of the tests performed on June 09, 2014 49

Figure 3.2: Layout of the Tests performed on June 09, 2014 50

Figure 3.3: Location of the tests performed on June 17, 2014 51

Figure 3.4: Layout of the tests performed 51

Figure 3.5: Location of the Tests performed on August 2, 2014 52

Figure 3.6: Layout of the Tests performed on August 2, 2014 53

Figure 3.7: Location of the tests performed on August 27, 2014 54

Figure 3.8: Layout of the tests performed on August 27, 2014 54

Figure 3.9: Location of the Tests performed on October 3, 2014 55

Figure 3.10: Layout of the Tests performed on October 3, 2014 56
Figure 3.11: Dynamic Cone Penetrometer Test Photos 57
Figure 3.12: Geogauge Test Photos 59
Figure 3.13: Nuclear Density Gauge Test Photos 60
Figure 4.1: DCPI profile across depth of the pavement 63
Figure 4.2: DCPI profile across depth of the pavement obtained from P6 65
Figure 4.3: Resilient Moduli Profile across depth of the pavement 66
Figure 4.1: Variation of Resilient Moduli in Different Layers 67
Figure 4.5: Variation of Unconfined Compressive Strength in base layer across width of pavement at Location-1 68
Figure 4.6: Variation of Young's Modulus across Pavement 69
Figure 4.7: Variability of Resilient Moduli with Young's Moduli (Cement Stabilized Base Layer) 70
Figure 4.8: Variation of Young's Moduli with change in Moisture Content 71
Figure 4.9: Variation of Young's Moduli with change in Wet Density 72
Figure 4.10: Variation of Young's Moduli with change in Dry Density 73
Figure 4.11: DCPI profile across depth of the pavement 74
Figure 4.12: DCPI profile across depth of the pavement obtained from P2 75
Figure 4.13: DCPI profile across depth of the pavement obtained from P2 76
Figure 4.14: Variation of Resilient Moduli in Different Layers 78
Figure 4.15: Variation of Unconfined Compressive Strength in base layer across width of pavement at Location-3 79
Figure 4.16: Variation of Young's Modulus across Pavement 80
Figure 4.17: Variability of Resilient Moduli with Young's Moduli (Cement Stabilized Base Layer) 81

Figure 4.18: Variation of Young's Moduli with change in Moisture Content 82
Figure 4.19: Variation of Young's Moduli with change in Wet Density 83
Figure 4.20: Variation of Young's Moduli with change in Dry Density 84
Figure 4.21: DCPI profile across depth of the pavement 85
Figure 4.22: DCPI profile across depth of the pavement obtained from P1 86
Figure 4.23: Resilient Moduli Profile across depth of the pavement 87
Figure 4.24: Variation of Resilient Moduli in Different Layers 88
Figure 4.25: Variation of Unconfined Compressive Strength in base layer across width of pavement at Location-5 89
Figure 4.26: Variation of Young's Modulus across Pavement 90
Figure 4.27: Variability of Resilient Moduli with Young's Moduli (Cement Stabilized Base Layer) 91
Figure 4.28: Comparison between Resilient Moduli values obtained from Field Tests and Literature (Cement Stabilized Base Layer) 93
Figure 4.29: Comparison between Resilient Moduli values obtained from Field Tests and Literature (Lime treated Subgrade Layer) 94
Figure 4.30: Comparison between Resilient Moduli values obtained from Field Tests and Literature (Compacted Subgrade Layer) 96
Figure 4.31: Comparison between UCS values obtained from Field Tests and Literature 98
Figure 4.32: Comparison between Young's Moduli values obtained from Field Tests and Literature 100

List Of Tables

Table 2.1: Values of B and 2τ0 for Different Types of Soil 27

Table 2.2: Properties of Test Materials (Ayers et al., 1989) 31

Table 2.3: Correlation between DCPI and Shear Strength (Ayers et al., 1989) 32

Table 2.4: Classification of Granular Soils from DCPI (Huntley, 1990) 35

Table 2.5: Classification of Cohesive Soils from DCPI (Huntley, 1990) 35

Table 2.6: DCP criteria (NDCP) for a penetration of 0 to 6 inch (0 to 150 mm) 36

Table 2.7: Limiting DCPI by MnDOT 36

Table 2.8: Typical Poisson's Ratio value for Different Types of Materials 42

Table 2.9: Geogauge and FWD suggested values to characterize base layer 44

Table 3.1: Site Locations of the Pavement Testing for Horseshoe Project, Dallas, TX ... 48

Table 3.2: Summary of the Tests performed in each location 56

Table 4.1: Location-wise Resilient Moduli values with Literature Moduli Values (Cement Stabilized Base Layer) 92

Table 4.2: Location-wise Resilient Moduli values with Literature Moduli Values (Lime Treated Subgrade Layer) 94

Table 4.3: Location-wise Resilient Moduli values with Literature Moduli Values (Compacted Subgrade Layer) 95

Table 4.4: Location-wise UCS values with Literature Values (Cement Stabilized Base Layer) 97

Table 4.5: Location-wise Young’s Moduli values measured with Geogauge and TX Pavement Design Moduli 99

CHAPTER 1

INTRODUCTION

1.1 Background

United States of America comprises of 4,064,000 miles of public road network throughout the entire country. The total length of the paved roads is 2,646,000 miles and the rest is the unpaved roads which is 1,418,000 miles long (Bureau of Transportation Statistics). The satisfactory performance of the road networks mainly depends on the quality control measures that were taken during the construction process. In this regard, proper quality control to ensure the necessary design steps to be performed accordingly needs to be taken during the construction of the pavement.

The loads coming from the ongoing vehicles mainly pass on to the layers of the pavement which mainly consists of base course, subbase course and the compacted subgrade underneath the surface course and the binder course. Hence, proper construction of the pavement beneath the paved surface is of utmost importance during the construction of the pavement structure. Proper design life can be ensured if only proper quality control is maintained throughout the whole construction process.

Several in-situ devices have been used throughout the decades to evaluate the material properties of the pavement during construction process which can be broken down into three main major categories (MnDOT):

1. Determination of shear strength:
    - (i) Dynamic Cone Penetrometer (DCP)
    - (ii) Rapid Compaction Control Device (RCCD)

2. Determination of Elastic Modulus:
    - (i) Dynatest Falling Weight Deflectometer (FWD)
    - (ii) Loadman Portable FWD (PFWD)

(iii) PRIMA PFWD

(iv) Humboldt Geogauge

3. Determination of Density:

(i) Sand Cone Method

(ii) Nuclear Density Gauge (NDG)

In the recent decades, popularity of Dynamic Cone Penetrometer and Geogauge are increasing due to their simplicity in use and less time required to estimate material qualities. Dynamic Cone Penetrometer has been used by many agencies throughout the years but the use of Geogauge for assessing the material quality is recent. Dynamic Cone Penetrometer is a simple hand-held device to measure the in-situ strength of base, subbase and subgrade and the thickness and location of underlying soil layers and has been used in geotechnical investigations for a few decades. This equipment can estimate the strength, pavement condition and variability of granular bases and subgrade soils of existing pavements.

Geogauge which was formerly known as Soil Stiffness Gauge is a hand-portable gauge used to measure lift stiffness and soil modulus for compaction process control. Geogauge measures the impedance at the surface of the soil i.e., the stress imparted to the surface and the resulting surface velocity as a function of time which provides the stiffness of the underlying material of the pavement. Few agencies including U.S. Army Corps of Engineers, Federal Highway Authority (FHWA), Minnesota Department of Transportation (MnDOT), New York State Department of Transportation (NYSDOT), North Carolina Department of Transportation (NCDOT) and Texas Department of Transportation (TxDOT) have recently been using Geogauge in their construction works.

1.2 Problem Statement

The Horseshoe Project is a $798 million design-build roadway construction project undertaken by the Texas Department of Transportation (TxDOT). The project was taken into account to improve the traffic flow through the heart of the downtown Dallas which includes construction improvements such as expansion, repaving and addition of new bridges and roadways along Interstates 30 and 35E and construction of a new signature bridge named the Margaret McDermott Bridge over I-30. The timeline to complete the whole project is from April 2013 to summer 2017 which will ensure the improved safety, increased capacity and improved mobility through the downtown Dallas.

Typically, as a part of the QA/QC program of the horseshoe project, the conventional core samples are collected to determine the strength and stiffness parameters to assess the construction quality. However, collecting the core samples followed by laboratory testing is time consuming and might be expensive. Moreover, the core collection is performed every few thousand feet and considered that collected core sample is representing the overall strength of the entire section. However, the strength and stiffness may vary within few feet. Therefore, adopting the insitu technique as a part of the QA/QC program will provide more data points which may help to improve the construction quality and compliance. The in-situ test such as DCP and Geogauge can be performed within the horseshoe project to assess the construction quality, uniformity, layer stiffness moduli as well as compaction level as a part of the QA/QC work.

1.3 Objectives

The major objective of this study is to utilize the in-situ test technique such as DCP and Geogauge to evaluate the construction quality and compliance with the design standard in different locations of the horseshoe project. The specific objective of the study includes:

- Perform DCP and Geogauge tests at different location of the Horseshoe project on monthly basis after placing the base layer.
- Determine the layer thickness from DCP Index profile along depth obtained from Dynamic Cone Penetrometer test.
- Assess resilient moduli values and unconfined compressive strength in different layers of the pavement using Dynamic Cone Penetrometer.
- Evaluate the variation of Young's moduli across the width of the pavement with the use of Geogauge.
- Compare of DCP and Geogauge test results.
- Compare DCP and Geogauge test results between current and previous studies.

1.4 Organization

A brief summary of the chapters included in this thesis is presented in the following paragraphs:

Chapter 1 provides an introduction and presents the problem statement and objectives of the study that has been conducted under Horseshoe Project.

Chapter 2 presents the background, an overview and use of Dynamic Cone Penetrometer and Geogauge in the recent research works carried out by different agencies across United States.

Chapter 3 presents the methodology of the field tests, the layout in which the tests at the field were carried out and procedures to analyze the data collected from field tests performed in different locations of Dallas, TX under Horseshoe Project.

Chapter 4 describes the analysis results of the in-situ tests performed with Dynamic Cone Penetrometer, Geogauge and Nuclear Density Gauge and the comparison of the results obtained from tests performed with the literature.

Chapter 5 discusses the comparison drawn to evaluate the qualitative use of Dynamic Cone Penetrometer and Geogauge as an in-situ pavement testing technique.

CHAPTER 2

LITERATURE REVIEW

2.1 Introduction

This chapter reviews the test devices (i.e., Dynamic Cone Penetrometer and Geogauge) that were used in this study. This summary contains history, background, working principle, existing correlations for soil measurements and the current uses of these two devices.

2.2 Dynamic Cone Penetrometer

2.2.1 Background

Efficient construction of pavement as well as its performance evaluation requires a proper and representative characterization of materials. In geotechnical engineering, in-situ penetration techniques have become popular and are being widely used to serve this purpose due to its simplicity and low cost of operation. Two of the most typical in-situ penetration tests which have been used due to this reason are the Standard Penetration Test (SPT) and the Cone Penetration Test (CPT). In SPT test, a sampler is driven into the soil with hammer blow whereas, the principle on which CPT is operated is quasi-static. Due to its nature of consuming much time during the construction phase, the need of a more time saving in-situ testing device was realized.

The Dynamic Cone Penetration test (DCP) was first developed by Scala in South Africa as an in-situ pavement evaluation technique for evaluating pavement layer strength (Scala, 1956). Dynamic Cone Penetrometer (DCP) has been used to measure the in-situ shear resistance of soil because a soil's shearing resistance is its ability to withstand load. But a newer form of the Dynamic Cone Penetrometer was designed by Dr. D. J. van Vuuren with a 30° cone in 1969. Afterwards, the Transvaal Roads Department in South Africa started using DCP to investigate road pavement in 1973 (Kleyn, 1975) with a 30° cone tip. Afterwards the results which were obtained using 30° and 60° cone tip were reported by

Kleyn.Kleyn found that when a DCP measurement is plotted against a CBR obtained from the lab experiments on a log-log graph, the relationship between these two parameters are linear. Despite giving much effort to find out a way to use the DCP curves as an indicator of pavement condition, Kleyn was unable to find any pattern that would give any indication about the pavement condition. Then in 1982, the final conclusion about the Dynamic cone Penetrometer was drawn by Kleyn after comparing sound pavement sections with failed pavement sections where he found a minimum strength or suitability for the base course. It has been extensively used in South Africa, United Kingdom, Australia, New Zealand and several States in the U.S.A. such as California, Florida, Illinois, Minnesota, Kansas, Mississippi and Texas for the characterization of the pavement layers and subgrades. The U. S. Corps of Engineers has also used DCP as an in-situ testing tool. The Dynamic Cone Penetrometer has been proven as an effective tool in measuring the strength parameter of the pavement layers and subgrade conditions.

Figure 2.1: Dynamic Cone Penetrometer

California Bearing Ratio (CBR) values for a soil were used as an indicator of shear strength for the pavement applications in military. CBR is measured with a standardized penetration shear test and usually performed on laboratory compacted test specimens during the design phase of the pavement. In these situations to determine the CBR value, destructive

test pits were usually dug to determine pavement layer thicknesses and characterization of subgrade materials. This test was time consuming and impractical during the construction of the pavement.

The Dynamic Cone Penetration (DCP) is a simple field test method, consumes less time in practical applications, require less maintenance and a continuous profile of the pavement layers can be achieved with higher accuracy. Manually driving mechanism is avoided in the operation of DCP. The greatest advantage of DCP over other in-situ pavement testing devices is that it can locate the zone of weakness within the pavement easily

2.2.2 Principle

The Dynamic Cone Penetrometer Test is performed by dropping a hammer of a specific weight from a certain height which constitutes features both of SPT and CPT. The DCP test is standardized by ASTM D 6951-03. The penetration depth per blow up to a depth needed is measured thus resembling this to SPT procedures which measures blow count using the soil sampler. A 60° cone is used to create a cavity during the DCP test instead of using the split spoon soil sampler, this operation makes it similar to CPT as well. The principles on which the DCP operates on seem to reduce many of the deficiencies that occurred during manually getting into the soil.

The Dynamic Cone Penetrometer can provide continuous measurements of the pavement layers and the underlying subgrade without digging the existing pavement which is encounters during CBR test [7]. It constitutes an upper fixed travel shaft which is 22.6 inch (575 mm) long with a 17.6 lbs (8 kg) falling weight which exerts an energy of about 78.5 N and a lower shaft of 39.4 inch (1000 mm) which contains an anvil and a replaceable cone with an apex angle of 60° and 0.8 inch (20 mm) diameter. The anvil stops the hammer from falling further than the standard falling height which ensures a constant driving force of the cone into the ground. An additional rod which is attached to the lower shaft is used as scale

to measure the penetration per blow.The shaft has a smaller diameter than the cone (16 mm) to reduce the skin friction during the penetration of the cone into the soil. A schematic of the DCP is given below in Figure 2.2.

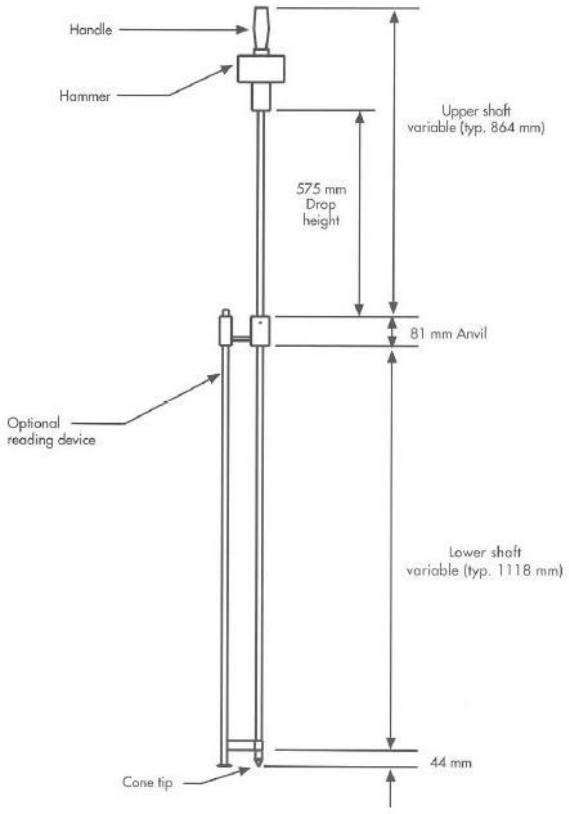

Figure 2.2: Dynamic Cone Penetrometer Schematic (Source: MnDOT DCP Design)

Few configuration options are available for the DCP in the market for the use which include changing the mass of the falling weight, type of tip and recording method. The standard hammer mass is 17.6 lbs (8 kg) but 10.1 lbs (4.6 kg) mass is also available for a weaker soil. The smaller mass weight can be used on soils with a CBR value up to 80. The bigger between these two is usually used for the pavement application. The pavement layers are compacted and requires more energy from the falling weight for the proper penetration to occur. The tip which is attached to the lower portion of the DCP can be replaceable point

or disposable cones. The replaceable point remains for a certain period of time until it becomes worn out or damaged beyond a certain limit and then it is replaced with a newer one. On the contrary, the disposable cone remains in the soil after every test. The main reason behind using disposable cones with the DCP is that it helps to remove the DCP shaft from the soil after the penetration process is performed.

Performing DCP test requires two persons where one person let the weight fall freely from a specified height and the other person records the measurement. The lower shaft can move independently with the scale attached to it for the measurement to be recorded. The scale stays on the ground surface so that the penetration of the shaft can be measured with respect to the ground surface. The cone tip is being placed on the surface being tested at first and afterwards, the test is performed by letting the fall freely. The cone must have to penetrate a minimum of 25 mm between recorded measurements. Data which are taken at less than 25 mm penetration increments sometimes results in inaccurate strength determinations hence, to be avoided. The number of hammer blows between measurements should be between 1, 2, 3, 5, 10, 20 depending on the cone penetration rate. The initial reading recorded before any hammer blow is counted as initial penetration corresponding to blow 0. The falling of the mass is repeated until the desired depth is reached and the penetration depth for each blow is measured for each hammer drop. The penetration procedure performed with the DCP is shown in Figure 2.3 (Salgado and Yoon, 2003).

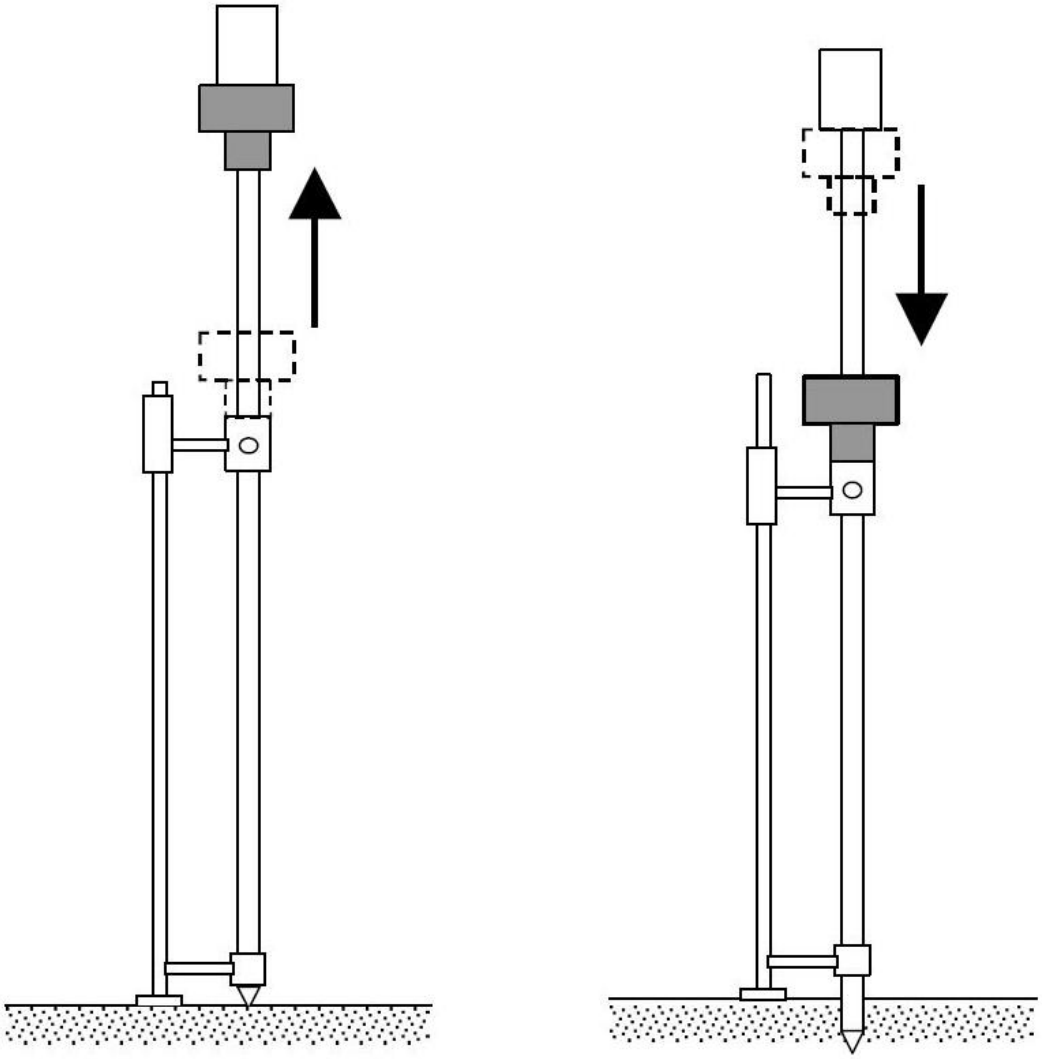

Figure 2.3: The Dynamic Cone Penetration (DCP) Test Procedure (Salgado and Yoon, 2003)

While determining the layer thickness, the slope of the curve between number of blows and depth of penetration (mm/blow) is denoted as the DCP Penetration Index (DCPI). It can be calculated as (Embacher, 2005):

$$\text{DCPI} = \frac{P(i+1)-P(i)}{B(i+1)-B(i)}$$

Where, DCPI = Dynamic Cone Penetration Index (mm/blow)

P = Penetration at *i*th or (*i*+1)th hammer drops (mm)

B = blow count for *i*th or (*i*+1)th hammer drops

A typical plot of DCP test results is presented below in Figure 2.4. The slope of this graph at any point represents the value of Dynamic Cone Penetration Index (DCPI) in mm/blow which indicates the amount of resistance the material is exerting towards the cone. The lower DCPI values indicates a stiffer soil and vice versa.

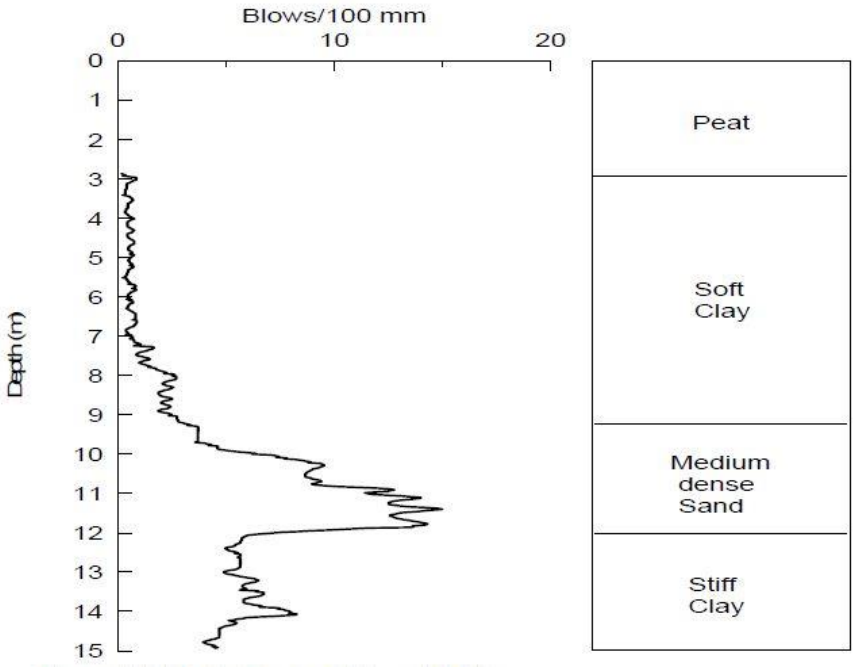

Figure 2.4: DCPI Profile of a Flexible Pavement (Gudishala, 2004)

A standard procedure should be followed while analyzing the data recorded from DCP measurement for a representative value of penetration per blow. For a specific location, a representative DCPI value for a certain amount of depth being considered can be obtained using any of the two methods mentioned below:

Arithmetic Average:

The arithmetic average is obtained using the following equation (Edil and Benson, 2005):

$$DCPI_{avg} = \Sigma_i^N (DCPI)/N$$

Where, N = Total number of DCPI recorded for a given depth

Weighted Average:

The weighted average is obtained from the following equation (Edil and Benson, 2005):

$$DCPI_{wt.avg} = \frac{1}{H} * \Sigma_i^N * (DCPI_i * Z_i)$$

Where, Z = Penetration Depth per Blow Set

H = Total Penetration Depth

2.2.3 Terminology

From the early stages of the development of DCP, many indices were derived from DCP data to characterize the pavement layers.

Kleyn et al. defined the DCP Structure Number (DSN) as the number of blows required to penetrate a layer of material (Kleyn et al., 1982). According to them, DSN of the i^{th} layer, DSN_i, can be defined as the number of blows required to penetrate the layer thickness h_i (mm/inch) at an average PR of DN_i (mm/inch) per blow.

$$DSN_i = h_i/DN_i$$

The pavement DSN was denoted as the number of blows required to penetrate the whole pavement structure:

$$DSN = \Sigma\, DSN_i$$

The pavement strength balance N_{DCP} was defined as the number of blows required to penetrate 10 cm (3.9 inch)

Over the past few decades, data taken from DCP measurements have also been represented in the following chart formats (Kleyn, 1975):

1. The Foundation Balance Graph: A plot of depth over PR with both axes in log scale which is presented in Figure 2.5.
    - The DCP Factor: The area enclosed by the foundation balance graph

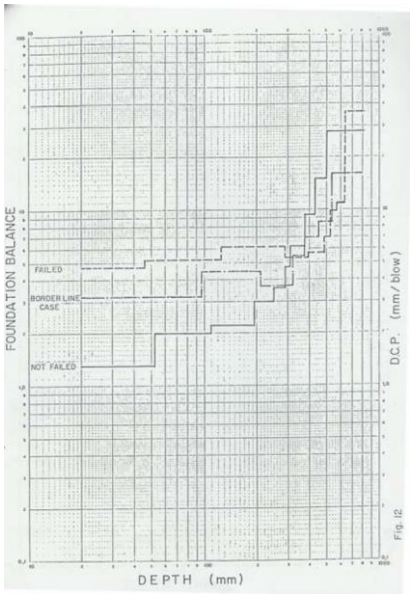

Figure 2.5: Foundation Balance Graph (Kleyn) (1 inch = 25.4 mm)

2. The Strength-Balance Curve (Presented in Figure 2.6:)

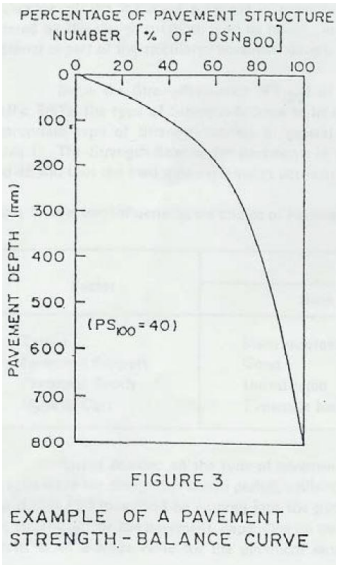

Figure 2.6: Strength-Balance Curve (Kleyn) (1 inch = 25.4 mm)

3. The Layer Strength Diagram: The depth in natural numbers and the PR in log scale
4. The DCP Curve: The number of blows needed to reach a certain depth

DCP data have been interpreted in different ways from the beginning of DCP being used for the pavement characterization. Below are some of the different forms of DCP measurements which measure the depth of penetration per blow:

i. Penetration Rate (PR)
ii. DCP Number (DN) (Kleyn, 1975)
iii. DCP Index (DI or DCPI) (Harison, 1989)
iv. Blow Number (BN)

In this report, measurement taken from DCP will be denoted as the DCPI.

2.2.4 Application Of Dynamic Cone Penetrometer

According to Kleyn, Maree and Savage (1982), Dynamic Cone Penetrometer can be used in construction projects to evaluate the following:

1. Potentially collapsible soils
2. Construction control
3. Efficiency of compaction
4. Stabilized layers
5. Subgrade moisture content

The MnDOT recommended two applications of DCP as a quality control device:

1. During the compaction of backfill of pavement edge drain trenches.
2. During the compaction of granular base layer.

Each layer of granular base layer requires less than 19 mm per blow (0.75 inches per blow) to ensure the proper compaction. This DCPI limiting value is valid for freshly compacted base materials because DCPI value decreases quickly with time and under traffic loading. MnDOT recommended using other devices along with DCP to ensure proper compaction. Based on the studies conducted by Siekmeier (1998), MnDOT revised the limiting penetration rate based on the agreement between the DCPI and percent compaction which are as follows:

1. 15 mm/blow in the upper 75 mm (3.0 inch)
2. 10 mm/blow at depth between 75 and 150 mm (3 and 6 inch)
3. 5 mm/blow at depth below 150 mm (6 inch)

They recommended the following:

(i) The test should be performed consistently and not more than one day after compaction while the base material is still damp.

(ii) The construction traffic should be distributed uniformly by requiring haul trucks to vary their path.

(iii) At least two dynamic cone penetrometer tests should be conducted at selected sites within each 800 cubic meters of constructed base course.

The Wisconsin DOT identified DCP and rolling wheel deflectometer as an effective tool in identifying weak areas of in-situ subgrade for construction acceptance (Corvetti & Schabelski, 2001).

Presence of shallow bed rock or less than 3 inch (75 mm) of asphalt concrete layer often result in misinterpretation of backcalculated moduli from falling weight deflectometer (FWD). DCP can accurately be used in these kinds of situations where weak subgrade or base layers can cause large deflections which exceed the calibration limit of the equipment. A stiffer material results in lower values of DCPI whereas, a soft material provides higher values of DCPI. The following Figure 2.7 presents the average strength profile of an existing flexible pavement.

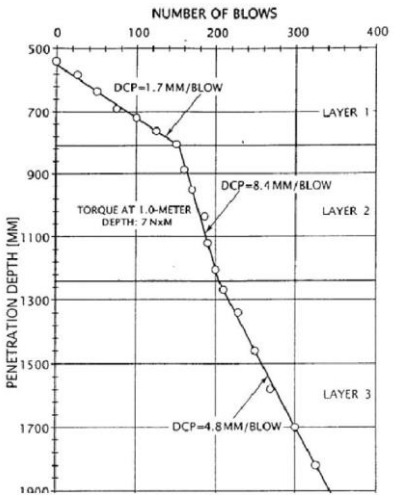

Figure 2.7: Average Strength Profile of a Flexible Pavement

Soil layer thickness can also be determined from the change in slope of the depth vs the profile of the accumulated blows. Livneh (1987) matched the layer thickness obtained from the measurements taken with the DCP to the thickness obtained from the test pits and hence, concluded that the DCP test is reliable to determine the layer thickness for evaluating any project.

2.2.5 Factors Affecting DCP Measurements

2.2.5.1 Material Effects

Many researchers have conducted research activities to evaluate the factors that might affect the measurements taken with the Dynamic Cone Penetrometer which include soil type, gradation, moisture content, density, plasticity and maximum aggregate size.

Kleyn& Savage (1982) concluded that the plasticity, density, moisture content and gradation influentially affect the measurements taken with the DCP. According to Hassan (1996), DCP measurements are significantly affected by moisture content, AASHTO soil classification, confining pressures and dry density for fine grained soils whereas, George (2000) suggested that the DCP data to be affected by the maximum aggregate size and the coefficient of uniformity. Harison (1987) observed the trend between DCPI, moisture content and dry unit weight which is presented below in the Figure 2.8.

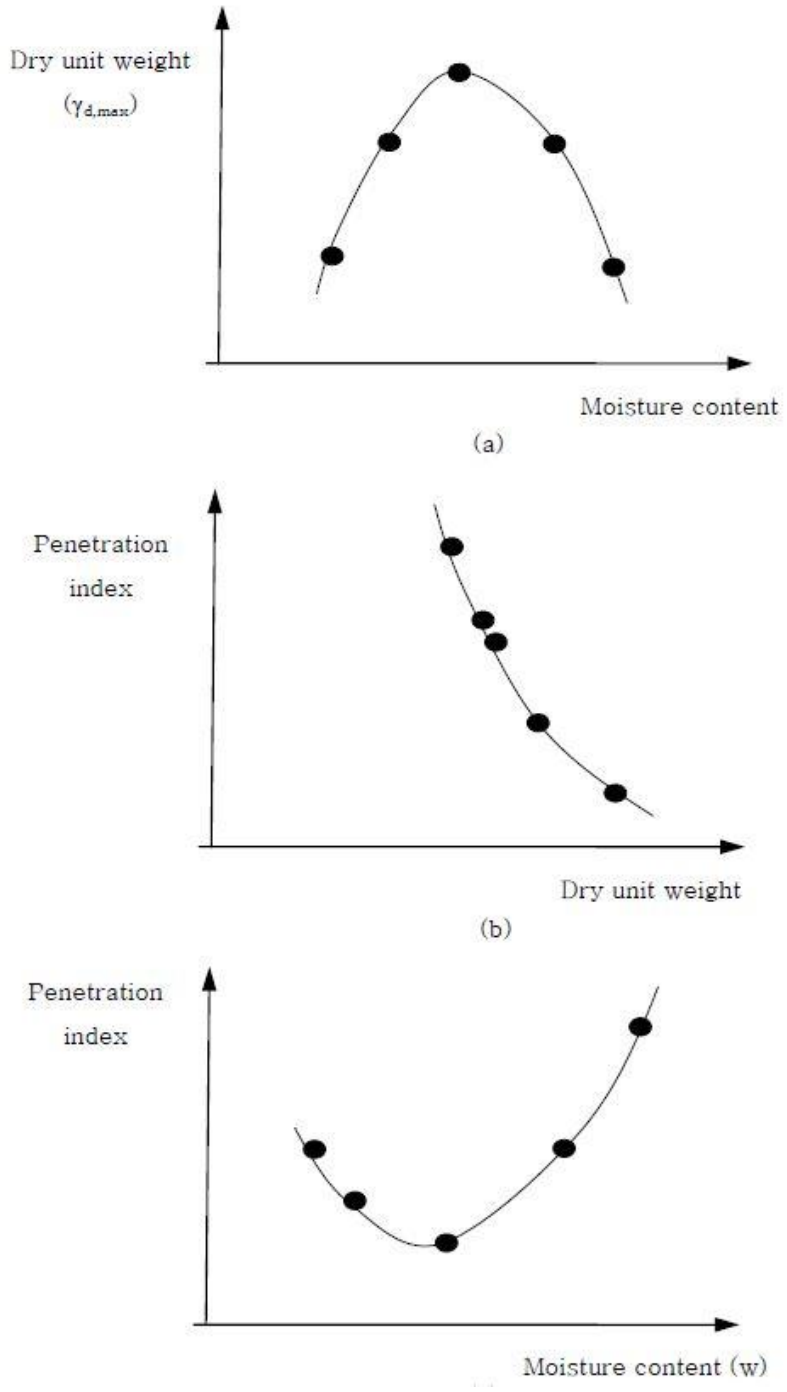

Figure 2.8: Trend among the trends obtained from Laboratory results (Harison, 1987)

2.2.5.2 Vertical Confinement Effects

The effect of vertical confinement on strength of soil obtained from the measurement taken with the DCP was studied by Livneh et al. (1995) and no effect of vertical confinement by rigid pavement structure or by upper cohesive layers on the DCP data of lower cohesive subgrade layers have been observed by them. However, vertical confinement effect by the upper asphaltic layers on the DCP data of the granular pavement layers has been observed. This influence might be occurred because of the friction developed in the DCP shaft by tilted penetration or by a collapse of the granular material on the shaft surface during penetration.

2.2.5.3 Side Friction Effect

Side friction often generated while penetrating is mainly due to the non-vertical penetration of DCP shaft in to the soil. It can also be generated while penetration occurs in a collapsible granular material. However, the amount side friction generated in cohesive soils is often small. According to Livneh (2000), a correction factor can be used to correct the DCP value for the side friction effect.

2.2.6 Existing Correlations Between DCP And California Bearing Ratio (CBR)

Penetration rates of the cone of Dynamic Cone Penetrometer into the base, sub-base and subgrade soil can be converted into CBR. Assessing the structural properties of a pavement layers often requires the DCP values to be converted into CBR. Different correlations were suggested between the DCPI (mm/blow) and CBR values.

Based on the previously performed researches, it has been observed that the relationship between DCPI and CBR values are often one of the following forms presented below:

Log-Log Equation: Log (CBR) = a + b (Log DCPI)

Where, CBR = California Bearing Ratio

DCPI = Dynamic Cone Penetration Index

a = constant ranging from 1.55 to 3.93

b = constant ranging from -0.55 to -1.65

Inverse Equation: CBR = D (DCPI) E + F

Where, D, E, F = Regression Constants

U.S. Army Corps of Engineers developed a relation between DCPI and CBR based on a wide range of granular and cohesive materials which was adapted by many researchers [12].

Log CBR = 2.465 – 1.12 (Log DCPI)

Or, CBR = $\frac{292}{DCPI\text{^}1.12}$

This correlation can be presented by the chart presented below:

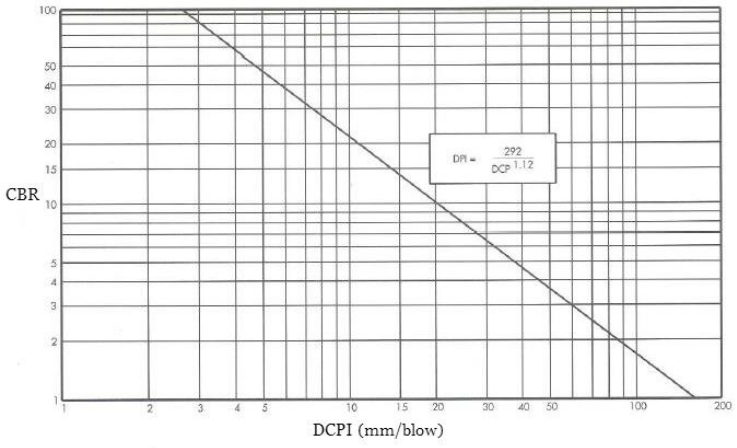

Figure 2.9: Correlation chart between CBR vs DCPI

Based on the field CBR and the average of three measurements taken with the DCP within an area with a radius of less than 1 ft (0.3 m), the North Carolina Department of Transportation (NCDOT) (Wu, 1987) suggested the following relationship:

Log (CBR) 2.64 – 1.08 (Log DCPI)

Or, CBR = $\frac{435}{PR\text{^}1.08}$ (R^2=0.79)

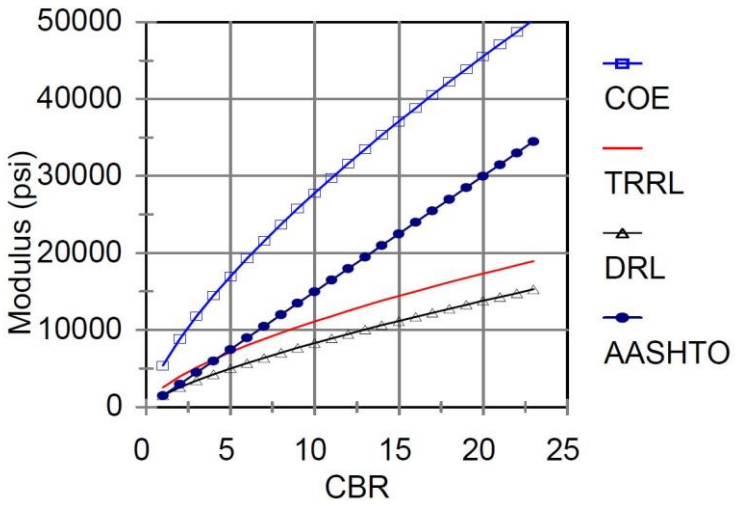

Figure 2.10: Comparison of Different CBR-Moduli Relationships (Wu and Sargand, 2007)

The study conducted by U.S. Army Corps of Engineers was based on the CBR values obtained from the lab experiments and the CBR values obtained by NCDOT were from field. It has been observed that the CBR values obtained from field is twice than the values obtained from lab experiments. The results of these two experiments were in good agreements, Webster et al. (1994) refined this equation and suggested correlations suitable for different soil types.

CBR = $\frac{1}{(0.002871*DCPI)}$ (for high plasticity clay soil (CH))

CBR = $\frac{1}{(0.017019*DCPI)\text{^}2}$ (for low plasticity clay soil (CL))

After performing DCP tests on 2000 sample of pavement materials in standard molds, Kleyn [8] recommended the following equation. He found out that the measurements taken from the DCP varied in a way as the CBR varies with the moisture content. According to him, DCP-CBR relationship was independent of moisture content.

$$\text{Log CBR} = 2.62 - 1.27 \text{ (log DCPI)}$$

Smith and Pratt suggested the following correlation based on a field study [9]:

$$\text{Log CBR} = 2.56 - 1.15 \text{ (log DCPI)}$$

Observing the small difference between the two relationships above, Livneh et al. (1994) proposed the following equation as the best correlation:

$$\text{Log CBR} = 2.46 - 1.12 \text{ Log (DCPI)}$$

Using a wide range of undisturbed and compacted fine-grained soil samples with or without saturation, Livneh and Ishia developed a correlation between DCPI and the in-situ CBR. Compacted granular soils were tested in flexible molds with variable controlled lateral pressures. The following relationship was developed by them [10]:

$$\text{Log CBR} = 2.2 - 0.71 \text{ (Log DCPI)}^{1.5}$$

Livneh, M. (1989) developed the following relationship based on field and laboratory tests:

$$\text{Log CBR} = 2.14 - 0.69 \text{ (Log DCPI)}^{1.5}$$

The following relationships were developed by Harrison for different soils [11]. According to him, soaking process has an insignificant effect on the CBR-DCP relationship

$$\text{Log CBR} = 2.56 - 1.16 \text{ Log (DCPI) (clayey-like soil where PR> 10 mm/blow)}$$

$$\text{Log CBR} = 2.70 - 1.12 \text{ Log (DCPI) (granular soil where PR<10 mm/blow)}$$

According to tests conducted by Coonse (1999) on piedmont residual soils, he developed an empirical relationship between CBR and DCP [12]. He concluded that the CBR-DCP relationship is independent of moisture content, dry density and soaking.

$$\text{Log (CBR)} = 2.53 - 1.14 \text{ (Log DCPI)}$$

Based on the tests performed on aggregate base course, Ese et al, (1994) developed the following correlation:

$$\text{Log (CBR)} = 2.44 - 1.07 \text{ (Log DCPI)}$$

Ese (Norwegian Road Research Laboratory) correlated field measurements taken with the DCP with lab CBR values. He suggested the following relationship:

$$\text{Log } (CBR_{lab}) = 2.438 - 1.65 \text{ (Log } DCPI_{field})$$

Where, CBR_{lab}= CBR values obtained from the lab experiments

CBR_{field}= CBR values obtained in the field

Webster et al. (1992) suggested the following relationship based on tests performed on various types of soil.

$$\text{Log (CBR)} = 2.46 - 1.15 \text{ (Log DCPI)}$$

Based on the coupled contribution of the subgrade and the aggregate base course material, Gabr et al. (2000) conducted a regression analysis to develop a relationship between CBR and DCP and afterwards, the model was validated using data set from four test sites.

$$\text{Log (CBR)} = 1.55 - 0.55 \text{ (Log DCPI)} \ (R^2=0.82)$$

Lee et al. (2014) suggested a correlation between these two parameters based on laboratory experiments on weathered sandy soil (SP, SM and SW-SM) in Korea with high R^2 value.

$$\text{Log (CBR)} = 3.93 - 1.47 \text{ (Log DCPI)} \ (R^2=0.93)$$

Abu-Farsakh et al. (2004) developed a relationship between the CBR value and DCPI which is given below:

$$\text{CBR} = \frac{5.1}{DCPI^{0.2}-1.41} \ (R^2=0.93)$$

Many correlations have been developed by the researchers and organizations around the world. Based on the results obtained from different sources, the equation developed by

U.S. Army Corps of Engineers was selected as the best correlation among all the equations and has been adopted.

2.2.7 Existing Correlation between DCP and Different Moduli

Structural analysis of Pavement requires moduli values and it can be derived based on the relation between moduli values and CBR. The following equation has been proposed by Huekelom and Klomp and adopted by the 1993 AASHTO Guide for Design of Pavement Structures to calculate subgrade resilient modulus (M_R) which was derived for the fine-grained soils with a soaked CBR or 10 or less. The resilient moduli value calculated on which the correlation was developed was 750 to 3000 times higher than the CBR values.

$$M_R = 1500\ CBR\ (M_R \text{ in psi})$$

$$\text{Or, } M_R = 10.34\ CBR\ (M_R \text{ in MPa})$$

According to Chen et al., the CBR value should be computed using the equation adopted by U.S. Army Corps of Engineers and the following equation should be used to predict the resilient moduli value from the measurements taken with DCP tests. Powell et al., of the Transport and Research Laboratory (TRRL) in the United Kingdom suggested the relationship between subgrade resilient modulus and CBR which is presented below:

$$M_R = 2550\ CBR^{0.64}\ (M_R \text{ in psi})$$

$$\text{Or, } M_R = 17.58\ CBR^{0.64}\ (M_R \text{ in MPa})$$

U.S. Army Corps of Engineers Research and Development Center Waterways Experiment Station (COE) developed the following equation:

$$M_R = 5409\ CBR^{0.711}\ (E \text{ in psi})$$

$$\text{Or, } M_R = 37.3\ CBR^{0.711}\ (E \text{ in MPa})$$

Danish Road Laboratory proposed the equation presented below:

$$M_R = 1500\ CBR^{0.73}\ (E \text{ in psi})$$

$$\text{Or, } M_R = 10\ CBR^{0.73}\ (E \text{ in MPa})$$

The moduli values computed from the above mentioned formulae vary significantly which is presented below in the chart.

A study was conducted by George et al. using the laboratory resilient modulus to develop a model from DCP parameters. Two different models were suggested by them which are given below:

1. Fine-grained Soils:

$$M_R = a_0 (DCPI)^{a1} (\gamma_{dr}^{a2} + (LL/w_c)^{a3})$$

Where , M_R = Resilient Modulus (MPa)

DCPI = Dynamic Cone Penetration Index (mm/blow)

w_c = Actual moisture content (%)

γ_{dr} = Density Ratio, Filed Density/Maximum Dry Density

LL = Liquid Limit (%)

a_0, a_1, a_2, a_3 = Regression Coefficients

2. Coarse-grained Soils:

$$M_R = a_0 (DCPI/Log\ c_u)^{a1} (w_{cr}^{a2} + \gamma_{dr}^{a3})$$

Where, M_R = Resilient Modulus (MPa)

DCPI = Dynamic Cone Penetration Index (mm/blow)

c_u = Coefficient of uniformity

w_{cr} = Moisture Ration, Field Moisture/Optimum Moisture Content

γ_{dr} = Density Ratio, Filed Density/Maximum Dry Density

a_0, a_1, a_2, a_3 = Regression Coefficients

A regression model was developed by Hassan for fine-grained soils at optimum moisture content.

$$M_R = 7013.065 – 2040.783 \ln (DCPI)$$

Where, M_R= Resilient Modulus in psi

DCPI = Dynamic Cone Penetration Index in inches/blow

According to Pen, the following two relationships between subgrade elastic modulus (Es) and DCPI can be defined as:

$$\text{Log (Es)} = 3.25 – 0.89 \text{ Log (DCPI)}$$

$$\text{Log (Es)} = 3.652 – 1.17 \text{ Log (DCPI)}$$

Where, Es = Subgrade Elastic Modulus (MPa)

DCPI = Dynamic Cone Penetration Index (mm/blow)

Chua related cone apex angle to a model to interpret the results of DCP to determine the elastic modulus using DCPI where the value of elastic modulus depends on the principal stress differences at failure ($2\tau_0$).

$$\text{Log (Es)} = B – 0.4 \text{ Log (DCPI)}$$

Where, Es = Elastic Modulus (MPa)

B = constant whose value depends on $2\tau_0$. Different conditions of $2\tau_0$ and B for various types of soil are given in the table below:

Table 2.1: Values of B and 2τ0 for Different Types of Soil

Soil Type	**$2\tau_0$**	**B**
Plastic Clay	25	2.22
Clayey Soil	50	2.44
Silty Soil	75	2.53
Sandy Soil	150	2.63

A regression analysis was conducted by Chen et al. between the FWD back-calculated resilient modulus and DCPI and the following relationship was proposed:

$$M_{FWD} = 338\ (DCPI)^{-0.39}\ \text{(for 10 mm/blow < DCPI < 60 mm/blow)}$$

Where, M_{FWD} = FWD back-calculated resilient modulus (MPa)

Pandey et al. developed a correlation between DCPI and backcalculated modulus from falling weight deflectometer, M_{FWD}, which is given below:

$$M_{FWD} = 357.87\ (DCPI)^{-0.6445}$$

FWD deflection data and DCPI were used byJianzhou et al. to predict the backcalculated subgrade modulus from measurements taken with DCP.

$$E_{FWD} = 338\ (DCPI)^{-0.39}$$

Where, E_{FWD} = Backcalculated Elastic Modulus (MPa)

And DCPI is in mm/blow

The correlation developed by Abu-Farsakh et al. (2004)between the DCPI and the back-calculated modulus obtained from FWD is given below:

$$\ln (M_{FWD}) = 2.35 + \frac{5.21}{\ln(DCPI)}\ (R^2=0.91)$$

De Beer suggested a relationship between elastic modulus of soil (Es) and DCPI:

$$\text{Log (Es)} = 3.05 - 1.07\ \text{Log (DCPI)}$$

Chai et al. suggested the following model based on the DCP test and CBR-DCPI relationships which was developed in Malaysia during 1987 to calculate the subgrade elastic modulus.

$$E = 17.6\ (269/DCPI)^{0.64}$$

Where, E = Subgrade elastic modulus in MN/m^2

DCPI = Dynamic Cone Penetration Index in blows/300 mm penetration

Chai et al. proposed a relationship correlating the backcalculated elastic modulus to DCPI which is given below:

$$E = 2224\ (DCPI)^{-0.996}$$

Where, E = Backcalculated Subgrade Elastic Modulus (MN/m^2)

Based on the DCPI of a large DCP with a 51 mm diameter cone and the elastic modulus of unbound aggregates and natural granular soils back-calculated from plate load tests (E_{PLT}) (in MPa), Konard and Lachance also suggested a relationship which is as follows:

$$\text{Log}\ (E_{PLT}) = -0.88405\ \text{Log}\ (DCPI) + 2.90625$$

Abu-Farsakh et al. (2004) conducted a detailed experimental program to assess the accuracy of in-situ test methods which include DCP, Static Plate Load test, Falling Weight Deflectometer test and CBR test data which were collected in the field. The correlations between the DCPI and both the initial modulus and the reloading stiffness of SPLT are given below:

Relation with Initial Modulus obtained from Plate Load Test in field:

$$E_i = \frac{17421.2}{PR^{2.05}+62.53} - 5.71\ (E_i \text{ in MPa})$$

$$\text{Or, } E_i = \frac{2526.7}{PR^{2.05}+62.53} - 0.828\ (E_i \text{ in ksi})\ (R^2=0.94)$$

Relation with Reloading Modulus obtained from Plate Load Test in field:

$$E_R = \frac{5142.61}{DCPI^{1.57}-14.8} - 3.49\ (E_R \text{ in MPa})$$

$$\text{Or, } E_R = \frac{745.87.}{DCPI^{1.57}-14.8} - 0.506\ (E_R \text{ in MPa})\ (R^2=0.95)$$

Based on the laboratory experiments conducted by Mohammadi et al. (2008), two different relationships between DCPI and Initial modulus ($E_{PLT(i)}$) and Reloading stiffness modulus ($E_{PLT(R^2)}$) were developed which are given below:

(i) $$E_{PLT(i)} = \frac{55.033}{DCPI^{0.54}}\ (R^2=0.83)\ (E \text{ in MPa})$$

$$E_{PLT(R^2)} = \frac{53.73}{DCPI^{0.74}} \ (R^2=0.94) \ (E \text{ in MPa})$$

(ii) $$E_{PLT(R^2)} = 0.16 \ (E_{PLT(i)})^{1.49} \ (R^2=0.94) \ (E \text{ in MPa})$$

Chen et al. (2005) developed a correlation using the DCP test results to determine the Young's modulus:

$$E = 78.05 \ (DCPI)^{-0.6645} \ (E \text{ in ksi})$$

$$\text{Or, } E = 537.76 \ (DCPI)^{-0.6645} \ (E \text{ in MPa})$$

R^2 value was found to be 0.855.

2.2.8 Existing Correlation Between DCP And Shear Strength Of Soil

Ayers et al. (1989) developed equations based on the laboratory tests performed on different base material for various confining pressures to evaluate the efficiency of the DCP for determining the shear strength of granular material. Laboratory DCP and triaxial tests were performed on sand, dense-graded sandy gravel, crushed dolomite ballast, and ballast with varying amounts of non-plastic crushed dolomitic fines to obtain the DCPI and shear strength to develop correlations which take form as:

$$DS = A - B \ (DCPI)$$

Where, DS = Shear Strength of soil

DCPI = Dynamic Cone Penetration Index

A, B = Regression Coefficients

The material properties and the correlations between DCPI and shear strength of the above mentioned materials and confining stress level are given in the Table 2.2 and Table 2.3.

Table 2.2: Properties of Test Materials (Ayers et al., 1989)

Material	G_S	C_u[i]	C_c[ii]	Maximum grain size (mm)	D_{10} (mm)	D_{30} (mm)	D_{60} (mm)
Sand	2.65	5.1	0.87	4.83	0.229	0.483	1.168
Sandy Gravel	2.55	80.0	1.01	25.4	0.102	0.914	8.128
Crushed Dolomitic ballast	2.63	1.70	0.99	38.1	18.03	23.11	29.97
Ballast with 7.5% NF[iii]	2.63	3.0	1.67	38.1	9.906	22.09	29.46
Ballast with 15% NF[iii]	2.63	9.2	5.22	38.1	3.048	21.08	27.94
Ballast with 22.5% NF[iii]	2.62	15.1	8.41	38.1	1.778	20.07	26.92

[i] C_u: Coefficient of uniformity

[ii] C_c: Coefficient of curvature

[iii] NF: Non-plastic fines

Table 2.3: Correlation between DCPI and Shear Strength (Ayers et al. 1989)

Material	Confining Stress (kPa)	Correlation
Sand	34.5	DS = 41.3 – 12.8 (DCPI)
	103.4	DS = 100.4 – 23.4 (DCPI)
	206.9	DS = 149.6 – 12.7 (DCPI)
Sandy Gravel	34.5	DS = 51.3 – 13.6 (DCPI)
	103.4	DS = 62.9 – 3.6 (DCPI)
	206.9	DS = 90.7 -5.8 (DCPI)
Crushed Dolomitic Ballast	34.5	DS = 64.1 – 13.3 (DCPI)
	103.4	DS = 139.0 – 40.6 (DCPI)
	206.9	DS = 166.3 – 16.2 (DCPI)
Ballast with 7.5% NF	34.5	DS = 87.2 – 78.7 (DCPI)
	103.4	DS = 216.1 – 213.9 (DCPI)
	206.9	DS = 282.1 – 233.2 (DCPI)
Ballast with 15% NF	34.5	DS = 47.5 – 0.45 (DCPI)
	103.4	DS = 184.2 – 215.5 (DCPI)
	206.9	DS = 206.4 – 135.7 (DCPI)
Ballast with 22.5% NF	34.5	DS = 49.7 – 23.1 (DCPI)
	103.4	DS = 133.1 – 68.6 (DCPI)
	206.9	DS = 192.1 - 95.7 (DCPI)

2.2.9 Correlation between DCPI and Unconfined Compressive Strength

McElvaney and Djatnika (1991) developed three equations to predict unconfined compressive strength (UCS) values from DCPI for 50%, 95% and 99% confidence level, respectively which are given below based on the laboratory results on soil-lime mixture. Individual and combined soil types were considered in the analysis. According to them, zero lime content has negligible effects on the correlations which suggest that the correlation is predominantly a function of strength and only valid for lower range of strain values.

Log UCS = 3.56 – 0.807 (Log DCPI) (50% probability of underestimation)

Log UCS = 3.29 – 0.809 (Log DCPI) (95% probability of underestimation)

Log UCS = 3.21 – 0.809 (Log DCPI) (99% probability of underestimation)

In-situ condition has been simulated in laboratory by Patel and Patel (2012) using soils from various locations of Gujarat, India which include CH, CI, CL, SC and SM-SC soil to correlate DCPI with the UCS values. The equation obtained is presented below:

$$UCS = 4.349\ (DCPI)^{-1.09}\ (R^2=0.968)$$

A multi variable relationship has been developed by Patel and Patel (2012) to predict the value of UCS from DCPI value:

$$UCS = 6.904701568 \cdot 10\text{-}1\ MDD - 1.146947823 \cdot 10\text{-}2\ OMC - 1.704888589 \cdot 10\text{-}2\ MLL + 0.299916777\ DCPI - 12.61710035$$

Where, MDD = Maximum Dry Density

OMC = Optimum Moisture Content

MLL = Modified Liquid Limit

The plot from this equation is given below in Figure 2.11:

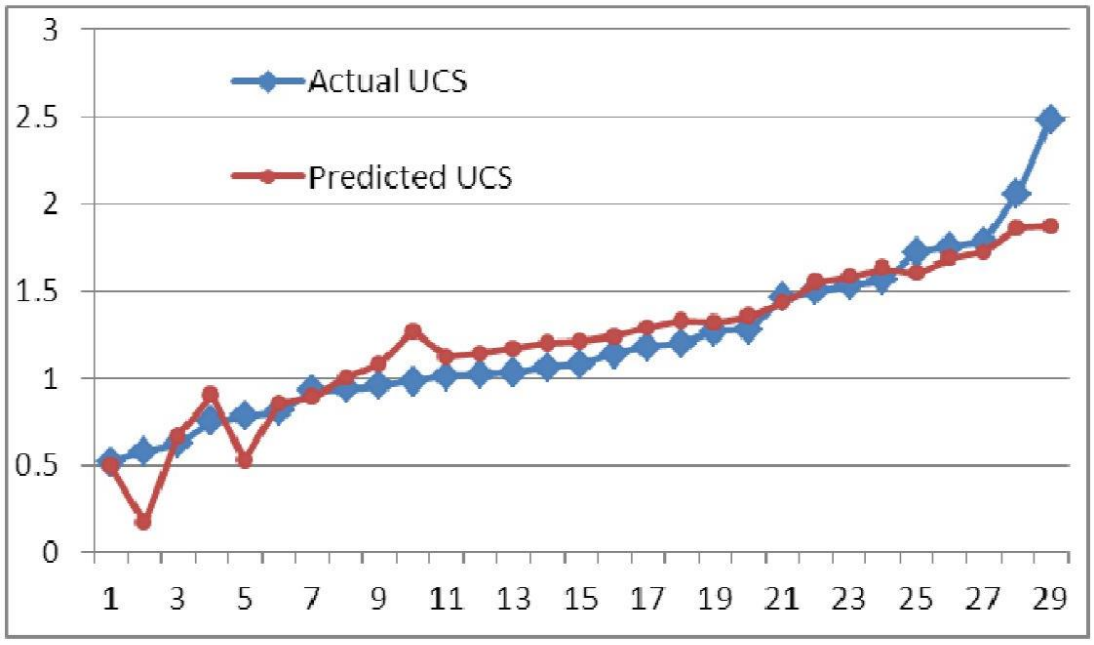

Figure 2.11: Comparison of Predicted UCS and Actual UCS

2.2.10 Soil Classification Based On DCPI

Huntley (1990) proposed a preliminary soil classification system from DCPI values based on a series of case histories in Herfordshire, U.K. which is shown in Table 2.4 and Table 2.5. He recommended that a understanding of the mechanics of skin friction on the upper shaft is needed to use this table. Here, n is the blows needed for the cone to penetrate 100 mm.

Table 2.4: Classification of Granular Soils from DCPI (Huntley, 1990)

Classificaiton	n Value Range		
		Sand	**Gravelly Sand**
Very Loose	<1	<1	<3
Loose	1-2	2-3	3-7
Medium Dense	3-7	4-10	8-20
Dense	8-11	11-17	21-33
Very Dense	>11	>17	>33

Table 2.5: Classification of Cohesive Soils from DCPI (Huntley, 1990)

Classification	n Value Range
Very Soft	<1
Soft	1-2
Firm	3-4
Stiff	5-8
Very Stiff to Hard	>8

Many agencies (i.e., state DOTs and U.S. Army Corps of Engineers) have implemented DCPI values for compaction QC (Amini 2003). Below is the Table 2.6 which shows the N_{DCP}criteria corresponding to a depth of penetration fromo to 6 inch (0 to 150 mm) according to various DOT agencies where N_{DCP} values were converted from DCPI values.

Table 2.6: DCP criteria (NDCP) for a penetration of 0 to 6 inch (0 to 150 mm)

Materials		ILDOT	Iowa DOT	MnDot	NCDOT
Frictional Soil		6.1[i]	3.4~4.4[ii]	12.5[iii]	4.0[iv]
Cohesive Soil	Silt		3.8~4.4[ii]	6.0[iii]	
	Clay				

[i]DCP blow counts associated with a CBR of 8

[ii] Iowa DOT classified the soil either “suitable soil” or “unsuitable soil” in each group of soil. The values show the ranges of it (Larsen et al., 2007)

[iii] The criteria of frictional soil apply for “granular” base layer, MnDOT recorded N_{DCP} values only for blow counts that higher than two (Burnham, 1997)

[iv] DCP blow counts associated with a CBR of 8 (Gabr et al., 2000)

MnDOT is one of the first states which have been using DCP from 1991 as a tool to evaluate the strength and uniformity of highway structures. MnDOT defined limiting DCPI values for each particular subgrade soil and base type after performing more than 700 DCP tests on Minnesota Road Research project which is presented in Table 2.7. This table was developed based on the assumption of the presence of adequate confinement near the testing surface and certainly do not cover all types of materials. It has been suggested by MnDOT that there is scope to extend the table for other types of base materials.

Table 2.7: Limiting DCPI by MnDOT

Material	**Limiting DCPI (mm/blow)**
Silty/Clay Subgrade	<25
Select Granular Subgrade	<7
Class 3 Special Gradation Granular Base Materials	<5

2.3 Soil Stiffness Gauge (Geogauge)

2.3.1 Introduction

Soil Stiffness Gauge measures the in-place stiffness of compacted soil. It is a QC/QA field tool that measures the uniformity of unbound pavement layers by measuring the variability in stiffness throughout a structure. Irregularities during the construction process can easily be detected with the Geogauge. [1]

The technology on which Geogauge operates was first developed by the defense industry for detecting land mines. The collaboration between Bolts, Beranek, and Newman of Cambridge, MA, CAN consulting Engineers of Minneapolis, MN, and Humboldt came up with the product Humboldt Stiffness Gauge which is currently known as Geogauge presented in Figure 2.12.

Figure 2.12: Geogauge

Geogauge weighs about 22 lbs (10 kilograms) without its case and about 34 lbs (15.5 kilograms) with its case, it has a diameter of 11 inch (280 mm) and a height of 10 inch (254 mm). The carrying case has a dimension of 18.5 inch (470 mm) x 16.5 inch (419 mm) x 13 inch (330 mm). Six D-cell batteries powers the operation of the Geogauge which cover almost 1000 to 1500 measurements. An annular ring connects the soil with the Geogauge

and it has an outside diameter of 4.50 inch (114 mm), an inside diameter of 3.50 inch (89 mm) and a thickness of 0.5 inch (13 mm).

2.3.2 Principle of Operation

The principle of Geogauge is to measure the impedance at the surface of the soil by measuring the stress imparted to the surface and the resulting surface velocity as a function of time. It is an effective portable device that can measure the in-situ stiffness of compacted layers rapidly by imparting small dynamic force to the soil through a ring-shaped foot at 25 steady state frequencies between 100 and 196 Hz. The displacement it imparts to the soil layer is less than 0.00005 inch (1.27×10^{-6} m). According to a laboratory study conducted by Sawangsuriya et al. (2001), the force generated by the Geogauge is 9 N. The stiffness is determined at each frequency and the average of the 25 measurements is displayed on the screen. The Stiffness is calculated using the following equation:

$$K = \frac{P}{\delta}$$

Where, K = Stiffness measured with the Geogauge (MN/m)

P= Applied Force

δ= Deflection imparted by the Geogauge

The shaker of the Geogauge applies a force and this force is transferred to the ground which is measured by differential displacement across the flexible plate by two velocity sensors which is presented in Figure 2.13.

The expression is as follows:

$$F_{dr} = K_{flex}*(X_2 - X_1) = K_{flex}*(V_2 - V_1)$$

Where, F_{dr}= Force applied by Shaker

K_{flex}= Stiffness of the Flexible Plate

X_1 = Displacement at Rigid Plate

X_2 = Displacement at Flexible Plate

V_1= Velocity at Rigid Plate

V_2= Velocity at Flexible Plate

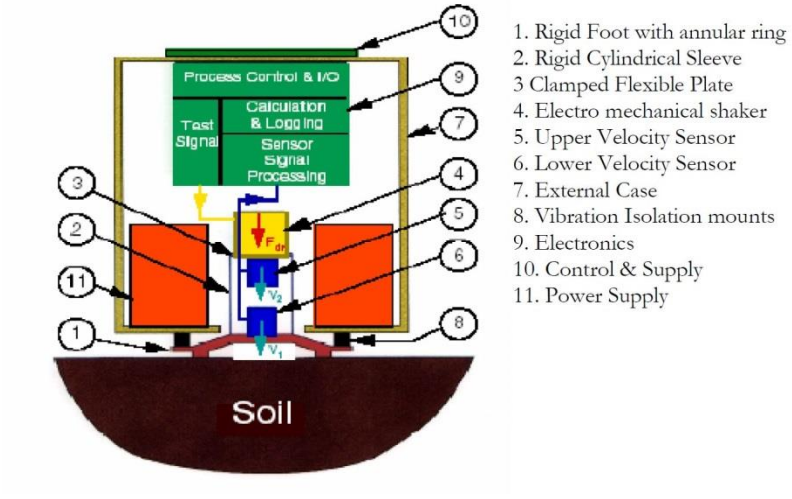

Figure 2.13: Schematic of Geogauge (Humboldt, 1998)

Previously conducted studies based on both finite element analyses and experimental studies indicated that the Geogauge has an influence radius which covers a range from 9 inch to 12 inch (220 mm to 310 mm).

2.3.3 Geogauge Stiffness And Moduli Calculation

The static stiffness, K, of a rigid annular ring on a linear elastic, homogeneous and isotropic half space has the following functional form (Egorov, 1965):

$$K = \frac{E*R}{(1-v^2)*\omega(n)}$$

Where, E= Modulus of Elasticity

v = Poisson's Ratio

R = Outside Radius of the Annular ring (2.25 inch)

ω(n) = a function of the ratio of the inside diameter and the outside diameter of the annular ring.

where, n= $\frac{r(in)}{r(out)}$ = Radius Ratio of the ring

For the ring geometry of the Geogauge, the parameter ω(n) is equal to 0.565. So,

$$K = \frac{1.77*R*E}{(1-v\text{^}2\ )}$$

Where, K = Stiffness measured with the Geogauge (MN/m)

E= Modulus of Elasticity

v = Poisson's Ratio

R = Outside Radius of the Annular ring (2.25 inch)

According to Lenke et al. (2003), the equations which were used as a principle of operation of the Geogauge is based on the assumption of infinite elastic half space. This assumption is violated in the pavement application because pavement sections consist of several finite thick layers which are made up of material with different strength properties.

The process of measurement takes about 75 seconds as a whole which plays a vital role to portray the vital role during QC/QA process. The stiffness, K can then be converted into elastic modulus, E, of soil using the equation proposed by CNA Consulting Engineers:

$$E= \frac{K*(1-v\text{^}2\ )}{1.77*R}$$

Where, E= Elastic Stiffness Modulus (MPa)

K= Stiffness measured with Geogauge (MN/m)

v= Poisson's ratio (assumed)

R= Radius of the Geogauge (2.25 inch)

Using the assumed Poisson's ratio, v, the shear modulus, G, can also be calculated using the following equation:

$$G= \frac{P*(1-v)}{3.54*R*\delta}$$

Where, P= Applied Load

R= Outer Radius of Annular Ring

δ= Induced Surface Deflection

v= Poisson's ratio (assumed)

Poisson's ratio has to be assumed to measure stiffness with the Geogauge. For a Poisson's ratio of 0.35, a factor of approximately 8.67 can convert the Geogauge Stiffness (MN/m) to a Stiffness Modulus (MPa). The Geogauge manufacturer (Humboldt) recommends that Geogauge should be used up to 70 MN/m while measuring layer stiffness and up to 610 MPa while measuring in-situ moduli value. According to a study conducted by Chen et al., (2000), it is recommended that Geogauge should be used only up to 23 MN/m and the reason behind this is that the Geogauge may lose accuracy when measuring stiffness greater than 23 MN/m.

Poisson's Ratio for different materials are shown in Table 2.8.

Table 2.8: Typical Poisson's Ratio value for Different Types of Materials

Material	Range	Typical Value
Portland Cement Concrete	0.15-0.2	0.15
Untreated Granular Materials	0.3-0.4	0.35
Cement treated Granular Materials	0.1-0.2	0.15
Cement treated fine-grained soils	0.15-0.35	0.25
Lime Stabilized Materials	0.1-0.25	0.2
Lime-Flyash Mixtures	0.1-0.15	0.15
Dense Sand	0.2-0.4	0.35
Fine grained Soil	0.3-0.45	0.4
Saturated Soft Soil	0.4-0.5	0.45

2.3.4 Geogauge Application

Portability, simplicity and less time of operation give Geogauge its main advantage over other in-situ testing devices. It can measure the in-situ stiffness of compacted soil at a rate of about one test per 1.25 minute and thus enabling it as a great tool for in-situ testing. Maintaining uniformity in paving application is of great importance and the mean stiffness of each layer plays a vital role on how the pavement fatigues, the lifetime of the pavement and the maintenance procedures. Geogauge paves the way to quick data collection and of large volume.

Non-uniform compaction during earthworks can cause premature failure and non-uniform structural stiffness is one of the indicators of these effects. Geogauge can easily detect the non-uniformities of earthworks while revealing voids and discontinuities in the material.

Non-destructive way of testing gives Geogauge the edge over other in-situ testing devices. Some cases require repeated measurements at the same location over time to satisfy the design and due to its non-destructive mode of operation, Geogauge can take numerous measurements at a single location. Geogauge can also be used to ensure satisfactory performance of pavement and if not, proper maintenance measures can be taken.

Measurement of density is one of main parameters in inspection of materials and structures. Geogauge can replace the conventional time-consuming devices. It provides a specific value within a short period of time.

2.3.5 Factors Affecting Geogauge Measurement

According to various studies, it has been observed that the density, moisture content, boundary conditions and stiffness of underlying layers all affect the Geogauge measurements.

2.3.6 Correlation Between Geogauge And Resilient Modulus

No attempt has been taken to correlate the Geogauge modulus to resilient modulus measured in laboratory. But a comparison study between resilient modulus measured in laboratory and Geogauge modulus measured in the field has been conducted [3][4].

According to Chen et al., the base moduli measured with the FWD are higher than those measured with the Geogauge [5]. Chen et al. suggested that a general relationship exists between the Geogauge stiffness and the FWD back-calculated modulus, M_{FWD}:

$$M_{FWD} = 37.65\ H_{SG} - 261.96$$

Where, M_{FWD} = Moduli measured with FWD (MPa)

H_{SG} = Stiffness measured with Geogauge (MN/m)

According to them, the quality of the base layers can be classified by FWD or Geogauge measurements which are provided in Table 2.9 below:

Table 2.9: Geogauge and FWD suggested values to characterize base layer

Base Quality	E(MPa) (Geogauge)	K (MN/m) (Geogauge)	M_{FWD} (MPa)
Weak	<87	<10	<140
Good	156-209	18-24	310-450
Excellent	>261	>30	>700

CNA Consulting Engineers conducted a number of field test to compare the modulus measured with the Quasi-Static Plate Load Test (QSPLT) with the Stiffness Modulus measured with the Geogauge. The results indicate that reloading elastic modulus obtained from QSPLT are similar to the Stiffness Modulus obtained from Geogauge. However, stiffness modulus measured with Geogauge is nearly 7 times higher than the initial loading modulus. From the results, it can be observed that the Geogauge stiffness modulus correlates better with initial modulus than with the reloading and unloading modulus obtained from QSPLT (Petersen et al., 2002)

$$E_{(QPLT)R} = 0.8962\ (E_G) + 25.9\ (R^2 = 0.23)$$

$$E_{(QPLT)u} = 0.6158(E_G) + 10.3\ (R^2 = 0.27)$$

$$E_{(QPLT)i} = 0.3388(E_G) + 84.7\ (R^2 = 0.66)$$

Where, $E_{(QPLT)R}$ = Reloading Modulus obtained from QSPLT

$E_{(QPLT)u}$ = Unloading Modulus obtained from QSPLT

$E_{(QPLT)I}$ = Initial Modulus obtained from QSPLT

E_G = Stiffness Modulus obtained from Geogauge

Wu et al. [6] proposed the following equation correlating the back calculated resilient modulus from FWD to Geogauge Stiffness.

$$M_R = 22.69\ e^{0.12*K_{SSG}}$$

Where, M_R = Resilient Modulus obtained from FWD (MPa)

K_{SSG} = Stiffness obtained from Geogauge (MN/m)

According to a study conducted by Gudishala, a correlation between Resilient Modulus and Stiffness Modulus obtained from Geogauge was developed for cohesive soil which is as follows:

$$M_R = 86.7 * \frac{\{E(Geo)\}\text{^}0.3}{w} + 2.2\gamma_d \ (R^2=0.67)$$

Where, M_R = Resilient Modulus (MPa)

$E_{(Geo)}$ = Modulus obtained from Geogauge (MPa)

w = measured Water Content (%)

γ_d= measured Dry Density (KN/m^3)

Another model was developed to predict resilient modulus from the moduli values obtained from Geogauge which was applicable for granular soils and it is as follows:

$$M_R = 20.3 * (E_{Geo})^{0.54} (R^2=0.83)$$

Where, M_R = Resilient Modulus (MPa)

$E_{(Geo)}$ = Modulus obtained from Geogauge (MPa)

He concluded that the resilient modulus of both cohesive and granular materials is stress dependent and is affected by physical properties of the material. However, according to him, models to predict the resilient modulus of granular materials are independent of soil properties.

Farsakh et al. (2004) conducted a study where potential of three in-situ testing devices (DCP, Geogauge, LFWD) was evaluated. A model was developed between the Geogauge data obtained both from laboratory and field with the Plate Load Test data and it has been

recommended to adopt the correlation which has been developed using field data to provide a better correlation.

$$E_{PLT(i)} = -75.58 + 1.62*E_G \ (R^2=0.87)$$

$$E_{PLT(R2)} = -65.37 + 1.50*E_G \ (R^2=0.90)$$

Where, E_G = Stiffness Modulus obtained from Geogauge

$E_{PLT(i)}$ = Initial Modulus obtained from PLT

$E_{PLT(R2)}$ = Reloading Modulus obtained from PLT

Regression analysis was conducted to develop a model relating Geogauge stiffness modulus to FWD back-calculated resilient moduli, M_{FWD}.

$$M_{FWD} = -20.07 + 1.17*E_G \ (R^2=0.81)$$

Where, M_{FWD} = FWD back-calculated Modulus

E_G = Stiffness Modulus obtained from Geogauge

During the same study, the Geogauge data based both on the laboratory experiments and field testing were used to develop a model between Stiffness Modulus obtained from Geogauge, E_G, and CBR value and the correlation based on the field data provided better correlation between these two parameters which is presented below:

$$CBR = 0.00392*(E_G)^2 - 5.75 \ (R^2=0.84)$$

Lee et al. (2014) performed laboratory tests using Soil Stiffness Gauge (SSG), Dynamic Cone Penetrometer (DCP) and Plate Load Test (PLT) and California Bearing Ratio (CBR) Test on three uncemented soil groups (poorly graded sand (SP), silty sand (SM), and well-graded sand with silt (SW-SM) and and conducted regression analysis to develop possible correlation of moduli values obtained from Geogauge with moduli values obtained from PLT and dry unit weight which are presented below:

$$E_{PLT} = 0.59*E_{SSG} \ (R^2=0.65)$$

$$\gamma d = \frac{20.6*\left(\frac{D50}{e}\right)*\text{ESSG}}{\left(\frac{D50}{e}\right)*\text{ESSG}+20.6}$$ (R^2=0.88)

Where, E_{PLT} = Moduli obtained from PLT (MPa)

E_{SSG} = Moduli obtained from Geogauge (MPa)

γd = Dry Unit Weight (KN/m^3)

e = Void Ratio

Chen et al. (1999) conducted field experiments to evaluate the potential of various non-destructive testing devices which include Humboldt Stiffness Gauge (HSG), Dirt Seismic Pavement Analyzer (D-SPA), Falling Weight Deflectometer and Olson Spectral Analysis of surface Waves (SASW) to determine the resilient moduli (M_R) of pavement layers and developed a correlation between Seismic Modulus (E_S) and Stiffness Modulus obtained from Geogauge (E_{HSG}).

$$E_S = 55.421*E_{HSG} - 162.94 \quad (R^2=0.8101)$$

It has been observed by Chen et al. (1999) that shear velocities less than 250 m/s link the base layer to be weak whereas, velocities greater than 400 m/s means that the base layer is in excellent condition.

2.3.7 Recent Use Of Geogauge

Minnesota Department of Transportation (MnDOT) has recently used Geogauge in trunk highway 610 project in Brooklyn Park, Minn. More than 1300 stiffness values have been measured using Geogauge in one of the sites. In the recent days, research organizations and the state transportation departments are using Geogauge to control the compaction process of subgrade and sub-base. Studies have been conducted to correlate the stiffness modulus to the resilient modulus

CHAPTER 3

SITE SELECTION AND TEST METHODOLOGY

3.1 Introduction

Assessing material properties to maintain proper quality control criterial while constructing pavement is of greatest importance to state departments of transportation agencies. In-situ testing techniques play an important role while evaluating material properties during the construction process. Five sites have been selected within Horseshoe Project in Dallas, TX under Texas Department of Transportation (TxDOT) to perform in-situ tests to evaluate the efficiency of Dynamic Cone Penetrometer and Geogauge as in-situ pavement testing equipment. Nuclear Density Gauge Test was performed in two of the locations to verify the data obtained with the Geogauge. The five pavement sites are: (1) Avery St., (2) I-35E Northbouth Frontage Road, (3) South Riverfront Blvd., (4) Jefferson Viaduct Blvd., and (5) Sylvan Ave. The site locations are presented in Table 3.1.

Table 3.1: Site Locations of the Pavement Testing for Horseshoe Project, Dallas, TX

Site	Location	Address
Location-1	Avery St.	229 Avery St, Dallas, TX 75208
Location-2	I-35E Northbound Frontage Road	1100 E Colorado Blvd, Dallas, TX 75203
Location-3	South Riverfront Blvd.	506 S Riverfront Blvd, Dallas, TX 75207
Location-4	Jefferson Viaduct Blvd.	612 S Riverfront Blvd, Dallas, TX 75207
Location-5	Sylvan Ave.	711 Turnpike Ave, Dallas, TX 75208

3.2 Site Location and Layout of The Tests

3.2.1 Location-1 (Avery St.)

The location is situated on Avery St near the Tom Landry Fwy (I-30), Dallas, TX. Nine points at 5' apart from each other were considered to perform the DCP and Geogauge test, respectively, on June 09, 2014. The location of the test and the layout of the points across the roadway are given below in Figure 3.1 and Figure 3.2, respectively. The pavement section consisted of three layers:

(i) Cement stabilized base with prime coat (0"~6")

(ii) Lime treated subgrade (6"~12")

(iii) Compacted subgrade (12"~)

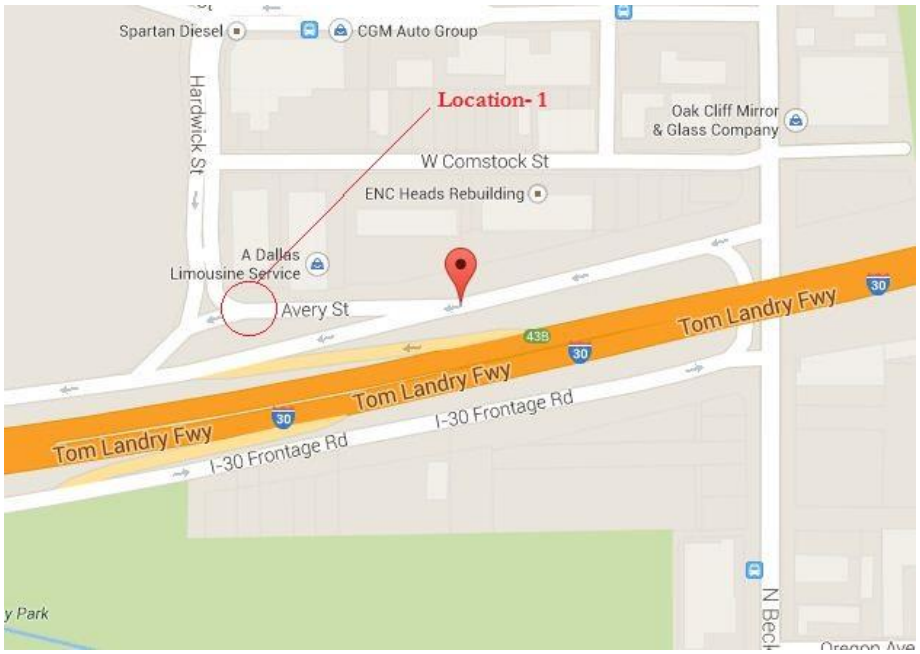

Figure 3.1: Location of the tests performed on June 09, 2014

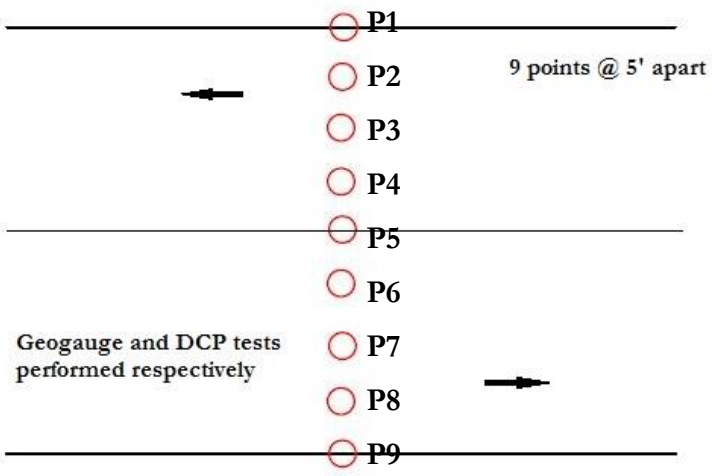

Figure 3.2: Layout of the Tests performed on June 09, 2014

3.2.2 Location-2 (I-35E Northbound Frontage Road)

The location is situated near the I-35E Northbound Frontage Road, Dallas, TX and tests were performed on June 17, 2014. Eight points at 5' apart from each other were considered to perform the Nuclear Density Gauge (NDG) and Geogauge tests respectively. Dynamic Cone Penetration test could not be performed on that day due to the higher strength acquired by the cement stabilized base course layer. The location of the tests performed and the layout of the tests are shown below in Figure 3.3 and Figure 3.4, respectively. The pavement section consisted of three layers:

(i) Cement stabilized base with prime coat (0"~6")

(ii) Lime treated subgrade (6"~12")

(iii) Compacted subgrade (12"~)

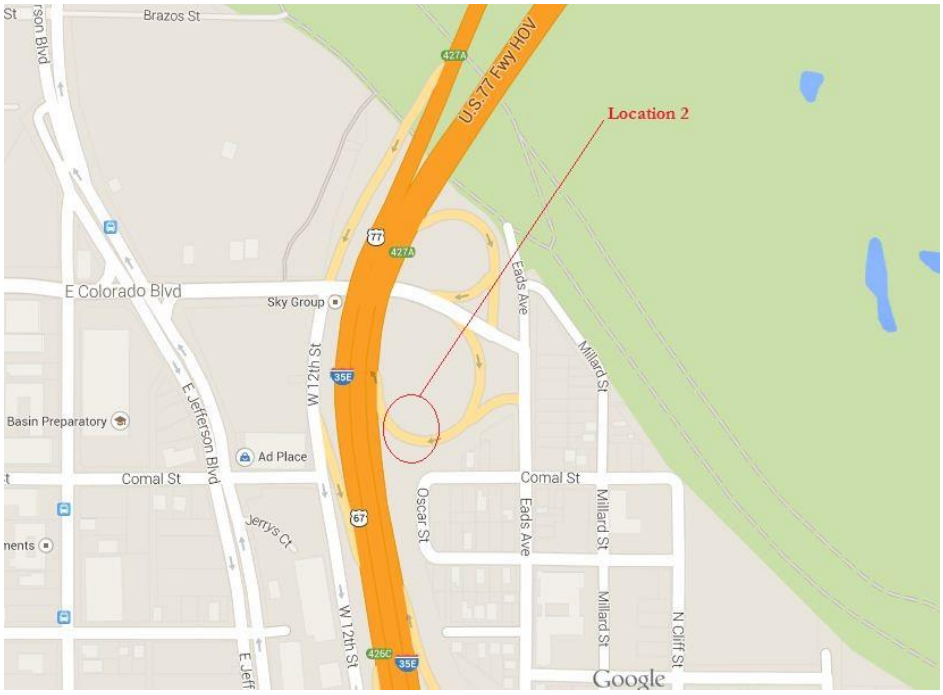

Figure 3.3: Location of the tests performed on June 17, 2014

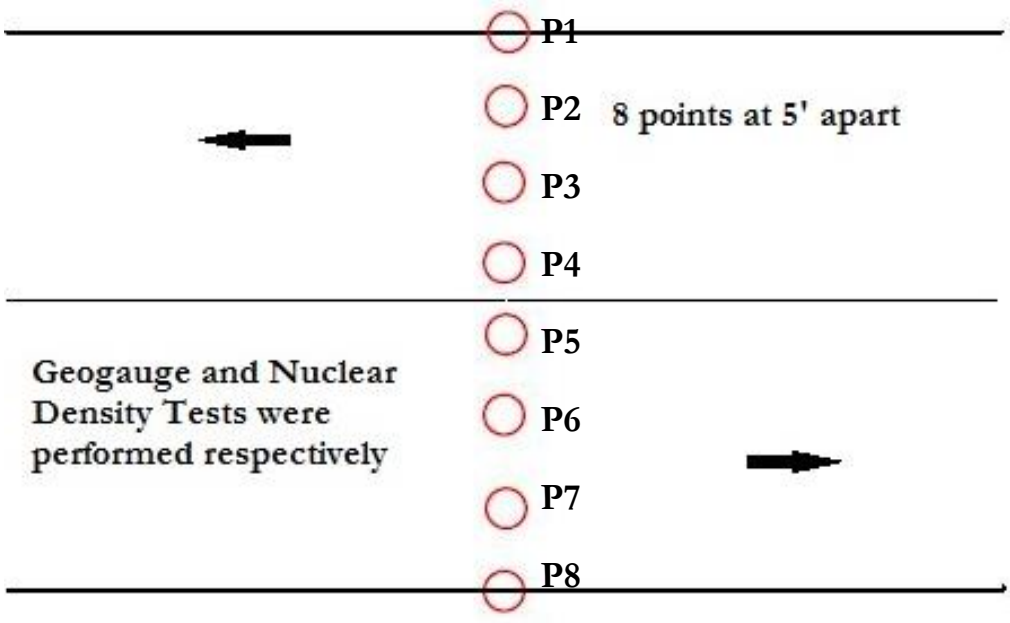

Figure 3.4: Layout of the tests performed

3.2.3 Location-3 (S Riverfront Blvd.)

The test location is located at the intersection of S Riverfront Blvd and S Houston St near the Tom Landry Fwy, Dallas, TX. Ten points at 7' apart were selected across the width of the road to perform the Dynamic Cone Penetration and Geogauge tests respectively after the placement of the cement stabilized base layer on August 2, 2014. The location and layout of the tests are presented in Figure 3.5 and Figure 3.6, respectively. The pavement section consisted of three layers:

(i) Cement stabilized base with prime coat (0"~6")

(ii) Lime treated subgrade (6"~19")

(iii) Compacted subgrade (19"~)

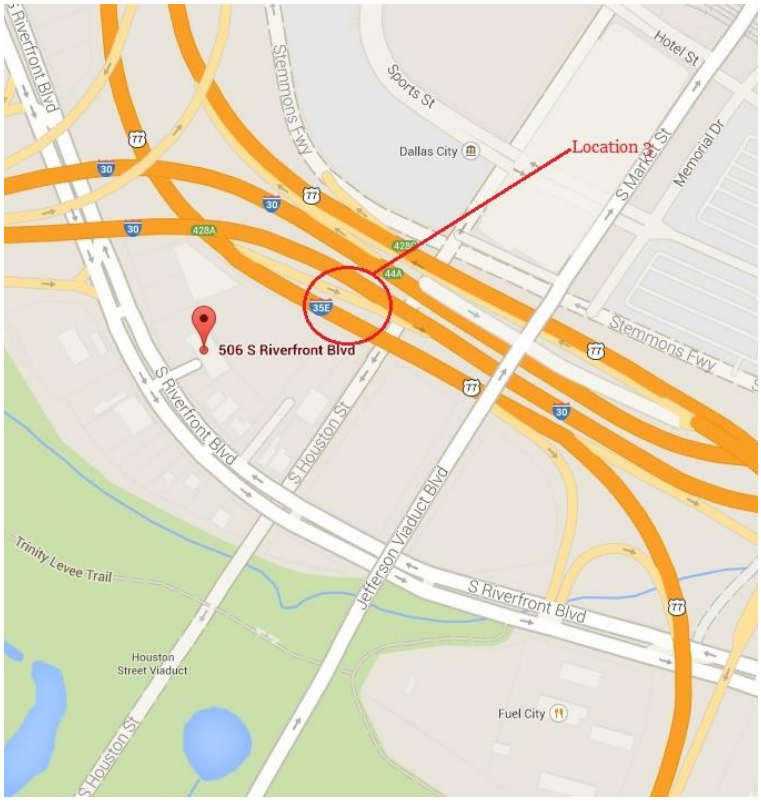

Figure 3.5: Location of the Tests performed on August 2, 2014

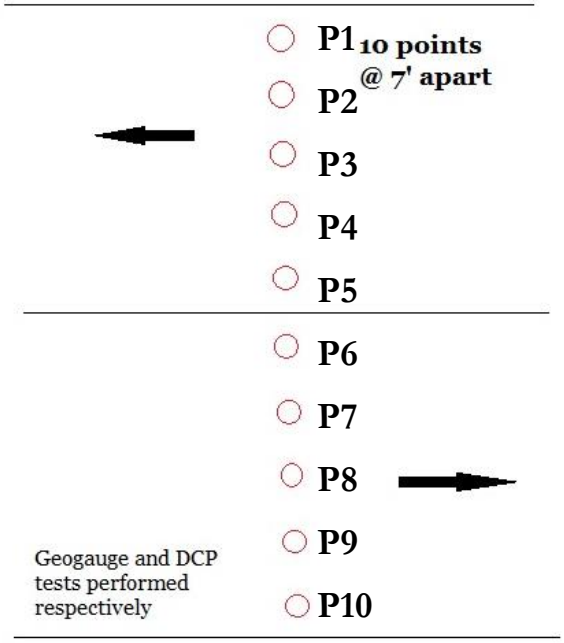

Figure 3.6: Layout of the Tests performed on August 2, 2014

3.2.4 Location-4 (Jefferson Viaduct Blvd.)

The field tests performed on August 27, 2014 took place near the Jefferson Viaduct Blvd., Dallas, TX which included Nuclear Density Gauge test and Geogauge Test. 6 points at 6 ft apart were considered to evaluate the material properties with the use of Nuclear Density Gauge and Geogauge. Dynamic Cone Penetrometer test was not performed when the refusal of the cone while penetration occurs. According to U.S. Army Corps of Engineers, test should be stopped if the cone does not penetrate 25 mm after 10 blows with the 17.6 lb hammer. The location of the tests performed and the layout of the test points are shown below in the Figure 3.7 and Figure 3.8, respectively.

The pavement section consisted of three layers:

(i) Cement stabilized base with prime coat (0”~6”)

(ii) Lime treated subgrade (6”~19”)

(iii) Compacted subgrade (19”~)

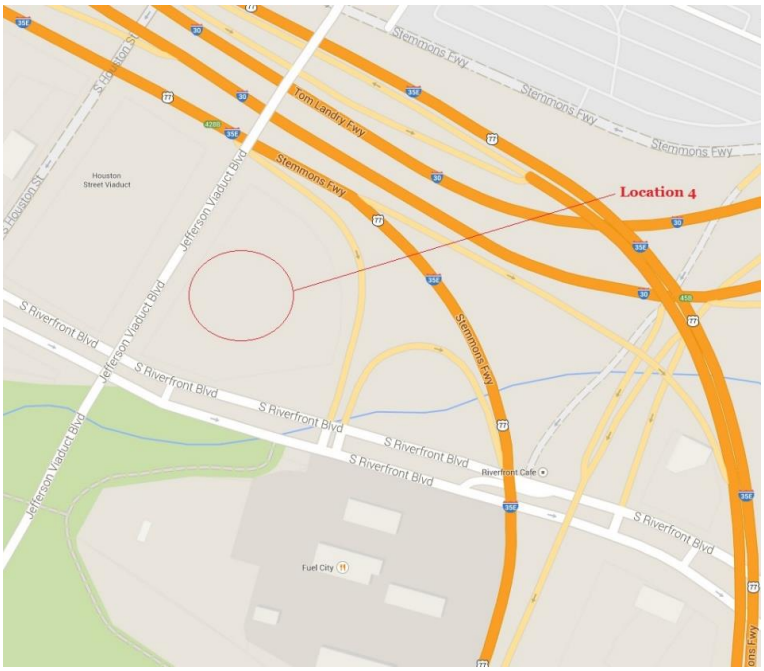

Figure 3.7: Location of the tests performed on August 27, 2014

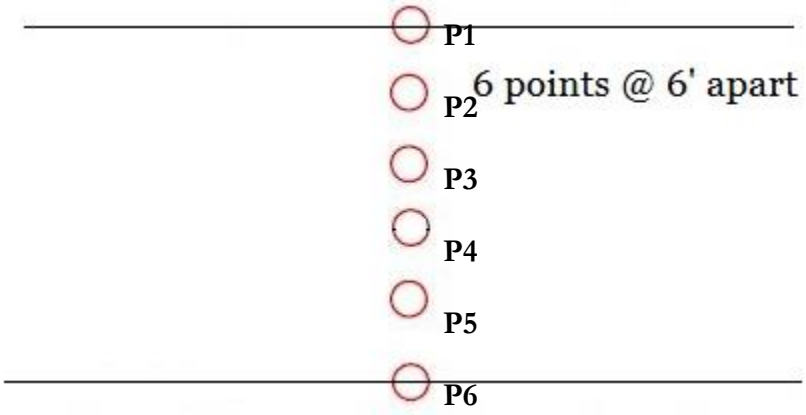

Figure 3.8: Layout of the tests performed on August 27, 2014

3.2.5 Location-5 (Near Sylvan Ave.)

The fifth location where the Dynamic Cone Penetrometer Test and Geogauge Test were performed was situated near the I-30 Westbound Frontage Road near Sylvan Ave., Dallas, TX. The tests were conducted on October 3, 2014 and included DCP and Geogauge tests, respectively. Five points (P1-P5) at 4 ft apart were considered to conduct both tests. The location of the tests performed and the layout of the test points are presented in Figure 3.9 and Figure 3.10, respectively. It is worth mentioning that P5 was located at the edge of the pavement whereas, P1-P4 were located at the middle portion of the roadway which can be seen from Figure 3.10. The pavement section consisted of three layers:

(i) Cement stabilized base with prime coat (0”~6”)

(ii) Lime treated subgrade (6”~12”)

(iii) Compacted subgrade (12”~)

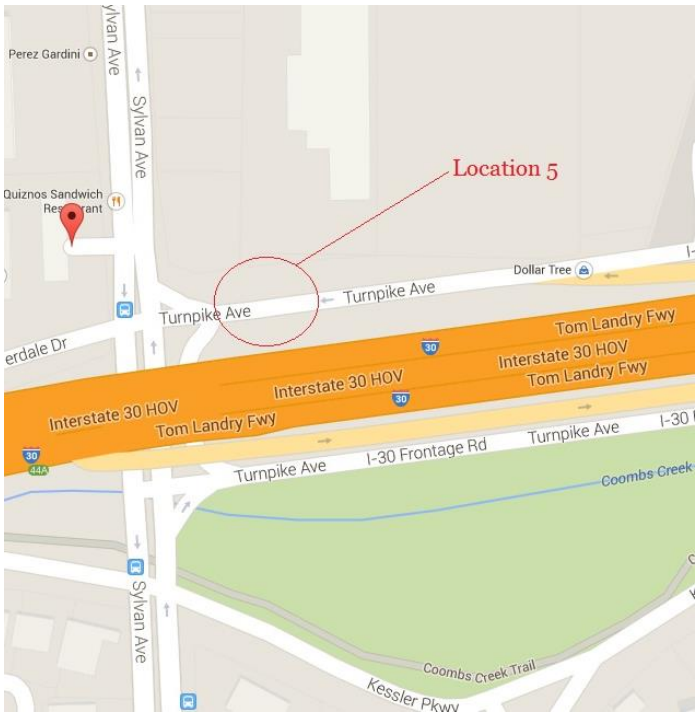

Figure 3.9: Location of the Tests performed on October 3, 2014

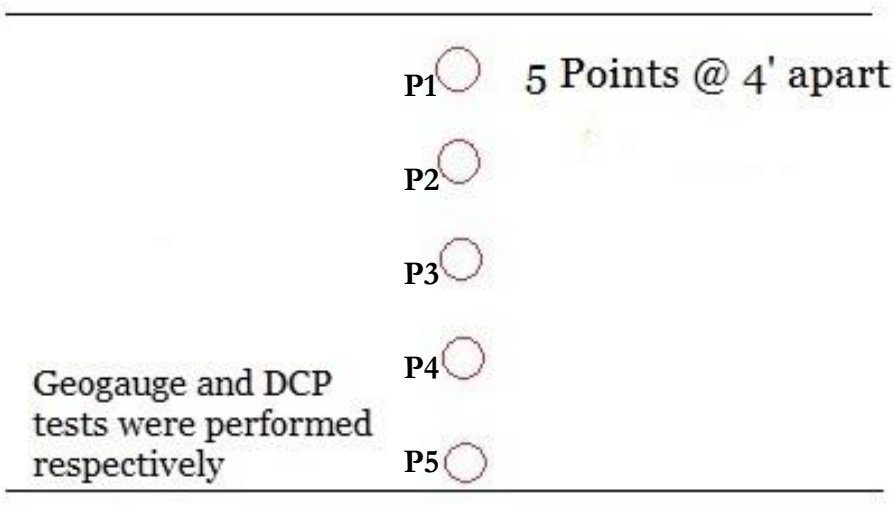

Figure 3.10: Layout of the Tests performed on October 3, 2014

3.2.6 Summary Of The Tests Performed In Each Location

Five locations were considered to perform Dynamic Cone Penetrometer Test and Geogauge test with Horseshoe Project under Texas Department of Transportation (TxDOT). The number of points considered for each test, the number of each test performed are given below in Table 3.2 in details.

Table 3.2: Summary of the Tests performed in each location

Location	Points considered	Distance between tested points (ft)	Dynamic Cone Penetrometer Test	Geogauge Test	Nuclear Density Gauge Test
Location-1	9	5’	✓	✓	x
Location-2	8	5’	x	✓	✓
Location-3	10	7’	✓	✓	x
Location-4	6	6’	x	✓	✓
Location-5	5	4’	✓	✓	x

3.3 Test Methodology and Analysis of Obtained Data

3.3.1 Dynamic Cone Penetration Test

The Dynamic Cone Penetrometer test was performed by raising and dropping the hammer to drive the cone through the pavement layers. Due to the smaller penetration depth in aggregate base course, no of blows for each 1" penetration was measured, recorded and later used to determine the DCP Index. Two persons performed the Dynamic Cone Penetrometer test while one person operated the hammer and the other person was positioned at the pavement surface to read and record the no of blows for each 1" penetration of the cone.

3.3.2 Analysis of Dynamic Cone Penetrometer (DCP) Data

While performing Dynamic Cone Penetrometer (DCP) tests, penetration depth for a set of blows was measured when the penetration depth exceeded 25 mm. According to Webster et al. (1992), a minimum 25 mm depth has to be acquired by the penetrating cone to avoid unnecessary strength determination. Some DCP test photos are presented in Figure 3.11.

Figure 3.11: Dynamic Cone Penetrometer Test Photos

3.3.2.1 DCP Index (DCPI)

DCP Index (DCPI) values were calculated according to a relationship proposed by Embacher, 2005:

$$DCPI = \frac{P(i+1)-P(i)}{B(i+1)-B(i)}$$

Where, DCPI = Dynamic Cone Penetration Index (mm/blow)

P = Penetration at *i*th or (*i*+1)th hammer drops (mm)

B = blow count for *i*th or (*i*+1)th hammer drops

While determining the average DCP Index for a layer considered, a relationship proposed by Edil and Benson (2005) was used which is given below:

$$DCPI_{avg} = \Sigma_i^N (DCPI)/N$$

Where, N = Total number of DCPI recorded for a given depth

3.3.2.2 Determination Of CBR

CBR values were calculated using a relationship proposed by the U.S. Army Corps of Engineers which was developed based on a wide range of granular and cohesive materials and later on, adopted by many researchers:

$$\text{Log CBR} = 2.465 - 1.12 (\text{Log DCPI})$$

$$\text{Or, CBR} = \frac{292}{DCPI\text{^}1.12}$$

Where, DCPI= Dynamic Cone Penetration Index

3.3.2.3 Determination Of Resilient Modulus (M_r)

Resilient Moduli values were calculated according to a relationship suggested by Huekelom and Klomp which has been adopted by the 1993 AASHTO Guide for Design of Pavement Structures. The proposed relationship is given below:

$$M_R = 1500 \text{ CBR } (M_R \text{ in psi})$$

Where, M_R= Resilient Modulus

3.3.2.4 Determination of Unconfined Compressive Strength (Qu)

Values of unconfined compressive strength from DCP measurements were calculated according to relationship proposed by Patel and Patel (2012) which was developed based on CH, CL, SC and SM-SC soil to correlated DCP and UCS value.

$$UCS = 4.349\ (DCPI)^{-1.09}\ (R^2=0.968)$$

3.3.3 Geogauge Test

For each point considered for Geogauge, at least three measurements were taken and then averaged to determine the stiffness of the pavement layer. Geogauge measurement is sensitive to the seating procedure of the foot. Close contact with the surrounding layer is necessary for the stiffness to be measured properly. Thus, to ensure close contact with the immediate pavement layer, a wet sand layer ($\frac{1}{4}$"$\sim\frac{1}{8}$") was placed on the pavement for the point to be measured with Geogauge. The wet sand layer ensured the proper contact between the Geogauge foot and the pavement layer. Some Geogauge test photos from the field tests are shown below in Figure 3.2.

Figure 3.12: Geogauge Test Photos

3.3.4 Analysis Of Geogauge Data

3.3.4.1 Determination of Young's Modulus, (E)

The value of stiffness, K (in MN/m) obtained from Geogauge has been converted into Young's Modulus (E) (in MPa) according to a relationship proposed by CAN Consulting Engineers. The relationship is given below:

$$E = \frac{K*(1-v\text{^}2)}{1.77*R}$$

Where, K = Stiffness measured with the Geogauge (MN/m)

E= Modulus of Elasticity (MPa)

v = Poisson's Ratio (assumed as 0.35)

R = Outside Radius of the Annular ring (2.25 inch)

3.3.5 Nuclear Density Gauge Test

Nuclear Density Gauge test was performed with the help of Texas Department of Transportation (TxDOT) officials at the site. Apart from operating the Gauge during measurement, every kind of cooperation was provided to TxDOT officials to ensure the proper measurement using Nuclear Density Gauge at site. Some of the test photos using Nuclear Density Gauge are shown in Figure 3.13.

Figure 3.13: Nuclear Density Gauge Test Photos

3.3.6 Analysis Of Nuclear Density Gauge Test Data

The Nuclear Density Gauge test was performed with the help of TxDOT officials at site. The density and moisture content data provided by the TxDOT officials were later used in this study to compare with the Geogauge test data at site.

CHAPTER 4

RESULTS AND ANALYSIS

4.1 Introduction

Field assessment for the in-situ tests was performed on base materials for Horseshoe Project. Analysis of the data obtained from the tests performed for the Horseshoe Project will be discussed in this chapter.

4.2 Data Collection

For the Horseshoe project, Dynamic Cone Penetrometer (DCP) and Geogauge tests have been performed on different test locations. Nuclear Density Gauge (NDG) test was also performed to evaluate the in-situ moisture content and density of the compacted material with the help of TxDOT officials.

4.3. Field Tests On Avery St. (Location-1)

4.3.1 Approximation Of Level Of Compaction From DCPI Profile With Depth

The DCP Index profiles obtained from the Dynamic Cone Penetrometer Tests performed on 9 points across the width of the roadway are presented in Figure 4.1.

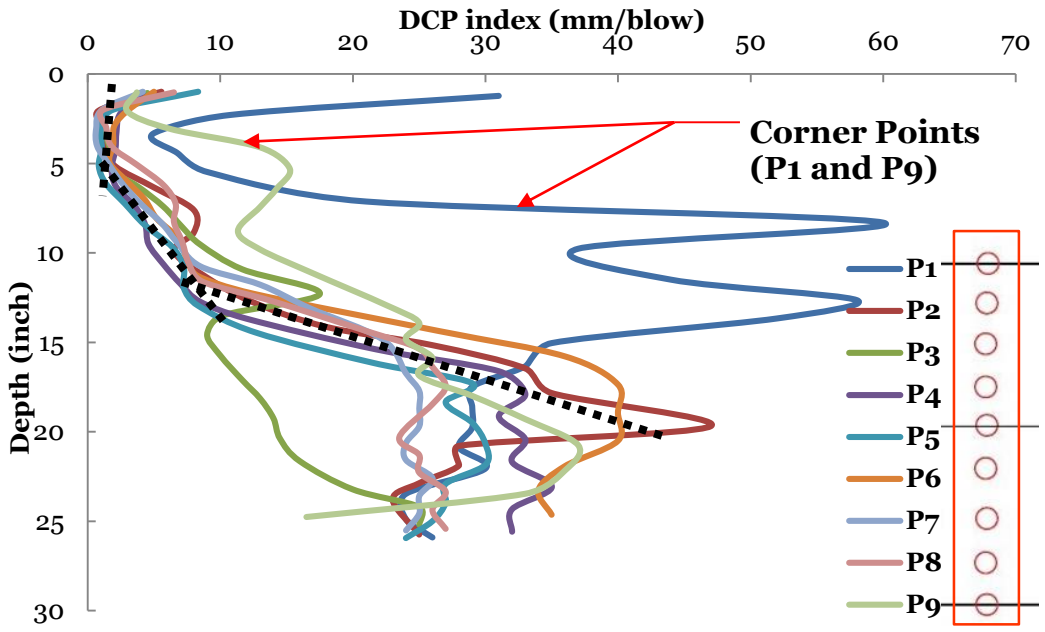

Figure 4.2: DCPI profile across depth of the pavement

DCPI values were observed within the range of 0-8 mm/blow for the upper 6" of cement stabilized base layer for P2-P8 points. A higher initial value of DCPI can be observed for each of the cases at the beginning of the penetration and this might happen due to the presence of open graded layer at the top of the pavement. It is worth mentioning that a heavy rainfall was observed before the test performed on June 9, 2014.

The values of DCPI vary from 3-22 mm/blow for the immediate 6" after the cement treated base layer which constitutes of 4% lime treated subgrade, for the points P2-P8. An increase in the values of DCPI from base layer to subgrade layer was observed which might have taken place due to the decrease in resistance of the subgrade layer than the base layer. The DCPI values vary within 8-47 mm/blow for the lower 12" (compacted subgrade) as presented in the drawings.

The DCPI values obtained from P1 and P9 points do not follow the same range obtained from P2-P8 points. It can be observed that for P1 and P9, the DCPI values vary within 4-

31 mm/blow for the upper 6” cement treated base layer, 11-60 mm/blow for 6” lime treated subgrade and 24-52 mm/blow for the lower 12” of compacted subgrade, respectively. DCPI profiles of P1 and P9 do not follow the range obtained from other points (P2-P8). P1 and P9 points were considered at the edge of the roadway which might indicate that the level of compaction along the edge of the roadway were not the same for all the three layers (cement treated base layer, lime treated subgrade layer, compacted subgrade layer) if compared to the compaction level obtained from the other points (P2-P8). There is a possibility that the level of confinement at the edge of the pavement might have affected the DCP penetration rate at the edge of the pavement.

4.3.2 Determination Of Layer Thickness From DCPI Profile

DCPI values obtained from a single point (here, P6) show that the values change significantly due to the change in the material properties for different layers which is presented below in Figure 4.2.

DCPI profile obtained from P6 that the DCPI values change gradually from layer to layer. Cement treated base layer provides lowest DCPI values and the compacted subgrade layer giving the highest DCPI values respectively. From the Figure 4.2, it can be seen that for the cement treated base layer, the DCPI values change from 1 mm/blow to 5 mm/blow providing a thickness of 6 inch for the cement treated base layer, whereas, for the lime treated subgrade layer, the DCPI values change from 4 mm/blow to 13 mm/blow which indicates a 6” thick lime treated subgrade layer following the base layer on the top. Afterwards, the DCPI increases with increasing depth and finally reaches a value of 40 mm/blow in the compacted subgrade layer. Based on the DCPI profile across depth of the pavement obtained from P6, three layers can easily be differentiated which indicates the effectiveness of using Dynamic Cone Penetrometer as an in-situ pavement testing equipment during construction.

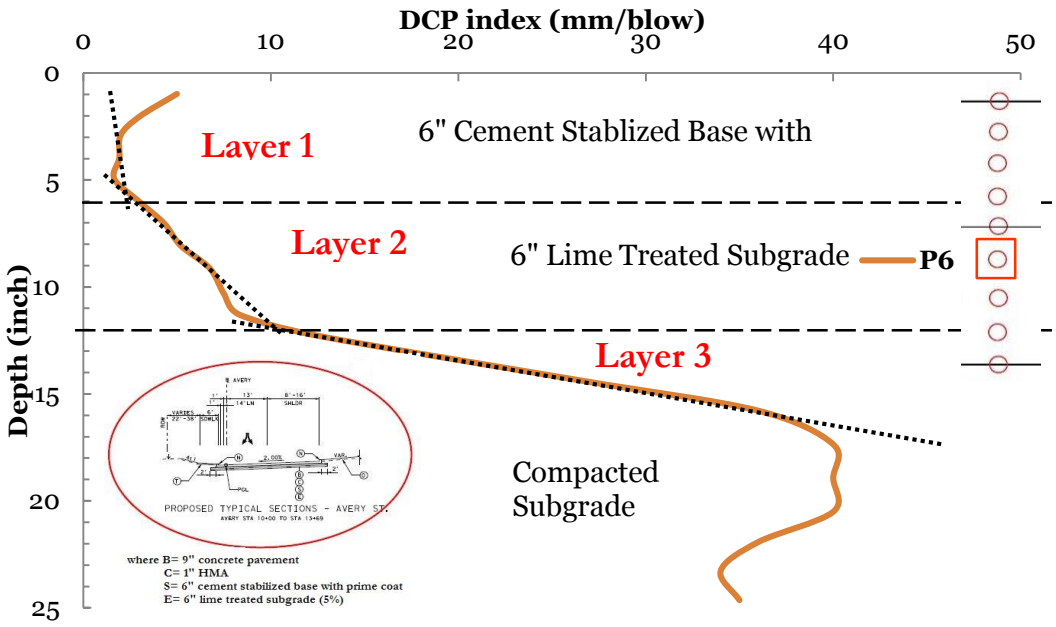

Figure 4.3: DCPI profile across depth of the pavement obtained from P6

Later the depth of each layer obtained from DCP Index profiles obtained from each points the tests have been performed was verified from the design thickness which can be seen from Figure 4.2. It can be seen that the depth of each layer distinguished from DCP Index profiles was observed within 0.5 inch from the design value. A linear trend of DCP Index values for each layer also provides a specific DCP Index value for a certain layer from which any effect of presence of hard layer or rock can be eliminated while calculating the material properties of a certain layer. Comparison of resilient moduli values obtained from the slope of the DCP Index profile and the average resilient moduli value obtained from each 1 inch segment of the pavement will be shown later in this chapter.

4.3.3 Resilient Moduli Profile Along Depth

The values of Resilient Moduli can be plotted with depth to see the variation of resilient moduli values across the depth of the pavement as the material properties changes across depth. It can be observed that for P2-P8, the resilient moduli values changes within a range of 40,744-713,948 psi for the upper 6" of cement treated base layer which is presented in Figure 4.3. Upper 6" cement treated base layer provided the highest resistance to the penetrating cone which results in higher range of resilient moduli values across this layer. For the immediate 6" lime treated subgrade layer, resilient moduli vary within a range of 17,749-138,218 psi for P2-P8. For compacted subgrade, Mr values vary from 5,869-40,744 psi.

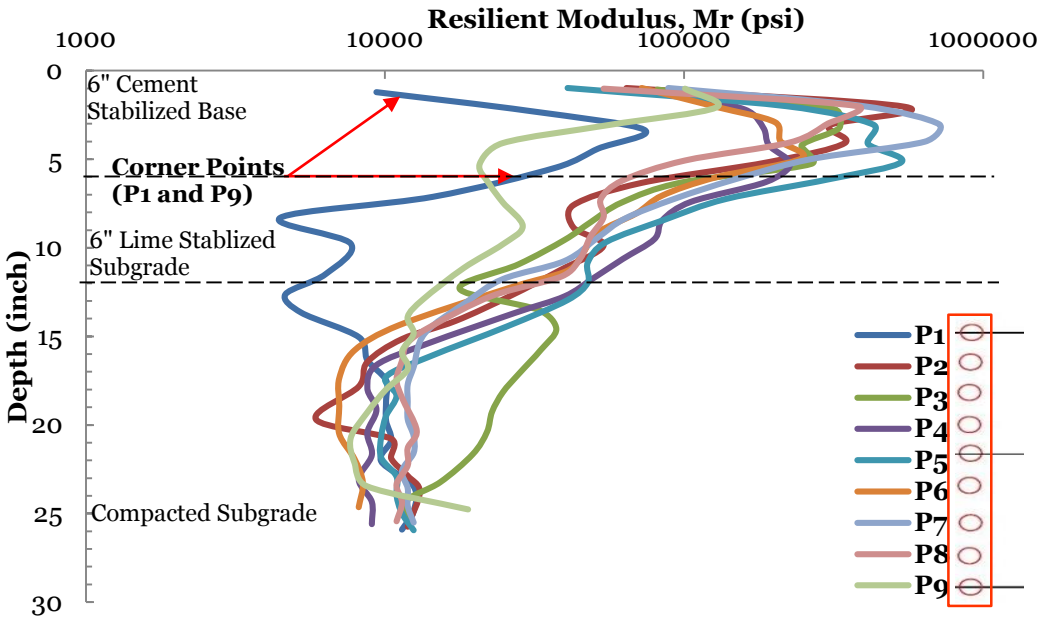

Figure 4.4: Resilient Moduli Profile across depth of the pavement

The upper 6" of cement treated base layer provides the highest support leading to a higher range of resilient moduli values for the upper layer. For the points considered both at the edge of the roadway, resilient moduli profiles are not same when compared to the other

points (P2-P8). For these two points (P1 and P9), the resilient moduli values were within a range of 9,355-127,940 psi for the upper 6" of cement treated base layer, 4,465-28,873 psi for the immediate 6" of lime treated subgrade layer and 7,673-18,958 psi for 12" of compacted subgrade as presented in Figure 4.3.

4.3.4 Variation Of Resilient Moduli In Different Layers

The resilient modulus was determined at each DCPI value. The predicted Mr value along the layer was averaged to determine the Mr at each point of the layer. The average resilient moduli values along each layer is presented in Figure 4.4.

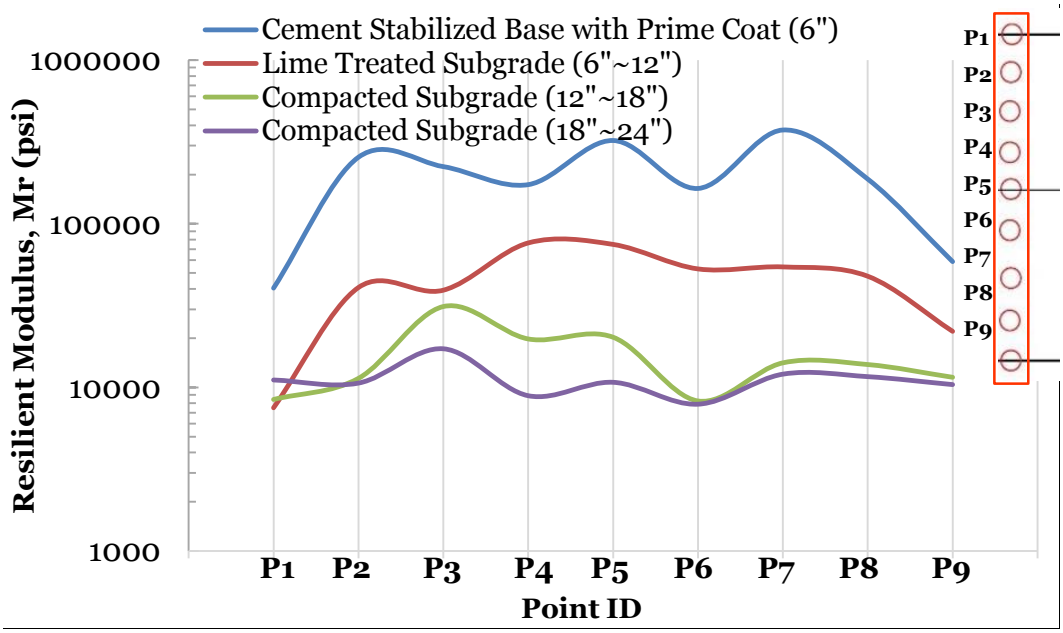

Figure 4.5: Variation of Resilient Moduli in Different Layers

Resilient moduli values in the upper 6" cement stabilized base layers vary from 40,500-374,078 psi. The resilient moduli vary from 7,513-73,351 psi for 6" lime treated subgrade layer and in the compacted subgrade layers, resilient moduli values were within a range 8,458-20,266 psi. For each of the three layers, the lowest value for each respective layer

is found at the edge of the roadway which might have occurred due to the lack of confinement at the edge of the pavement.

4.3.5 Variation Of Unconfined Compressive Strenth In Base Layer Across Width Of The Pavement

Figure 4.5 shows the variation of unconfined compressive strength (UCS) of the points considered in the topmost 6" cement stabilized base layer across the width of the pavement. The lowest UCS was found at both edges of the pavement (P1 and P9). The UCS value at the edge of the pavement varied between 73.7 psi – 76.4 psi whereas, for the other points (P2-P8), UCS was observed within a range of 269.4 psi – 619.2 psi. The UCS value across the width of the pavement was calculated according to a relationship proposed by Patel and Patel (2012).

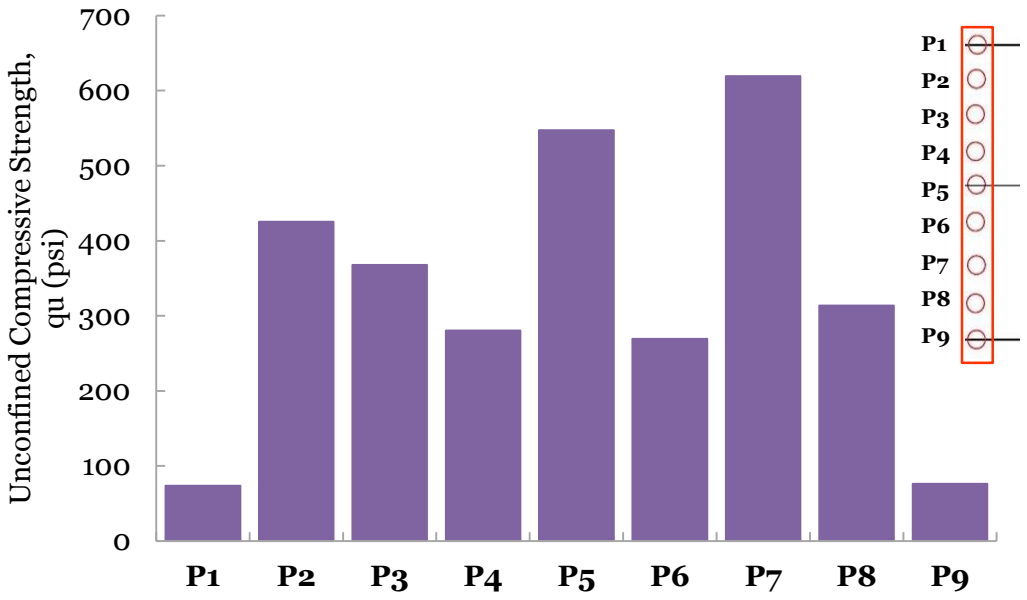

Figure 4.6: Variation of Unconfined Compressive Strength in base layer across width of pavement at Location-1

The UCS value across the width of the pavement was calculated according to a relationship proposed by Patel and Patel (2012).

4.3.6 Variation Of Young's Moduli From Geogauge

For the location on Avery St near Tom Landry Fwy (I-30), Dallas, TX, nine points at 5' apart were considered to be measured with Geogauge. Proper contact was ensured before each measurement with the placement of wet sand layer between the Geogauge foot and the pavement layer. Young's moduli values measured with Geogauge will be considered as the property of the top layer of the pavement (cement stabilized base with prime coat). It can be seen from the graph presented in Figure 4.6 that the lowest Young's Modulus value (28,900 psi) was found at the corner point (P9) of the pavement section. Young's Moduli value varied from 42,337 psi to 66,696 psi for P1-P8 points. The highest moduli value was obtained at P5 (66,696 psi) which was at the middle of the pavement.

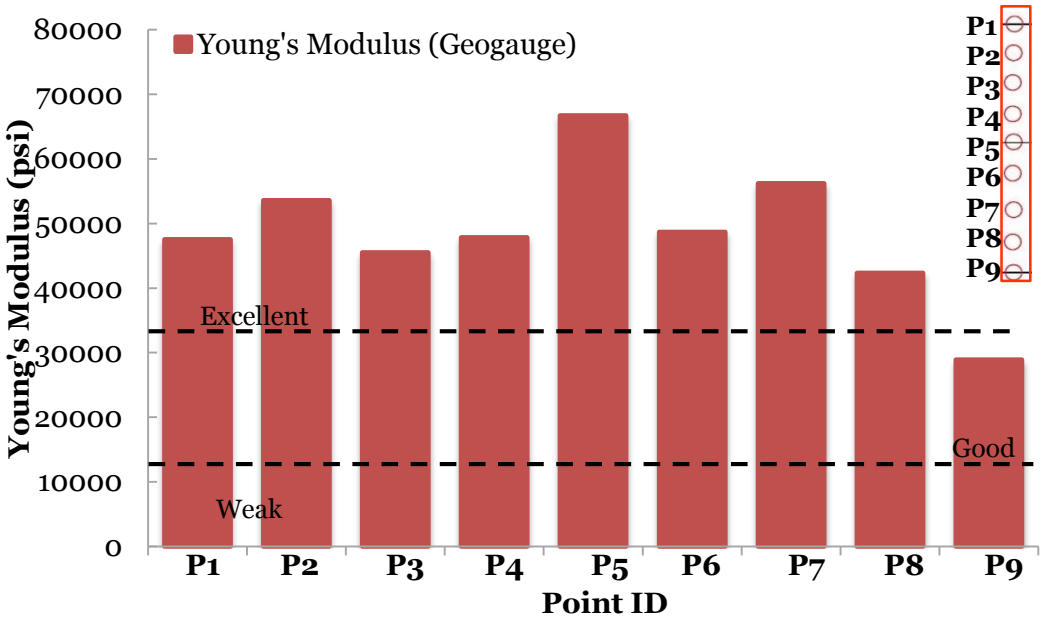

Figure 4.7: Variation of Young's Modulus across Pavement

According to base quality values of Humboldt Geogauge by Chen et al. (1999), Values obtained from P1-P8 maintained 'excellent' moduli values throughout the width of the pavement whereas, P9 showed 'good' quality of base layer which was measured with Geogauge.

4.3.7 Comaprison Of Resilient Moduli From DCP Measurement With Young's Moduli From Geogauge For Cement Stabilized Base Layer With Prime Coat

This layer constitutes the uppermost layer of the pavement section (6"). Resilient moduli was calculated for each 1" of the cement stabilized base layer and then averaged over the thickness of the layer, this average resilient moduli values obtained from DCP measurement are compared with the Young's Moduli values measured with Geogauge shown in Figure 4.7.

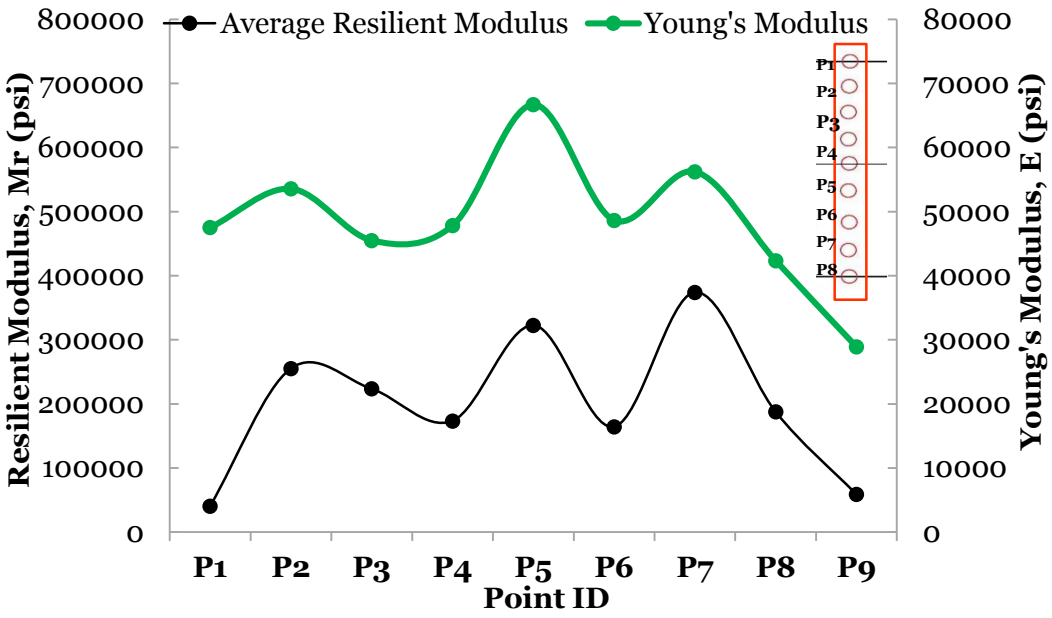

Figure 4.8: Variability of Resilient Moduli with Young's Moduli (Cement Stabilized Base Layer)

It can be seen that the trends obtained from DCP and Geogauge measurements are similar. Clearly, there is a visible trend between the resilient moduli values obtained from

DCP measurements and the Young's Moduli values measured with Geogauge. Although there is a possibility of the increase in resilient moduli value if DCP rod penetrates through a crushed concrete aggregate while obtaining the average material properties of a certain layer, Geogauge can clearly capture this effect into its measurement which can be observed from the similar trend provided by both DCP and Geogauge.

4.4 Field Tests Near I-35E Northbouth Frontage Road (Location-2)

4.4.1 Variation Of Young's Moduli With Moisture Content

Eight points at 5' apart from each other across the roadway were considered to measure the variation of moduli values with Geogauge, Nuclear Density Gauge tests were also performed at these points to see the variation of moisture content, dry density and wet density with the change in moduli values. It has been observed that the moduli values measured with Geogauge are affected with the slight change in moisture content which is presented below in Figure 4.8.

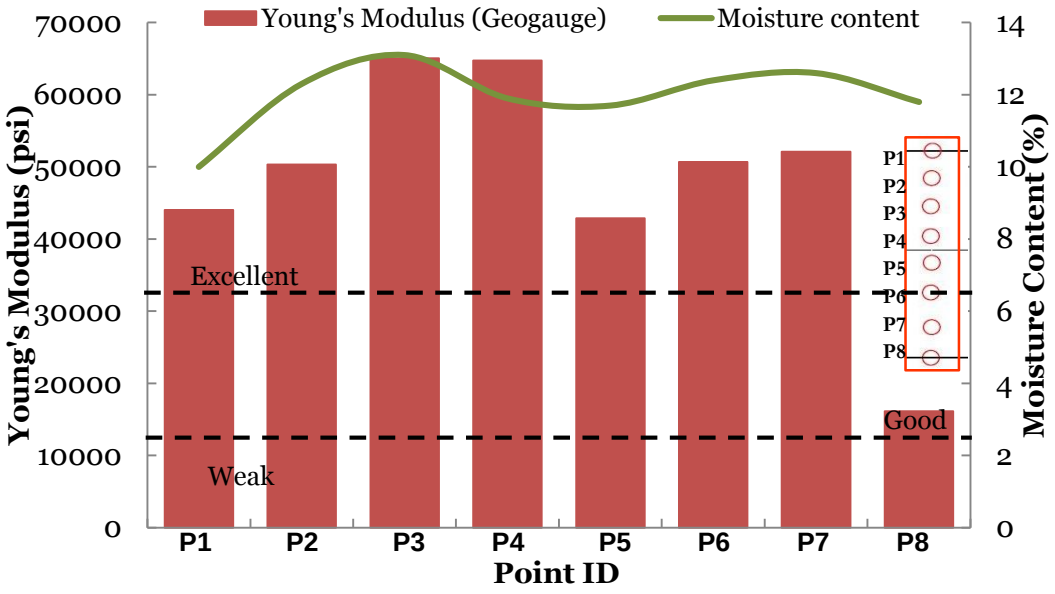

Figure 4.9: Variation of Young's Moduli with change in Moisture Content

The moduli values seem to increase with the increase in moisture content in the materials. At all the points which were considered for the Geogauge and Nuclear Density Gauge (NDG) tests to be performed, it was observed that the moduli values increase in all cases as the moisture content increases. P1 and P8 were considered at the edge of the pavement for the measurements to be taken, both were supposed to show the like-wise moduli values because of level of compaction at both points. P1 was not totally located at the edge of the roadway but rather more compacted areas were left apart from the width of the road which was considered for the measurements. According to the base characterization values provided by Chen et al., (1999), P1-P7 showed 'excellent' base quality while P8 which is located at the edge of the pavement was of 'good' quality.

4.4.2 Variation Of Young's Moduli With Change In Density

Change in Young's Moduli values can be compared with the change in wet density measured with Nuclear Density Gauge which is presented in Figure 4.9.

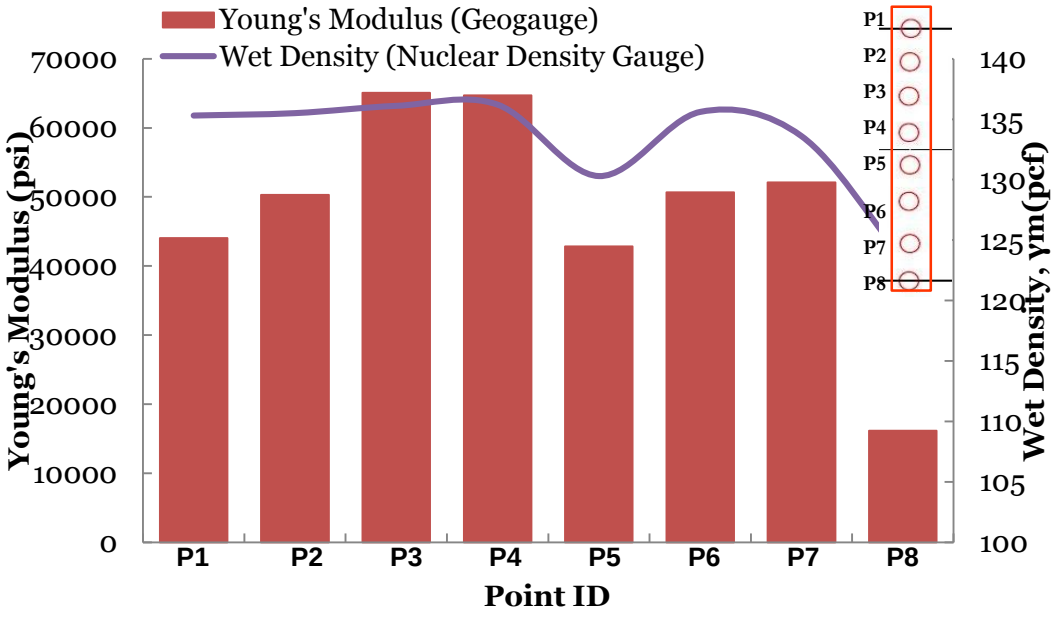

Figure 4.10: Variation of Young's Moduli with change in Wet Density

The Young's Moduli values increase with the increase in wet density. At P5, a sudden decrease in moduli value can be observed with a sudden drop of wet density. This might happen due to the non-uniformity of the compaction procedure during the placing of the cement treated base layer or lime treated subgrade. As Geogauge takes 12 inch into account while measuring the stiffness or moduli of the layer beneath, the non-uniformity of compaction during the placing of material within the upper 12" depth might lead to a decreased moduli value.

The same trend can also be found when moduli values measured at different points are plotted with the change in dry density measured with the Nuclear Density Gauge (NDG) which is presented below in Figure 4.10.

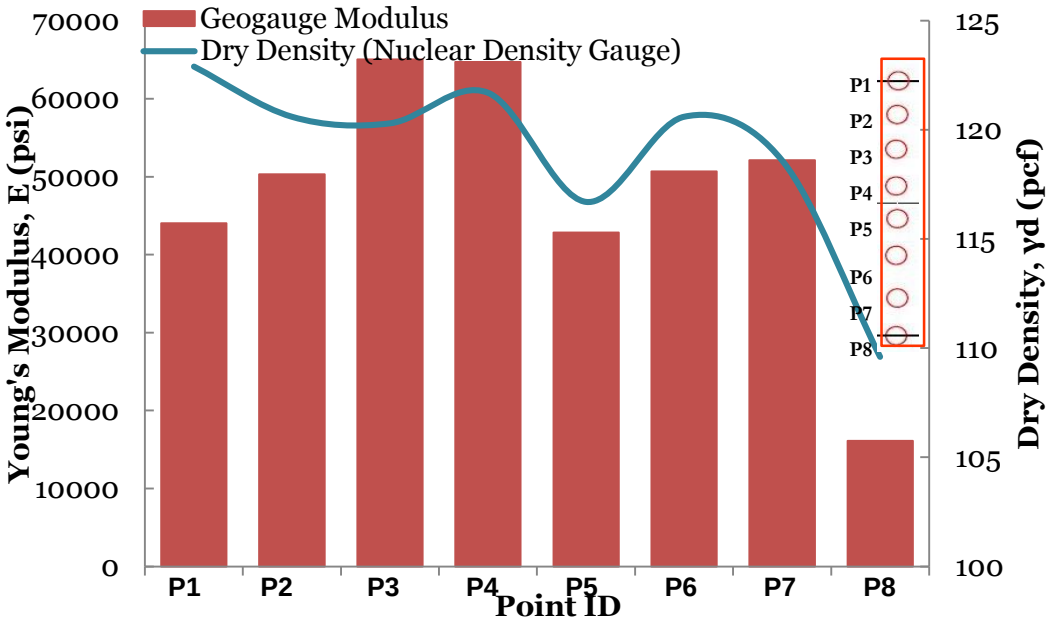

Figure 4.11: Variation of Young's Moduli with change in Dry Density

4.5 Field Tests Near South Riverfront Blvd. (Location-3)

4.5.1 Approximation Of Level Of Compaction From DCPI Profile With Depth

DCP Index values obtained from the DCP tests performed on August 2, 2014 was been plotted with depth to obtain the DCP Index profile along depth of the pavement from the ten points. The DCP Index profile from the tests performed on ten points near the S Riverfront Blvd, Dallas, TX is presented in Figure 4.11.

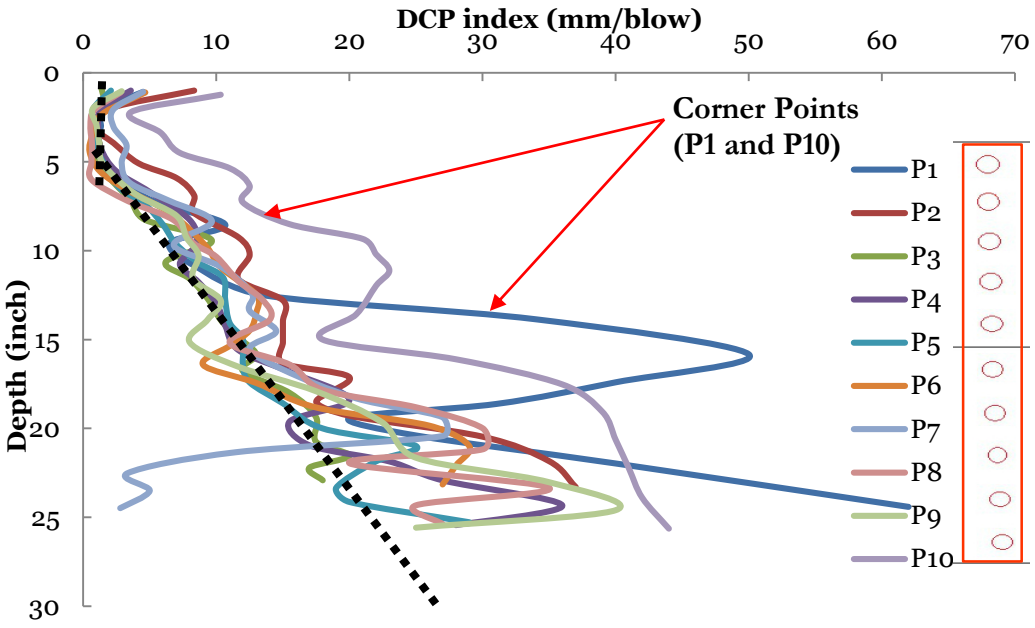

Figure 4.12: DCPI profile across depth of the pavement

Figure 4.11 shows that the DCPI profiles for P2-P9 points follows a trend for top 6" cement stabilized base layer and immediate 13" lime treated subgrade afterwards. A higher DCPI value was observed at the top of the pavement. For 6" cement stabilized base with prime coat layer, the DCPI values vary from 0.5 mm/blow to 7 mm/blow for P2-P9 considered. The DCPI profiles obtained from the corner points (here, P1 and P10) did not follow the same trend which was observed for the other points (here, P2-P9). Higher confinement seems to lessen at the edge of the pavement, this might act as a reason for the way-off

trend than the DCPI profiles obtained from P2-P9. For the 13" lime treated subgrade layer, the DCPI varied from 3.3 mm/blow to 25 mm/blow for the points from P2 to P9 considered.

4.5.2 Determination Of Layer Thickness From DCPI Profile

Different trend of DCPI values for different materials will facilitate the use of DCPI profile along depth to distinguish layers of the pavement section. Considering the DCPI profile obtained from P2, different layers of the pavement section can easily be distinguished from the trend that has been observed for separate layers of the pavement. DCPI profile along depth for point P2 has been presented below in the Figure 4.12.

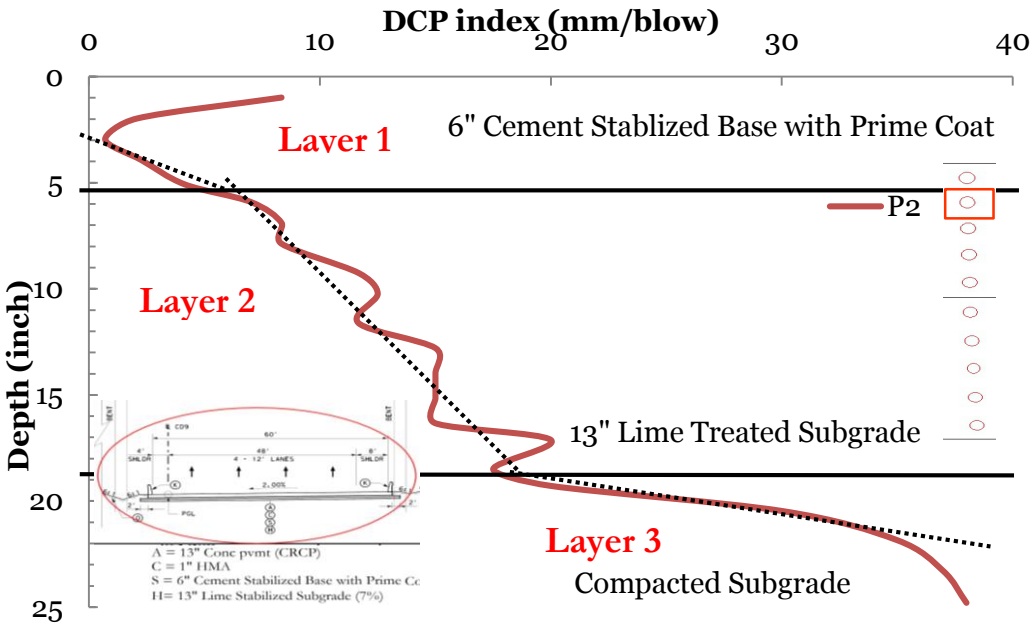

Figure 4.13: DCPI profile across depth of the pavement obtained from P2

From the DCPI profile obtained from P2 point, it can clearly be seen that the DCPI value change gradually from one layer to another. For instance, DCPI value was observed within 0.69 mm/blow - 7 mm/blow for the top 6" cement stabilized base layer. Afterwards, it started increasing gradually for the immediate 13" lime treated subgrade of the pavement section. The higher DCPI value for the first inch of the pavement was ignored while determining the

layer thickness because there might be a possibility that higher initial DCPI value may result due to positioning of the DCPI rod at the beginning of the pavement or the climatic effect on the top of the pavement. For the next 13” lime treated subgrade, the DCPI value varied from 8.3 mm/blow to 20 mm/blow and for the next part of the pavement which is compacted subgrade, the DCPI values started increasing gradually afterwards.

The determination of different layers using DCPI profiles along the depth of the pavement was later verified with the design thickness of the pavement section. It has been found that the layer thickness obtained from the DCPI profiles varied within a range of 0.5 inch when compared with the design thickness.

4.5.3 Resilient Moduli Profile Along Depth

The resilient moduli value obtained for different DCPI values for each 1” of the pavement was plotted with the depth to see the change of moduli values across the depth of the pavement which is presented in Figure 4.13.

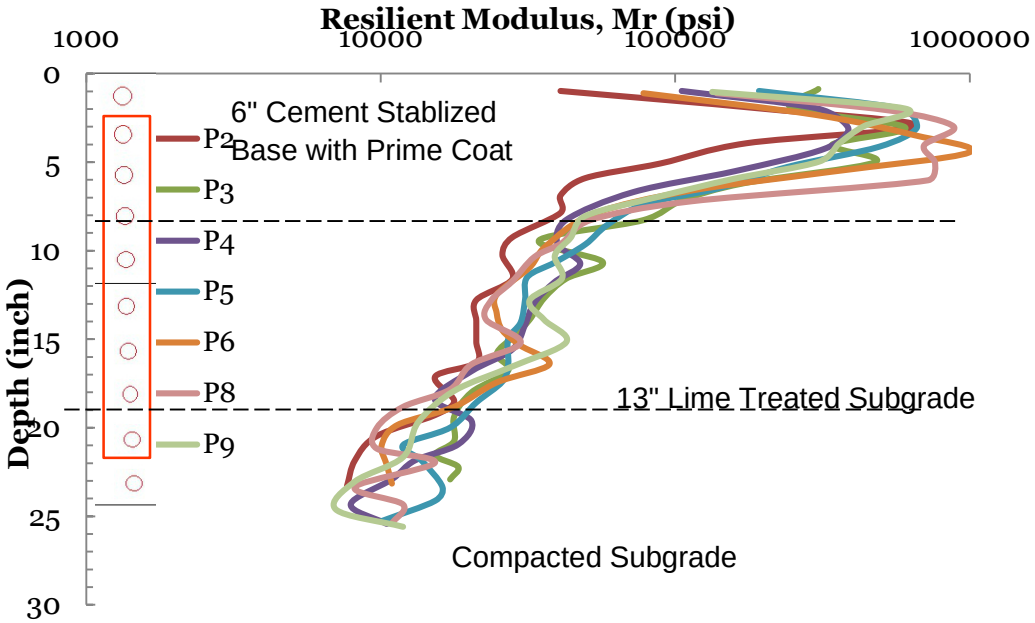

Figure 4.14: DCPI profile across depth of the pavement obtained from P2

The highest resilient moduli was provided by the top 6” of cement stabilized base layer with prime coat which will sustain most of the loads coming from the ongoing vehicles. For the top 6” of the pavement, the resilient moduli varied from 44,744 psi to 994,525 psi which was calculated from DCPI values of P2-P9 points considered. For the immediate 13” lime treated subgrade, the resilient moduli value were within a range of 11,903 psi – 113,700 psi for P2-P9 points. It is worth mentioning that resilient moduli values obtained from P2-P9 points were shown to provide a certain specific trend which can also be verified from DCPI profile along depth plot. The points at both edges of the pavement did not seem to follow the same trends.

4.5.4 Variation Of Resilient Moduli In Different Layers

The resilient moduli value obtained for three different layers (cement stabilized base layer with prime coat, lime treated subgrade and compacted subgrade) have been plotted point-wise to see the change in moduli values due to the change of material properties. The DCPI for each 1” of the pavement section has provided with a specific moduli value and the values for a certain layer have been averaged to obtain a single resilient moduli value for a certain layer which is presented below in Figure 4.14.

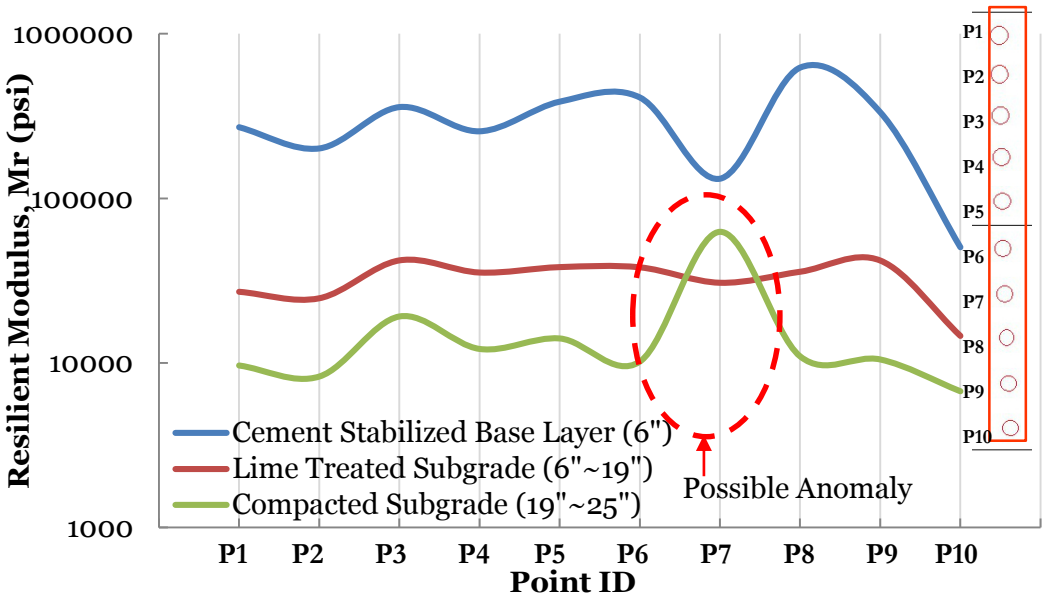

Figure 4.15: Variation of Resilient Moduli in Different Layers

It can be seen that the resilient moduli values for the topmost 6" cement stabilized base layer with prime coat varied from 131,423 psi to 623,285 psi, 14,556 psi – 41,950 psi for immediate 13" lime treated subgrade beneath the base layer. From the resilient moduli profile, it is clearly visible that there might be possible anomaly in the compacted subgrade. There might be a possibility that a hard layer may exist in the compacted subgrade which might lead to lesser DCPI value and thus higher resilient moduli value at that certain point (P7). Detection of possible hard layer in the middle of the pavement can also be understood from the variability plot of resilient moduli value for the points considered which will be shown later.

4.5.5 Variation Of Unconfined Compressive Strenth In Base Layer Across Width Of The Pavement

Figure 4.15 shows the variation of UCS in the base layer of the ten points considered for the DCP tests to be performed across the width of the pavement. The lowest UCS value

(81.9 psi) was found at P10 which is located at the edge of the pavement. From P1 to P9, the UCS value varied from 210 psi – 1023.5 psi where the highest UCS value was found at P8.

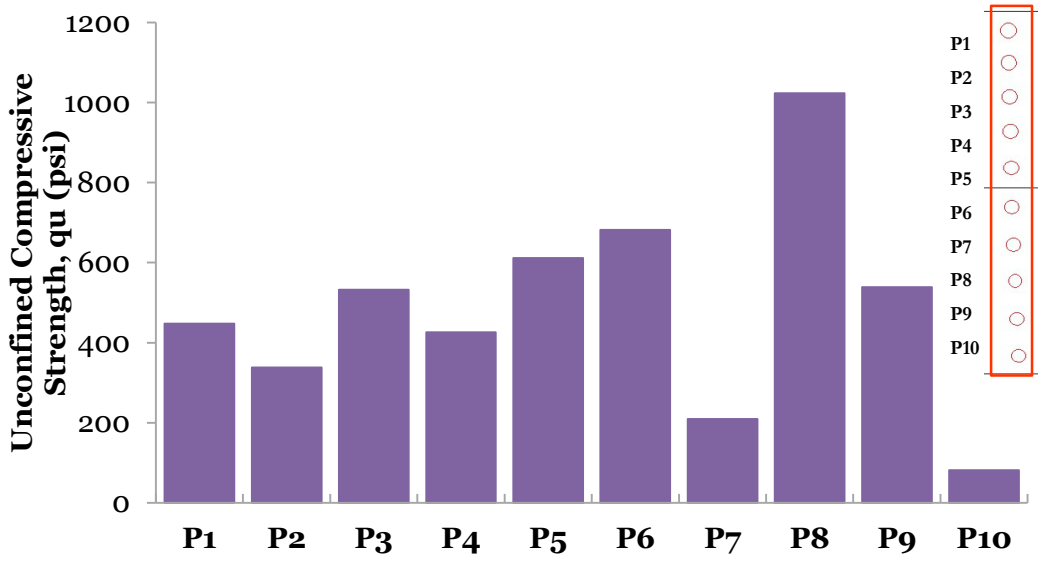

Figure 4.16: Variation of Unconfined Compressive Strength in base layer across width of pavement at Location-3

4.5.6 Variation Of Young's Moduli From Geogauge

Ten points at 7 ft apart were considered near the S Riverfront Blvd., Dallas, TX near I-35E for the field tests on August 2, 2014. First test performed on a single point was Geogauge test because it takes measurement without disturbing the pavement layer. A wet sand layer was placed before placing the Geogauge foot onto the soil to ensure the proper contact between the Geogauge foot and the pavement material. At lease, three close measurements were taken to avoid any error in taking measurements and then averaged to evaluate material properties for a certain test point considered. The variation of Young's moduli (E) across the width of the pavement can be seen from the Figure 4.16. For the top base layer of the pavement, the Young's modulus for the layer considered varied from 26,384 psi to 76,320 psi. The highest value was found at P8 with the use of Geogauge

which also satisfies the moduli value obtained with the use of Dynamic Cone Penetrometer which can be seen from Figure 4.16.

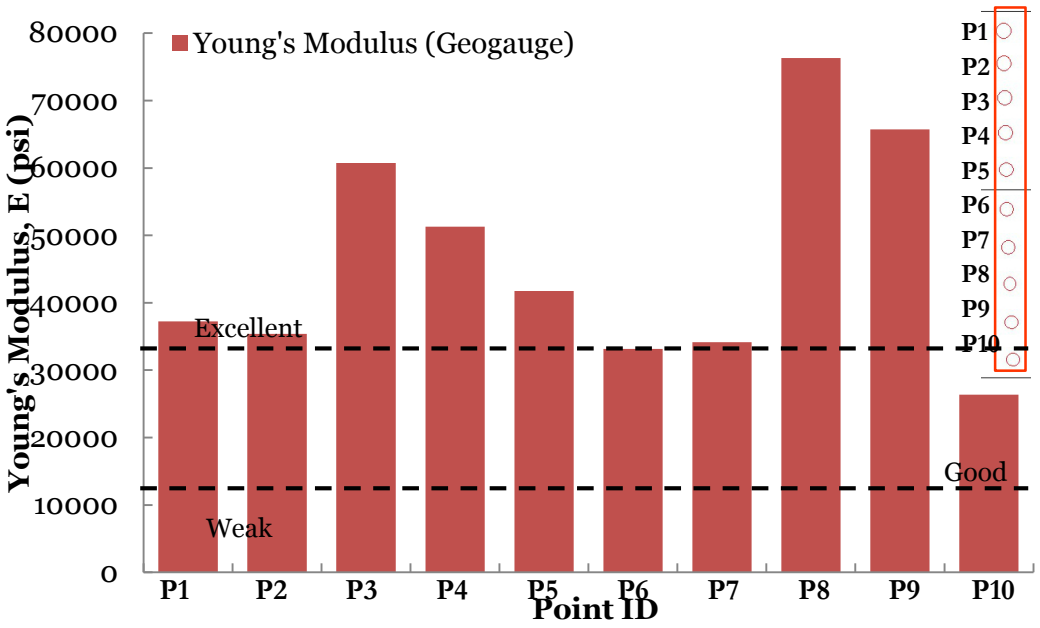

Figure 4.17: Variation of Young's Modulus across Pavement

From the values presented in Figure 4.16, All the points (P1-P10), except P6 and P10, showed 'excellent' base quality whereas P6 and P10 provided 'good' base quality according to the base quality characterization values provided by Chen et al., (1999).

4.5.7 Comaprison Of Resilient Moduli From DCP Measurement With Young's Moduli From Geogauge For Cement Stabilized Base Layer With Prime Coat

For the 6" cement stabilized base layer with prime coat, variability of resilient moduli values were plotted for all the points considered which is shown in Figure 4.17.

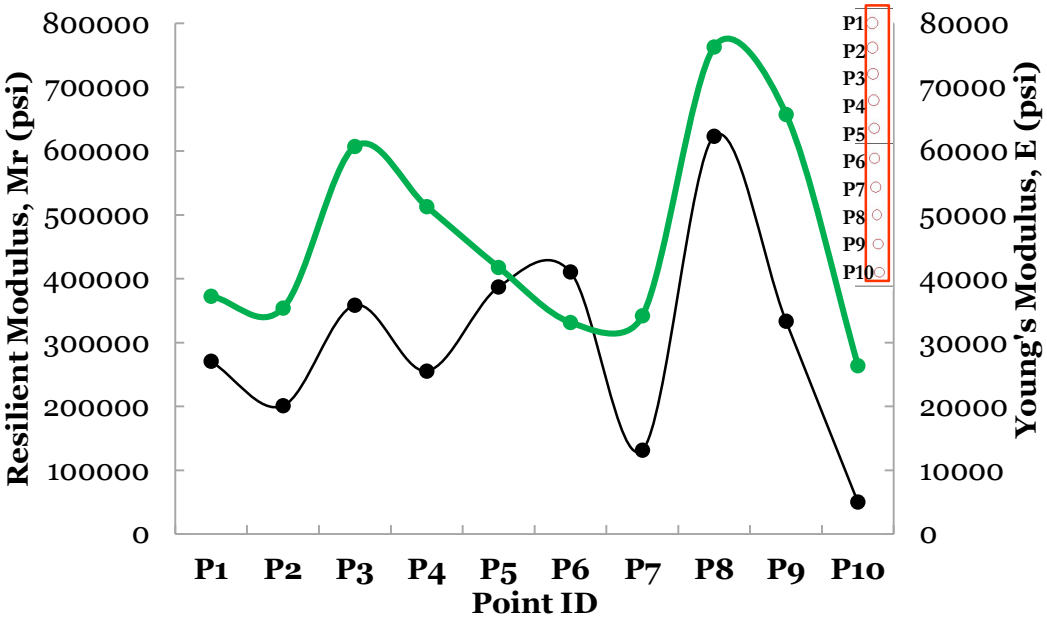

Figure 4.18: Variability of Resilient Moduli with Young's Moduli (Cement Stabilized Base Layer)

From the Young's moduli values across the points (P1-P10) measured with Geogauge that the Geogauge is able to capture the effect of presence of any crushed concrete aggregate in the layer where resilient moduli value measured with DCP is higher and thus showing a similar trend like a trend which was observed in values of Young's moduli measured with Geogauge.

4.6 Field Tests Near Jefferson Viaduct Blvd. (Location-4)

4.6.1 Variation Of Young's Moduli With Moisture Content

Six points were considered for NDG and Geogauge tests to be performed near the Jefferson Viaduct Blvd., Dallas, TX Variation in Young's moduli (E) was plotted with the change in moisture content measured with Nuclear Density Gauge as presented in Figure 4.18. Three close measurements were averaged to obtain a single modulus value for a single point considered. It has been observed that the Young's moduli value measured with Geogauge varied from 8,447 psi to 57,737 psi. The lowest modulus was found at one edge

of the pavement (P6). The moisture content (w) measured with Nuclear Density Gauge varied from 11.2% to 14.6% for P1-P6. All the properties measured with NDG was at the depth 6 inch from the top of the pavement which represents cement stabilized base layer with prime coat.

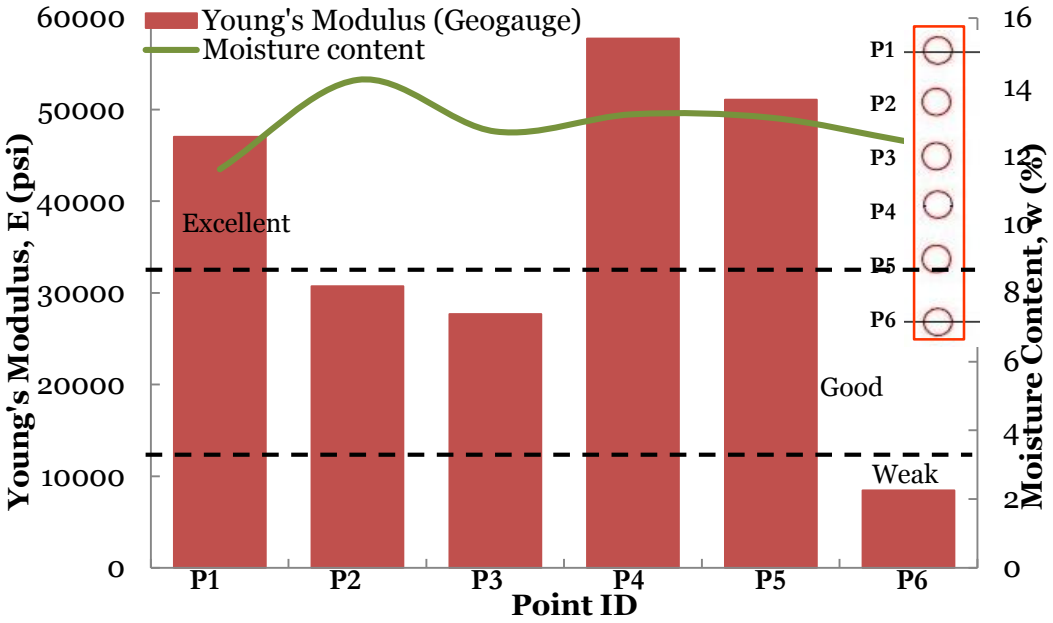

Figure 4.19: Variation of Young's Moduli with change in Moisture Content

It can be observed that the point ID- P1, P4 and P5 showed 'excellent' base quality whereas, P2 and P3 showed 'good' base quality. On the other hand, P6 which is located at the edge of the pavement, provided 'weak' base layer support according to the characterization value provided by Chen et al., (1999).

4.6.2 Variation Of Young's Moduli With Change In Density

The change in Young's moduli measured with Geogauge with the change in wet density measured with Nuclear Density Gauge is shown in Figure 4.19 below. It is evident that with the increase in wet density, Young's moduli values increase across the points considered

along the width of the pavement. The wet density varied from 109.6 pcf to 125.9 pcf. The lowest wet density was found at the edge of the pavement (P6).

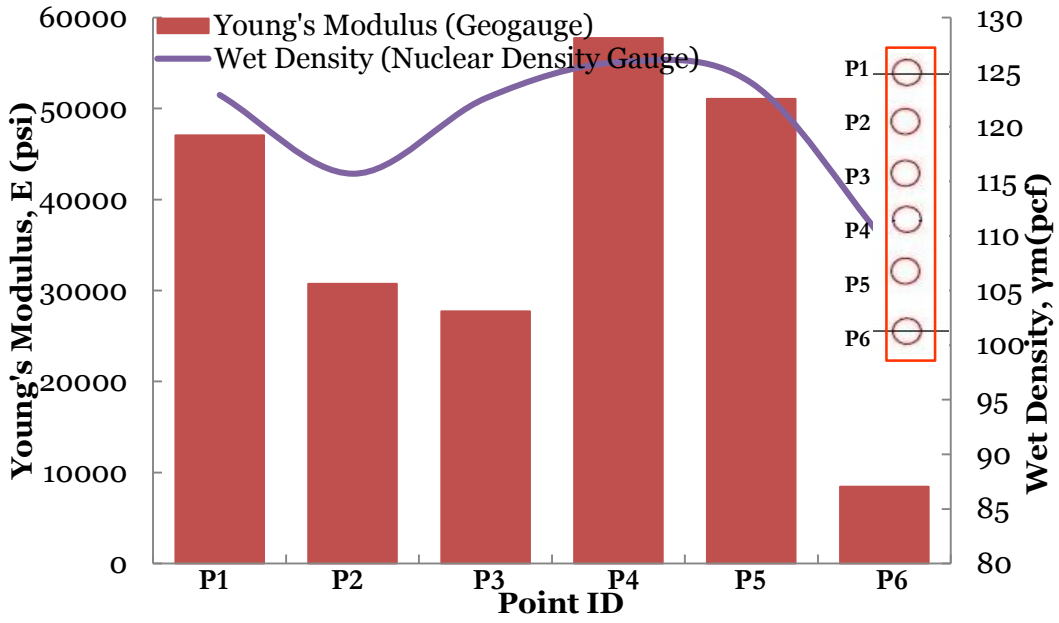

Figure 4.20: Variation of Young's Moduli with change in Wet Density

The same trend was also observed when dry density across the points was plotted against the Young's moduli value measured with Geogauge as presented in Figure 4.20. As the Dry density increases, Young's moduli values increase and the vice versa. The dry density of the points considered was observed within a range of 97.5 pcf – 111.2 pcf.

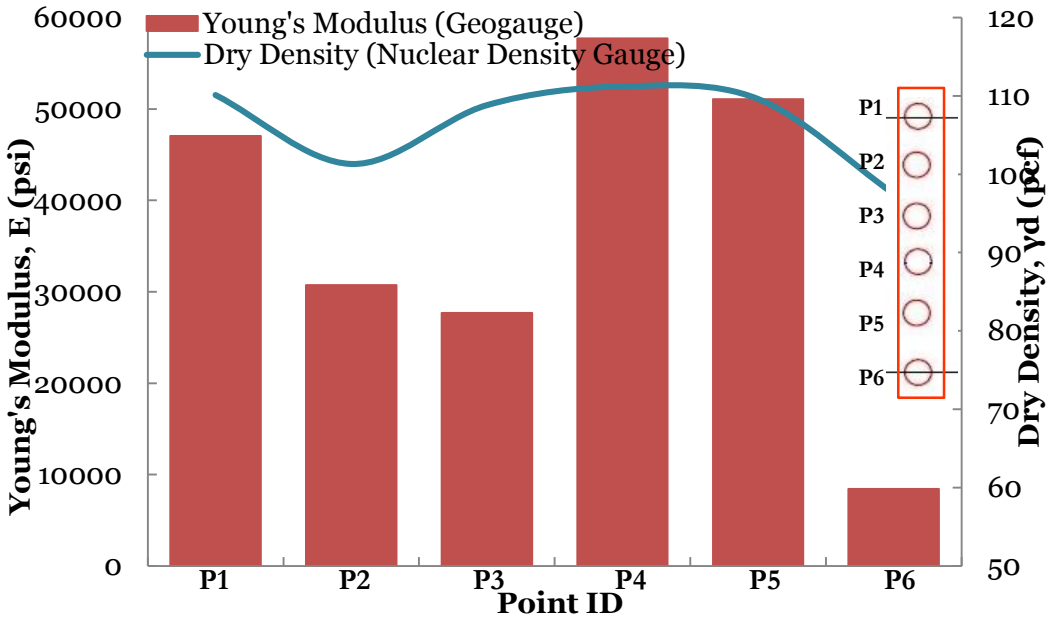

Figure 4.21: Variation of Young's Moduli with change in Dry Density

4.7 Field Tests Near Sylvan Ave. (Location-5)

4.7.1 Approximation Of Level Of Compaction From DCPI Profile With Depth

DCP Index values obtained for 1" penetration into the pavement layer by the DCP rod is plotted against the depth to obtain the DCPI profile along depth which is presented below

in Figure 4.21. All the points (P1-P4) followed the same trend in three different layers except P5. There might be a possibility that P5 was located at the edge of the roadway

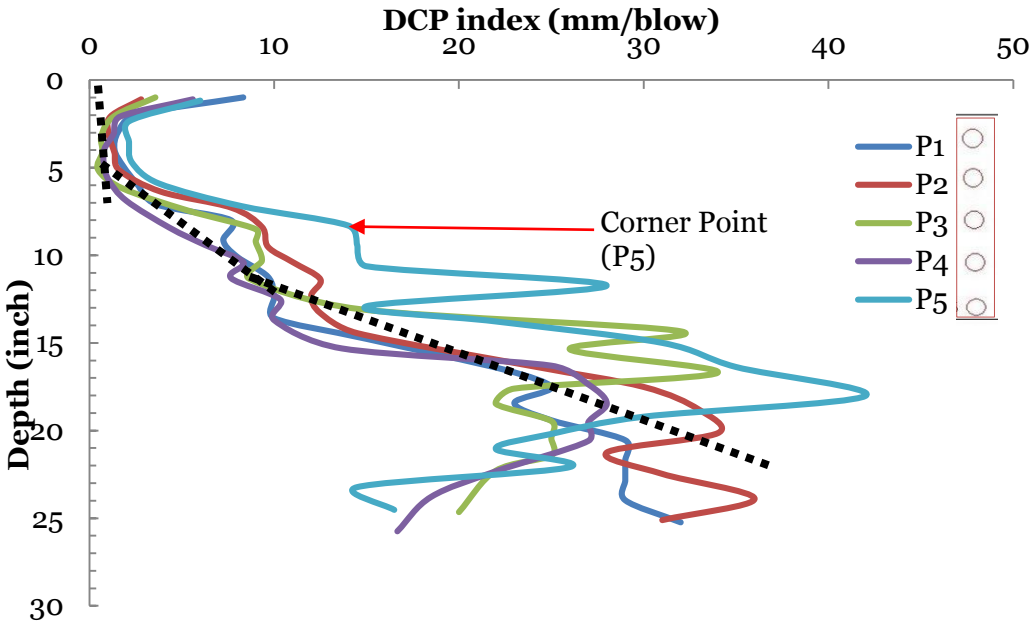

Figure 4.22: DCPI profile across depth of the pavement

Figure 4.21 shows that for the cement stabilized base layer, DCPI value varied from 0.5 mm/blow to 8 mm/blow while for the lime treated subgrade, DCPI remained within a range of 2 mm/blow – 12.5 mm/blow for P1-P4. For the compacted subgrade layer, DCPI fluctuated between a range of 10 mm/blow – 36 mm/blow.

4.7.2 Determination Of Layer Thickness From DCPI Profile

Different DCPI variation for different types of materials in the pavement section was used to distinguish each layer of the pavement as presented in Figure 4.22. DCPI profile obtained from P2 can easily be used to differentiate three separate layers for the pavement.

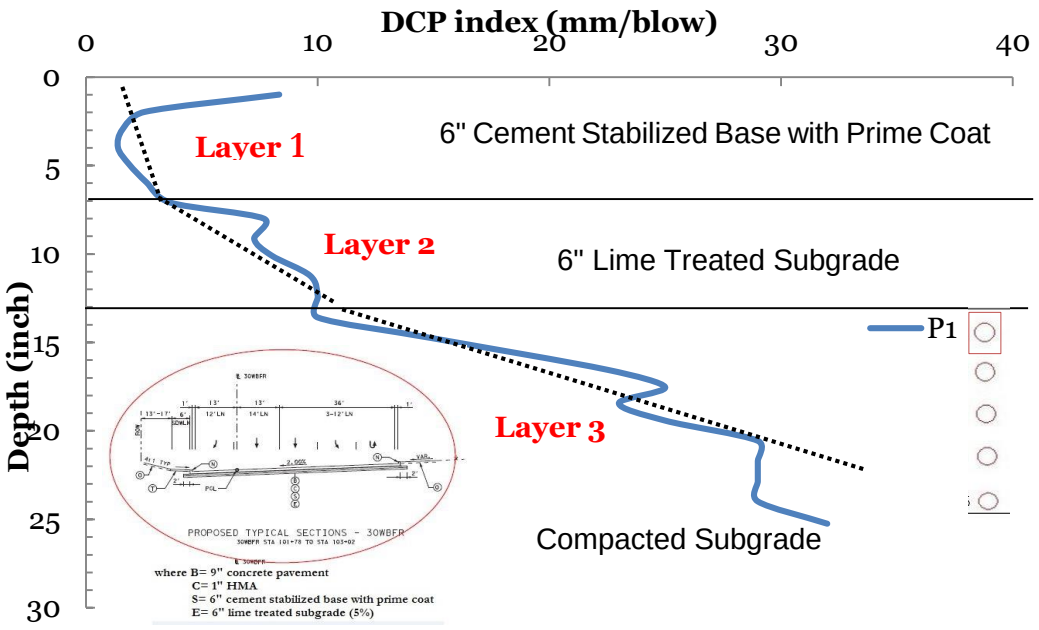

Figure 4.23: DCPI profile across depth of the pavement obtained from P1

Figure 4.22 shows that DCPI change within 1.3 mm/blow – 8.3 mm/blow for the top 6" cement stabilized base layer and varied between 3.6 mm/blow – 10 mm/blow for the immediate 6" lime treated subgrade and between 10 mm/blow – 32 mm/blow for the rest of the compacted subgrade. Higher initial DCPI was ignore while establishing the thickness of the top layer in this case. Later, these determined thicknesses of the layers were verified with the design thickness to evaluate the efficiency of Dynamic Cone Penetrometer as an in-situ pavement evaluation equipment. The determined thicknesses was within 0.5 inch when compared with the design thickness.

4.7.3 Resilient Moduli Profile Along Depth

The resilient moduli values calculated from the DCPI obtained from each 1" depth of the pavement section are plotted against the depth to obtain the resilient moduli profile along depth which is presented in Figure 4.23.

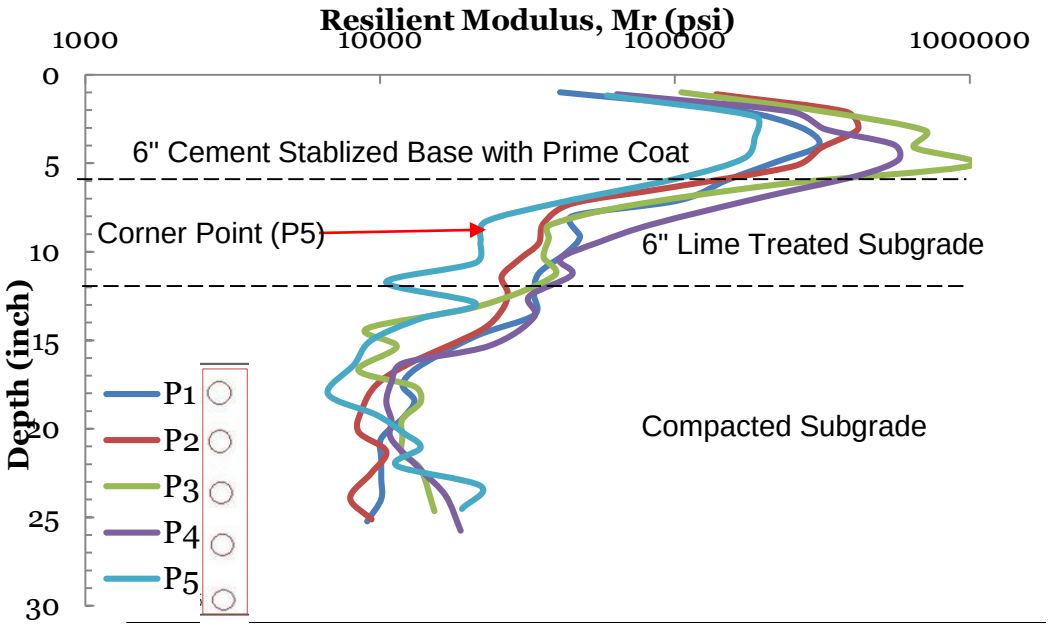

Figure 4.24: Resilient Moduli Profile across depth of the pavement

The top 6" cement stabilized base layer provided the highest resilient moduli values among the three layers encountered. The resilient moduli varied within a range of 40,745 psi – 573,704 psi for the topmost 6" cement stabilized base layer for P1-P4 considered whereas, for the immediate 6" lime treated subgrade, variation was within 25,873 psi – 201,480 psi. Resilient moduli values varied from 7,913 psi – 33,220 psi in the compacted subgrade layer for P1-P4 points.

4.7.4 Variation Of Resilient Moduli In Different Layers

Three different layers (cement stabilized base with prime coat, lime treated subgrade and compacted subgrade) provided three ranges of resilient moduli values which can be seen layer-wise from Figure 4.24. For cement stabilized base layer, resilient moduli varied from 190,345 psi to 502,206 psi while for lime treated subgrade, it varied from 32,990 psi to 76,660 psi. Resilient moduli values were observed within a range of 12,422 psi – 16,094 psi for compacted subgrade layer.

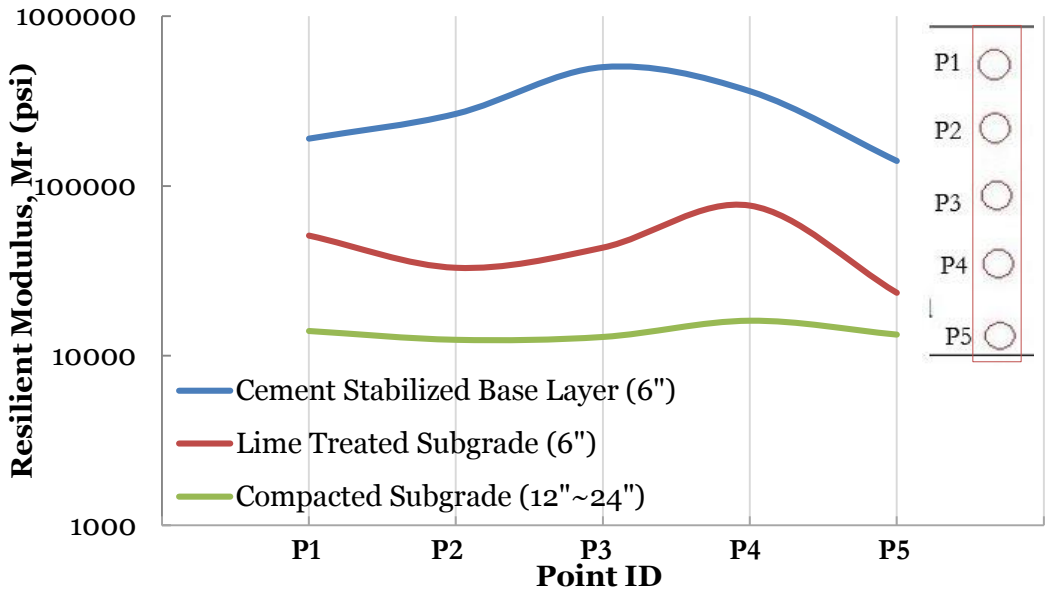

Figure 4.25: Variation of Resilient Moduli in Different Layers

4.7.5 Variation Of Unconfined Compressive Strenth In Base Layer Across Width Of The Pavement

Figure 4.25 presents the variation of unconfined compressive strength (UCS) in the top 6" cement stabilized base layer across the width of the pavement section. From P1-P5 considered, the UCS value varied from 238.2 psi – 829 psi where the lowest value was found at P5 and the highest value of UCS was found at P3 which was located in the middle of the width of the pavement.

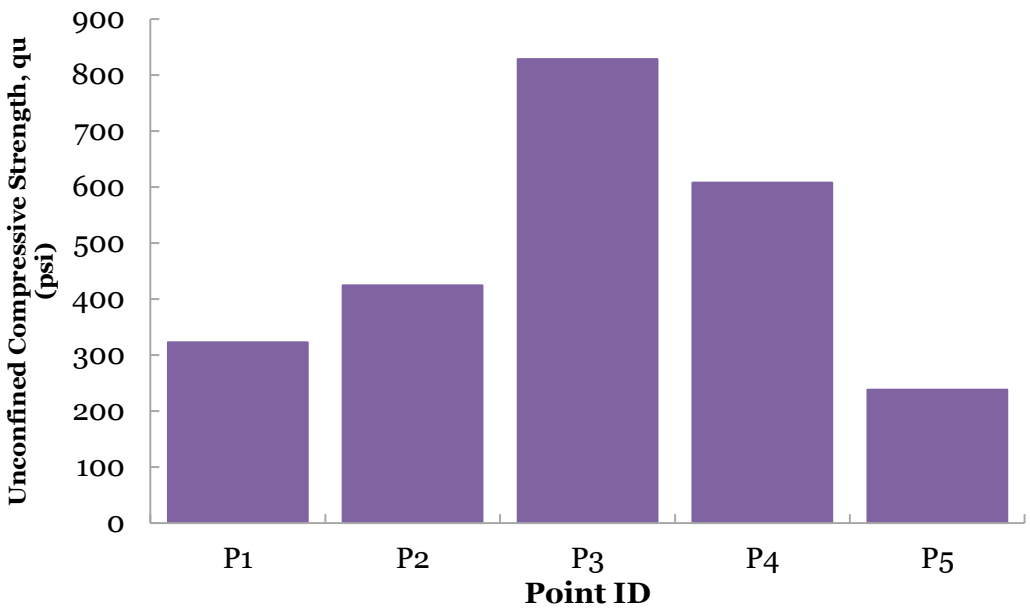

Figure 4.26: Variation of Unconfined Compressive Strength in base layer across width of pavement at Location-5

4.7.6 Variation Of Young's Moduli From Geogauge:

Wet sand layer was placed on the ground before taking measurement with Geogauge on five points set at 4 ft apart. Three close measurements were taken at each point considered to eliminate any scope of errors while measuring with Geogauge because proper contact between Geogauge foot and pavement layers is needed to ensure good measurement. The variation in Young's moduli across the five points is presented in Figure 4.26. From P1-P5, Young's moduli measured with Geogauge varied from 60,490 psi to 75,410 psi for the tests performed on October 3, 2014.

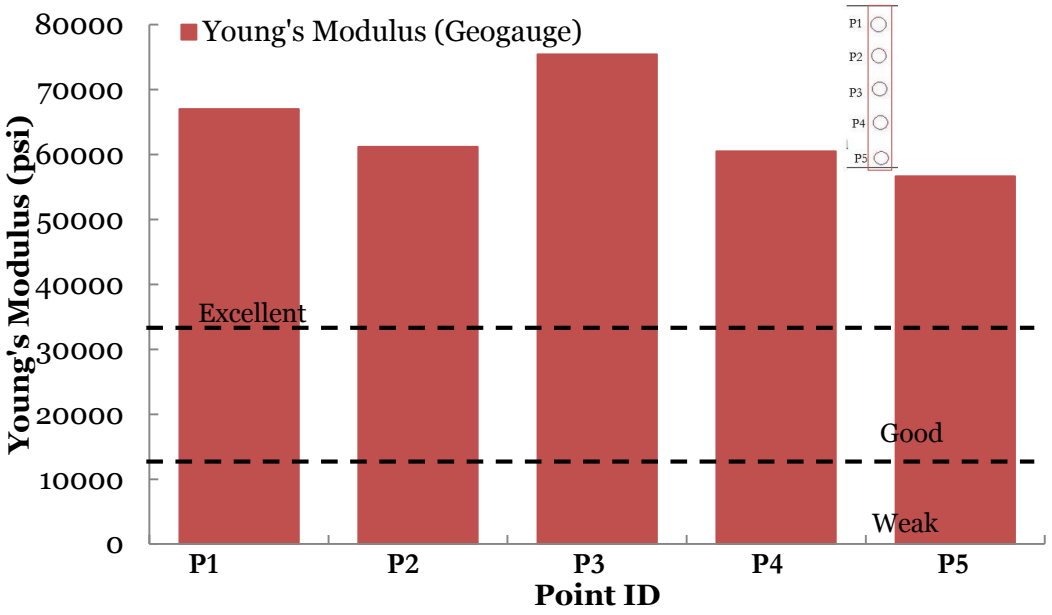

Figure 4.27: Variation of Young's Modulus across Pavement

All the points (P1-P5) provided 'excellent' base layer support according to the values characterization values provided by Chen et al., (1999) which can be seen from Figure above.

4.7.7 Comaprison Of Resilient Moduli From DCP Measurement With Young's Moduli From Geogauge For Cement Stabilized Base Layer With Prime Coat

Within P1-P5 considered, P3 showed highest variability in resilient moduli values within a range of 140,629 psi – 502,493 psi. Overall, Young's moduli values measured with Geogauge showed similar trend with the resilient moduli measured with Dynamic Cone Penetrometer which is shown below in Figure 4.27. Geogauge takes 9"~12" into account while taking it measurement, it is evident from the trend that the 6" cement stabilized base layer seems to have the major effect on the values measured with Geogauge because of its similarity with resilient moduli trend measure with DCP.

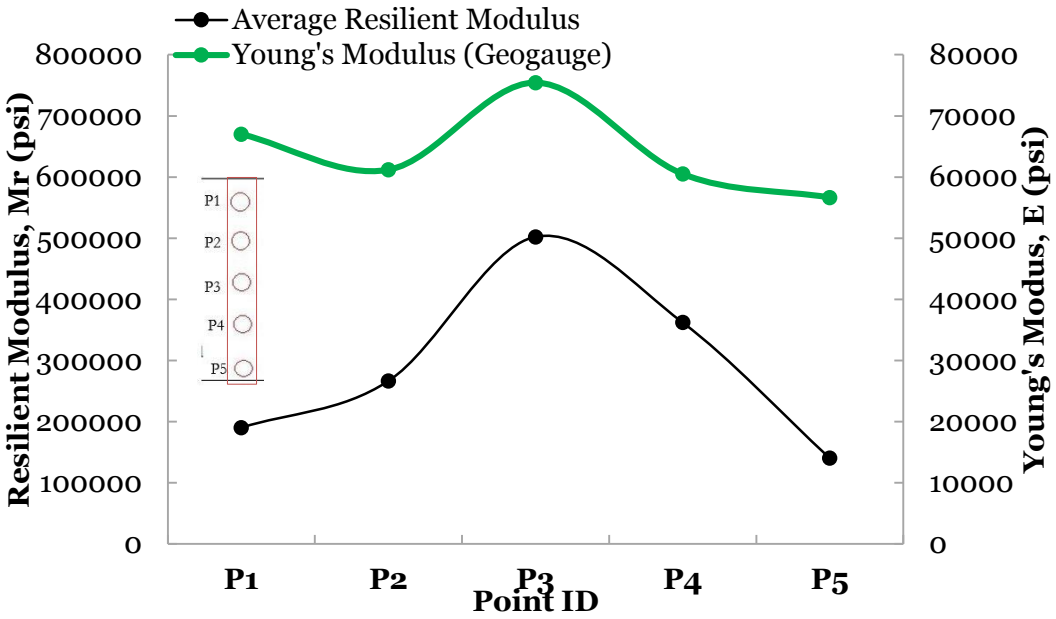

Figure 4.28: Variability of Resilient Moduli with Young's Moduli (Cement Stabilized Base Layer)

4.8 Comparison With Literature

4.8.1 Comparison Of Resilient Modulus From DCPI

4.8.1.1 Cement Stabilized Base With Prime Coat

Gaspard (2000) evaluated the resilient moduli values of cement stabilized base material for different cement content. The average resilient moduli value determined by Gaspard based on extensive field test performed for cement stabilized base materials for 7%, 8%, 9% and 10% cement content were 174,000 psi, 229,000 psi, 237,000 psi and 145,000 psi, respectively. While in Texan condition, laboratory test conducted on stabilized 4.5% and 3% cement treated base materials by Guthrie et al. (2001) generated a mean resilient moduli value of 381,170 psi and 276,722 psi, respectively. To compare resilient moduli value to other values mentioned in literature, resilient moduli values from every point considered for a location are averaged to obtain a specific moduli value for a certain location for 6" cement stabilized base layer with prime coat which is presented in Figure

4.28. Three locations (Avery St, S Riverfront Blvd. and Sylvan Ave.) where the DCP tests performed provided three specific resilient moduli value for the top cement stabilized base layer. The location-wise resilient moduli values and values determined by Gaspard (2000) and Guthrie et al. (2001) are given in the Table 4.1 below.

Table 4.1: Location-wise Resilient Moduli values with Literature Moduli Values (Cement Stabilized Base Layer)

Location	Resilient Modulus, Mr (psi)	Material Type	Test Type
Location-1 (Avery St.)	200,030	Cement Stabilized Base Materials	Field Test
Location-3 (S Riverfront Blvd.)	302,110	Cement Stabilized Base Materials	Field Test
Location-5 (Sylvan Ave.)	292,407	Cement Stabilized Base Materials	Field Test
7% Stabilized CTB (Gaspard, 2000)	174,000	Cement Stabilized Base Materials	Field Test
8% Stabilized CTB (Gaspard, 2000)	229,000	Cement Stabilized Base Materials	Field Test
9% Stabilized CTB (Gaspard, 2000)	237,000	Cement Stabilized Base Materials	Field Test
10% Stabilized CTB (Gaspard, 2000)	145,000	Cement Stabilized Base Materials	Field Test
3% Stabilized CTB (Guthrie et al., 2001)	276,722	Cement Stabilized Base Materials	Laboratory Test
4.5% Stabilized CTB (Guthrie et al., 2001)	381,170	Cement Stabilized Base Materials	Laboratory Test

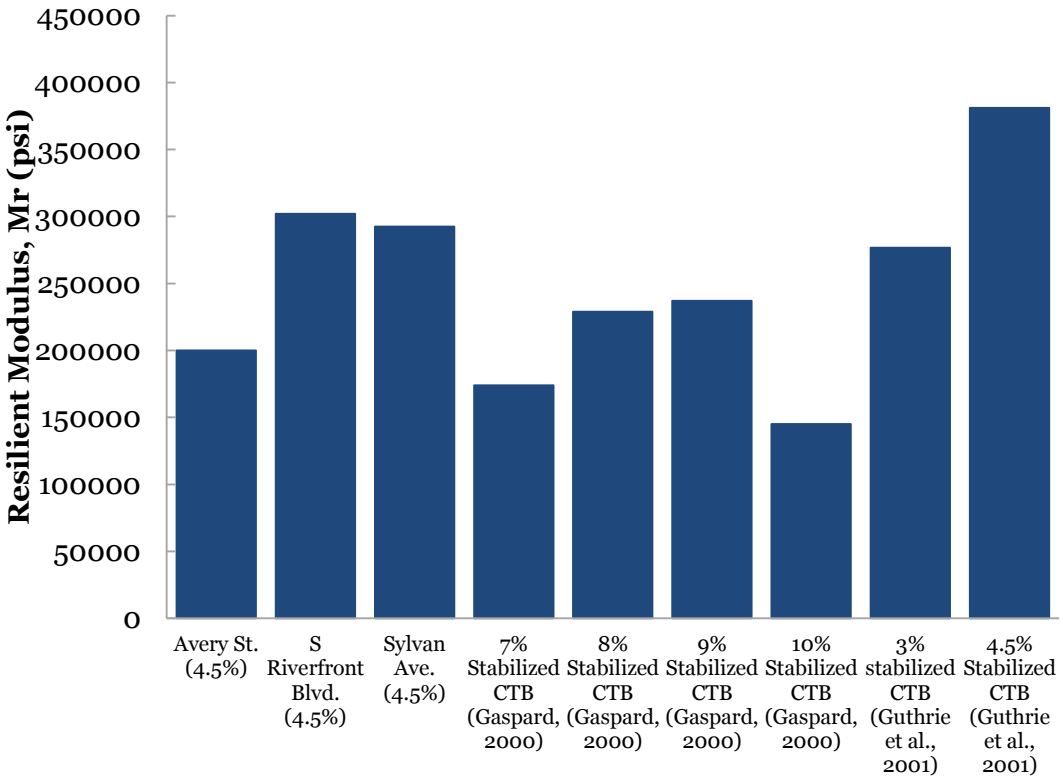

Figure 4.29: Comparison between Resilient Moduli values obtained from Field Tests and Literature (Cement Stabilized Base Layer)

4.8.1.2 Lime Stabilized Subgrade

Sargand (2000) conducted Dynamic Cone Penetrometer Test on lime treated Livingston soil in Ohio to determine the limiting DCPI value for subgrade acceptance and he concluded that the limiting DCPI for lime treated Livingston subgrade soil is 5.23 mm/blow. This DCPI value is converted into resilient modulus and thus compared to the average moduli value obtained by averaging the value from each successive 1" depth of the lime treated subgrade which is presented in Figure 4.29. Table 4.2 shows the resilient moduli values obtained from field tests performed at Avery St, S Riverfront Blvd. and Sylvan Ave., respectively.

Table 4.2: Location-wise Resilient Moduli values with Literature Moduli Values (Lime Treated Subgrade Layer)

Location	Resilient Modulus, Mr (psi)	Test Type	Material Type
Location-1 (Avery St.)	46,229	Field Test	Plastic Clay
Location-3 (S Riverfront Blvd.)	32,813	Field Test	Plastic Clay
Location-5 (Sylvan Ave.)	45,509	Field Test	Plastic Clay
Livingston Lime Treated Soil (Sargand, 2000)	68,668	Field Test	–
Lime Stabilized Texas soil (Little et al., 1995)	70,000	Laboratory Test	Plastic Clay

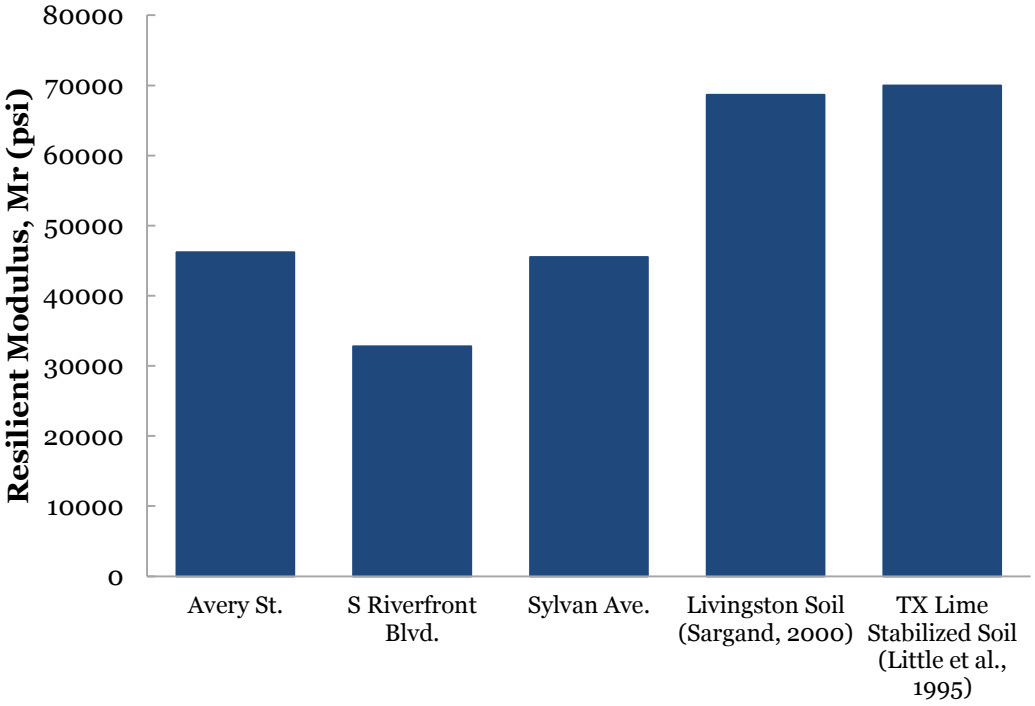

Figure 4.30: Comparison between Resilient Moduli values obtained from Field Tests and Literature (Lime treated Subgrade Layer)

From Figure 4.29, it can be seen that the resilient moduli values obtained for lime-treated subgrade layer varied at Location-1 varied 32.7% from the moduli value obtained from the test performed on Livingston soil, resilient moduli obtained from Location-3 varied 52.2% and moduli value from Location-5 varied 33.7%, respectively. According to Little et al., (1995), resilient moduli of lime stabilized subgrade soil can reach up to 70,000 psi.

4.8.1.3 Compacted Subgrade

Sargand (2000) performed resilient modulus test on the soil sample collected for US30 and DEL23 projects in Ohio. The resilient moduli values obtained from different tests performed by Sargand are presented below in Table 4.3 with the average moduli value obtained from the field tests performed at three different locations in Dallas, TX.

Table 4.3: Location-wise Resilient Moduli values with Literature Moduli Values (Compacted Subgrade Layer)

Location	Resilient Modulus, Mr (psi)	Test Type	Material Type
Location-1 (Avery St.)	13,052	Field Test	Plastic Clay
Location-3 (S Riverfront Blvd.)	16,413	Field Test	Plastic Clay
Location-5 (Sylvan Ave.)	13,750	Field Test	Plastic Clay
DEL23 (Sample 107) (Sargand, 2000)	17,700	Field Test	A-7-6
DEL23 (Sample 110) (Sargand, 2000)	9,100	Field Test	A-4
US30 (E876) (Sargand, 2000)	12,600	Field Test	A-4
US30 (W876) (Sargand, 2000)	9,200	Field Test	A-4

The comparison between the literature values and resilient moduli values obtained from field tests performed at three different locations are presented in Figure 4.30.

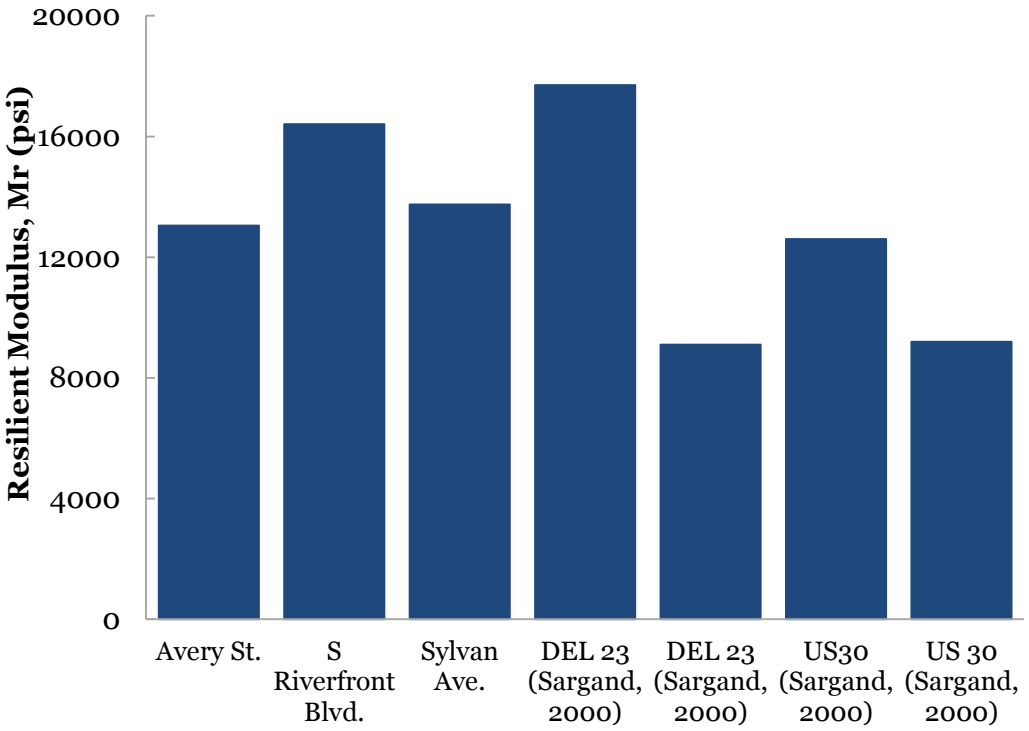

Figure 4.31: Comparison between Resilient Moduli values obtained from Field Tests and Literature (Compacted Subgrade Layer)

4.8.2 Comparison Of Unconfined Compressive Strength (UCS) From DCPI For Cement Stabilized Base Materials With Laboratory Data And Literature

A relationship between DCPI and UCS proposed by Patel and Patel (2012) was used to calculate UCS value from DCPI obtained from each 1" depth of the cement stabilized base layers. The UCS value calculated from field tests performed on Location-1, Location-3 and Location-5 were within a range of 400-550 psi. According to a study conducted by Guthrie et al. (2001), UCS value increased with the increase in cement content from 1.5% to 4.5% where, for 1.5% cement content, the unconfined compressive strength for 7 day curing period was 596 psi whereas, for 3% cement content, the UCS value for 7 day curing time

was 653 psi and for 4.5% cement content, the UCS value was 822 psi respectively. According to laboratory test performed on Grade-1 and Grade-2 base material provided by the TxDOT, the UCS value was found to be as 320 psi for Grade-1 materials (6% cement content) for 7 days curing period whereas, the UCS value was found to be 355 psi for Grade-2 materials (6% cement content) for 7 days curing period which is shown in Figure 4.31. The details are presented in Table 4.4.

Table 4.4: Location-wise UCS values with Literature Values (Cement Stabilized Base Layer)

Location	Unconfined Compressive Strength, qu (psi)	Test Type	Material Type
Location-1 (Avery St.)	403	Field Test	Cement Stabilized Base Materials
Location-3 (S Riverfront Blvd.)	534	Field Test	Cement Stabilized Base Materials
Location-5 (Sylvan Ave.)	484	Field Test	Cement Stabilized Base Materials
6% Stabilized CTB (Grade 1 material) (7 day)	396	Laboratory Test	Cement Stabilized Base Materials
6% Stabilized CTB (Grade 2 material) (7 day)	430	Laboratory Test	Cement Stabilized Base Materials
1.5% Stabilized CTB (Guthrie et al., 2001) (7 day)	596	Laboratory Test	Cement Stabilized Base Materials
3% Stabilized CTB (Guthrie et al., 2001) (7 day)	653	Laboratory Test	Cement Stabilized Base Materials
4.5% Stabilized CTB (Guthrie et al., 2001) (7 day)	822	Laboratory Test	Cement Stabilized Base Materials

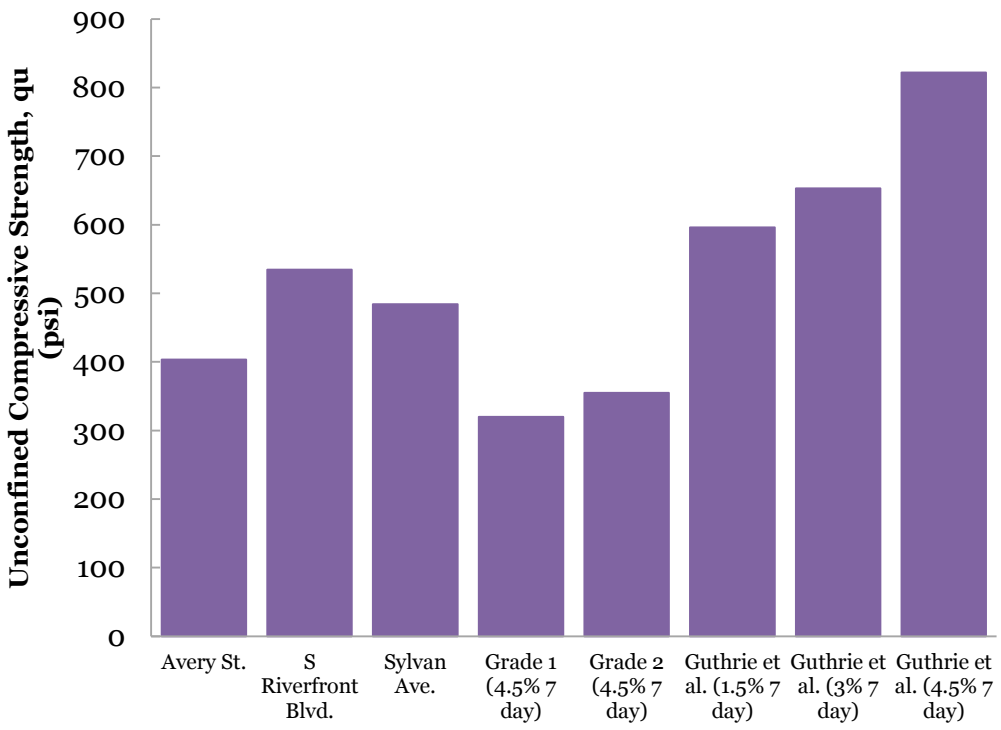

Figure 4.32: Comparison between UCS values obtained from Field Tests and Literature

4.8.3 Comparison Of Young's Modulus From Geogauge

Young's moduli values obtained from five locations will be compared with TX Pavement design modulus criteria for both cement stabilized base material and lime treated base materials. Being on a conservative side, the determined value of the moduli will be compared to the lower end of the range of the pavement design moduli criteria provided. Table 4.5 shows the different Young's Moduli values determined at five locations and the criteria for TX pavement design moduli values.

Table 4.5: Location-wise Young's Moduli values measured with Geogauge and TX Pavement Design Moduli

Location	Young's Modulus, E (psi)	Material Type
Location-1 (Avery St.)	67,615	Cement Treated Base Material
Location-2 (I-35E Northbound Frontage Road)	48,237	Cement Treated Base Material
Location-3 (S Riverfront Blvd.)	46,215	Cement Treated Base Material
Location-3 (Jefferson Viaduct Blvd.)	37,123	Cement Treated Base Material
Location-5 (Sylvan Ave.)	64,145	Cement Treated Base Material
TX Design Modulus (Pavement Design Guide, TxDOT, 2011)	80,000	Cement Treated Base Material
TX Design Modulus (Pavement Design Guide, TxDOT, 2011)	30,000	Lime Stabilized Subgrade

From Figure 4.32, it is evident that Young's moduli values obtained from five locations are higher than the design moduli of lime treated subgrade and lower than the design moduli of cement stabilized base. Young's moduli value obtained from the field tests reflect the material property of both 6" cement treated base and possibly 6" lime treated subgrade, it is highly likely that the Young's moduli values will be between the range provided for CTB and lime treated subgrade layer which can be observed from Figure 4.32.

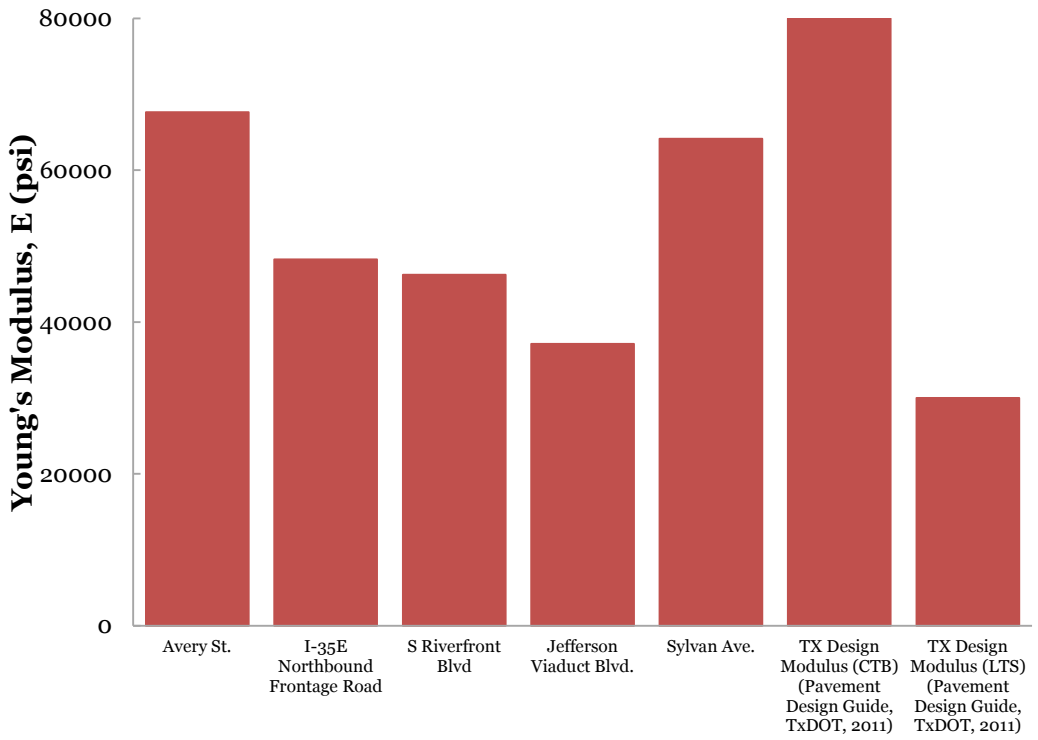

Figure 4.33: Comparison between Young's Moduli values obtained from Field Tests and Literature

CHAPTER 5

CONCLUSIONS AND RECOMMENDATIONS

Efficiency of in-situ pavement testing techniques plays the most important role during the construction period of pavement because it will ensure the proper design life of the pavement. Five sites within Horseshoe Project around Dallas, TX were selected for this study. The objective of this study was to evaluate the efficiency of two in-situ equipment i.e., Dynamic Cone Penetrometer and Geogauge, as in-situ testing technique with Nuclear Density Gauge as a supporting equipment in Texan climatic condition. Resilient moduli values obtained from Dynamic Cone Penetrometer test and Young's moduli values obtained from Geogauge were compared with each other to see the efficiency of a single in-situ equipment performing singularly to ensure proper pavement construction. The summary and conclusion derived from this extensive study are given in the following sections.

5.1 Summary And Conclusions

The results of the tests conducted with Dynamic Cone Penetrometer and Geogauge with the support of Nuclear Density Gauge can be summarized as:

- DCPI profile along depth of the pavement follow similar trend for similar types of pavement material in flexible pavement structure.
    - For cement stabilized base layer, DCPI varies from o.5 mm/blow to 8 mm/blow
    - For lime treated subgrade, DCPI varies from 2 mm/blow to 22 mm/blow
    - For compacted subgrade, DCPI varies from 8 mm/blow to 47 mm/blow
- From DCPI profile, layer thickness can efficiently be determined with a maximum margin of 0.5 inch which proves its effectiveness as an in-situ testing equipment.

- Resilient moduli along the depth of the pavement also follow similar trend in different types of base and subgrade materials but the opposite of the trend that DCPI profile represents.
    - For cement stabilized base layer, Mr varies from 40,500 psi to 623,285 psi
    - For lime treated subgrade, Mr varies from 7,513 psi – 76,660 psi
    - For compacted subgrade, Mr varies from 8,458 psi – 20,266 psi
- For cement stabilized base layer which was the topmost 6" of the pavement, the unconfined compressive strength varied within a range of 210 – 1,023.5 psi.
- Young's moduli measured with Geogauge also found to follow similar trend for the cement stabilized base layer with prime coat. Young's moduli values vary from 8,447 psi to 76,320 psi for the cement stabilized base.
- Young's modulus measured with Geogauge was found to be consistent with the density values measured with Nuclear Density Gauge.

5.2 Recommendations

To make the current study more effective, it is recommended that the work is further continued as mentioned in this section:

- Continue in-situ testing on freshly compacted base materials to evaluate the influence of the local base materials on the results obtained from Dynamic Cone Penetrometer Test and Geogauge test.
- Extensive laboratory program should be conducted to assess the effect of local base materials and develop possible correlations.

References

1. Scullion, T., Guthrie, S., & Sebesta, S. (2003). *Field performance and design recommendations for full depth recycling in Texas* (No. FHWA/TX-03/4182-1,).
2. Alshibli, K., Nazzal, M., & Seyman, E. (2004). *Assessment of in-situ test technology for construction control of base courses and embankments* (No. FHWA/LA. 04/389,). Baton Rouge,, LA, USA: Louisiana Transportation Research Center.
3. Petry, T. M., & Little, D. N. (2002). Review of stabilization of clays and expansive soils in pavements and lightly loaded structures-history, practice, and future.*Journal of Materials in Civil Engineering*, *14*(6), 447-460.
4. Salgado, R., & Yoon, S. (2003). Dynamic cone penetration test (DCPT) for subgrade assessment. *Joint Transportation Research Program*, 73.
5. Gabr, M. A., Hopkins, K., Coonse, J., & Hearne, T. (2000). DCP criteria for performance evaluation of pavement layers. *Journal of performance of constructed facilities*, *14*(4), 141-148.
6. Chou, E., Fournier, L., Luo, Z., & Wielinski, J. (2004). *Structural Support of Lime or Cement Stabilized Subgrade Used with Flexible Pavements* (No. FHWA/OH-2004/017,).
7. Little, D. N. (1995). *Stabilization of pavement subgrades and base courses with lime*.
8. Little, D. N. (1987). *Evaluation of structural properties of lime stabilized soils and aggregates*. National Lime Association.
9. Guthrie, W. S., Sebesta, S., & Scullion, T. (2002). *Selecting optimum cement contents for stabilizing aggregate base materials* (No. FHWA/TX-05/7-4920-2,). Texas Transportation Institute, Texas A & M University System.
10. Wu, S., & Sargand, S. M. (2007). *Use of dynamic cone penetrometer in subgrade and base acceptance* (No. FHWA/ODOT-2007/01). ORITE.

11. Gaspard, K. J. (2000). *Evaluation of Cement Treated Base Courses* (No. Report No. 00-1TA,).
12. Mohammadi, S. D., Nikoudel, M. R., Rahimi, H., & Khamehchiyan, M. (2008). Application of the Dynamic Cone Penetrometer (DCP) for determination of the engineering parameters of sandy soils. *Engineering Geology*, *101*(3), 195-203.
13. Gudishala, R. (2004). *Development of resilient modulus prediction models for base and subgrade pavement layers from in situ devices test results* (Doctoral dissertation, Louisiana State University).
14. Jones, D., & Harvey, J. T. (2005). Relationship between DCP, Stiffness, Shear Strength, and R-value. *Institute of Transportation Studies*.
15. Lee, C., Kim, K. S., Woo, W., & Lee, W. (2014). Soil Stiffness Gauge (SSG) and Dynamic Cone Penetrometer (DCP) tests for estimating engineering properties of weathered sandy soils in Korea. *Engineering Geology*, *169*, 91-99.
16. Amini, F. (2003). *Potential applications of dynamic and static cone penetrometers in MDOT pavement design and construction*. Jackson State University.
17. Patel, M. A., & Patel, H. S. Experimental Study on Various Soils to Corelate Test Results of PBT, UCS, DCP and CBR.
18. Chen, D. H., Wu, W., He, R., Bilyeu, J., & Arrelano, M. (1999). Evaluation of in-situ resilient modulus testing techniques. *Geotechnical Special Publication. ASCE*, *86*, 1-11.
19. Chen, D. H., Wu, W., He, R., Bilyeu, J., & Arrelano, M. (1999). Evaluation of in-situ resilient modulus testing techniques. *Geotechnical Special Publication. ASCE*, *86*, 1-11.

20. Chen, D. H., Wang, J. N., & Bilyeu, J. (2001). Application of dynamic cone penetrometer in evaluation of base and subgrade layers. *Transportation Research Record: Journal of the Transportation Research Board*, *1764*(1), 1-10.
21. Brown, E. R., & Foo, K. Y. (1989). EVALUATION OF VARIABILlIY IN RESILIENT MODULUS TEST RESULTS (ASTM D 41 23).
22. Richardson, David N., et al. *Resilient Moduli of Typical Missouri Soils and Unbound Granular Base Materials*. No. OR09. 016. 2009.
23. Zollinger, Dan G., Moon Won, and Andrew J. Wimsatt. *Subbase and Subgrade Performance Investigation for Concrete Pavement*. Texas Transportation Institute, Texas A&M University System, 2009.
24. Patel, M. A., & Patel, H. S. (2012). Experimental Study to Correlate the Test Results of PBT, UCS, and CBR with DCP on Various soils in soaked condition.*International Journal of Engineering (IJE)*, *6*(5), 244.
25. Mishra, D., Tutumluer, E., Moaveni, M., & Xiao, Y. (2012). Laboratory and field measured moduli of unsurfaced pavements on weak subgrade. In *GeoCongress 2012@ sState of the Art and Practice in Geotechnical Engineering* (pp. 1381-1390). ASCE.
26. Wachiraporn, S., Sawangsuriya, A., Sunitsakul, J., & Sramoon, W. (2010). Stiffness and Strength Based In-Place Evaluation of Compacted Unbound Materials. In *Paving Materials and Pavement Analysis* (pp. 347-354). ASCE.
27. Chen, D. H., Wang, J. N., & Bilyeu, J. (2001). Application of dynamic cone penetrometer in evaluation of base and subgrade layers. *Transportation Research Record: Journal of the Transportation Research Board*, *1764*(1), 1-10.

28. Siekmeier, J., Pinta, C., Merth, S., Jensen, J., Davich, P., Camargo, F., & Beyer, M. (2009). *Using the dynamic cone penetrometer and light weight deflectometer for construction quality assurance* (No. MN/RC 2009-12).
29. George, K. P. (2004). Prediction of resilient modulus from soil index properties.
30. Lee, W., Bohra, N. C., Altschaeffl, A. G., & White, T. D. (1994). Subgrade Resilient Modulus for Pavement Design and Evaluation: Implementation Report.
31. ELIAS, M., HELWANY, S., & TITI, H. (2006). Determination of Typical Resilient Modulus Values for Selected Soils in Wisconsin.
32. Khoury, N., Brooks, R., Boeni, S. Y., & Yada, D. (2012). Variation of resilient modulus, strength, and modulus of elasticity of stabilized soils with postcompaction moisture contents. *Journal of Materials in Civil Engineering*, *25*(2), 160-166.
33. Hossain, M. S., & Apeagyei, A. K. (2010). *Evaluation of the Lightweight deflectometer for in-situ determination of pavement layer moduli* (No. FHWA/VTRC 10-R6).
34. Alshibli, K., Nazzal, M., & Seyman, E. (2004). *Assessment of in-situ test technology for construction control of base courses and embankments* (No. FHWA/LA. 04/389,). Baton Rouge,, LA, USA: Louisiana Transportation Research Center.
35. Lopez, A., & Velarde, J. (2014). Developing In-Situ Moisture-Modulus Relationships for Compacted Subgrade Geomaterials. In *Transportation Research Board 93rd Annual Meeting* (No. 14-2129).
36. Parker Jr, F. (1991). Estimation of paving materials design moduli from falling weight deflectometer measurements. *Transportation Research Record*, (1293).
37. Ping, W. C. V., & Sheng, B. Evaluation of Resilient Modulus and Modulus of Subgrade Reaction for Florida Pavement Subgrades.
38. White, D. J. (2005). Fly Ash Soil Stabilization for Non-Uniform Subgrade Soils.

39. Fiedler, S. A., Main, M., & DiMillio, A. F. (2000). In-place stiffness and modulus measurements. *GEOTECHNICAL SPECIAL PUBLICATION*, 365-376.
40. Webster, S. L., Grau, R. H., & Williams, T. P. (1992). *Description and application of dual mass dynamic cone penetrometer* (No. WES/IR/GL-92-3). ARMY ENGINEER WATERWAYS EXPERIMENT STATION VICKSBURG MS GEOTECHNICAL LAB.
41. Siekmeier, J. A., Young, D., & Beberg, D. (2000). Comparison of the dynamic cone penetrometer with other tests during subgrade and granular base characterization in Minnesota. *ASTM Special Technical Publication*, *1375*, 175-188.
42. Kessler, K. (2009). Use of DCP (Dynamic Cone Penetrometer) and LWD (Light Weight Deflectometer) for QC/QA on Subgrade and Aggregate Base. In *Material Design, Construction, Maintenance, and Testing of Pavements@ sSelected Papers from the 2009 GeoHunan International Conference* (pp. 62-67). ASCE.
43. Abu-Farsakh, M. Y. (2005). The use of dynamic cone penetrometer to predict resilient modulus of subgrade soils.
44. Mohammad, L. N., Herath, A., Abu-Farsakh, M. Y., Gaspard, K., & Gudishala, R. (2007). Prediction of resilient modulus of cohesive subgrade soils from dynamic cone penetrometer test parameters. *Journal of Materials in Civil Engineering*,*19*(11), 986-992.
45. White, D. J., Vennapusa, P. K., Becker, P., White, C., & Engineer, B. C. (2013). Cement Stabilization of Subbase and Subgrade.
46. Ayers, M. E. (1990). *Rapid shear strength evaluation of in situ granular materials utilizing the dynamic cone penetrometer* (Doctoral dissertation, University of Illinois at Urbana-Champaign).

47. Sanchez, E. (2010). *Use of dynamic cone penetrometer versus other field and lab tests for subsurface characterization* (Doctoral dissertation, UNIVERSITY OF NEVADA, RENO).
48. Hassan, A. B. (1996). *The effects of material parameters on Dynamic Cone Penetrometer results for fine-grained soils and granular materials* (Doctoral dissertation, Oklahoma State University).

Biographical Information

Ahmed Nawal Ahsan graduated with a Bachelor of Science in Civil Engineering from Bangladesh University of Engineering and Technology, Dhaka, Bangladesh in April, 2012. After graduation, he started his career as QA/QC Engineer in Basic Engineering Ltd. in a contract project of Chevron, Bangladesh. He started his graduate studies at The University of Texas at Arlington in Summer 2013. During his study, he got the opportunity to work as a graduate research assistant under supervision of Dr. Sahadat Hossain. The author's research interests include In-situ pavement testing, Slope stability analysis, Numerical modeling, and Bioreactor Landfills.